Universidade Federal do Rio Grande do Norte
Centro de Ciências Exatas e da Terra
Programa de Pós-Graduação em Física

Chiral phases and Landau-forbidden transitions in one dimension

Natal - RN

Rafael Ávila Macêdo

February 2022

Universidade Federal do Rio Grande do Norte - UFRN
Sistema de Bibliotecas - SISBI
Catalogação de Publicação na Fonte. UFRN - Biblioteca Setorial Prof. Ronaldo Xavier de Arruda - CCET

Macêdo, Rafael Ávila.
Chiral phases and Landau-forbidden transitions in one dimension / Rafael Ávila Macêdo. - 2022.
138f.: il.

Dissertação (Mestrado) - Universidade Federal do Rio Grande do Norte, Centro de Ciências Exatas e da Terra, Programa de Pós-Graduação em Física. Natal, 2022.
Orientador: Rodrigo Gonçalves Pereira.

1. Física - Dissertação. 2. Chiral phase - Dissertação. 3. Deconfined quantum criticality - Dissertação. 4. Landau paradigm - Dissertação. 5. Bosonization - Dissertação. 6. Pseudospins - Dissertação. I. Pereira, Rodrigo Gonçalves. II. Título.

RN/UF/CCET CDU 53

Elaborado por Joseneide Ferreira Dantas - CRB-15/324

Abstract

The common lore in statistical physics suggests that phases and transitions of matter are generally classified by what is called the Landau-Ginzburg-Wilson paradigm. In two dimensions, however, quantum models can exhibit "deconfined" continuous transitions between ordered phases, which are forbidden by the Landau classification. On this thesis, we introduce a one-dimensional quantum spin model with three ordered phases: A chiral spin state, where the system orders into three-spin "fluxes", an antiferromagnetic state, and a novel phase which we denote as the Klein paramagnet. We find that all transitions from the chiral phase are continuous and beyond the Landau paradigm.

Keywords: Chiral phase, Deconfined quantum criticality, Landau paradigm, Bosonization, Pseudospins

Resumo

O conhecimento comum em física estatística sugere que fases da matéria e suas transições são geralmente classificadas pelo chamado paradigma de Landau-Ginzburg-Wilson. Em duas dimensões, entretanto, modelos quânticos podem apresentar transições contínuas "deconfinadas" entre fases ordenadas, proibidas pela classificação de Landau. Nesta dissertação, introduzimos um modelo de spin em uma dimensão com três fases ordenadas: um estado de spin quiral, onde o sistema se ordena em "fluxos" de três spins, um estado antiferromagnético, e uma nova fase nunca antes estudada que denominamos de paramagneto de Klein. Encontramos que todas as transições que envolvem a fase quiral são contínuas e fora do paradigma de Landau.

Palavras-chave: Fase quiral, Criticalidade quântica deconfinada, paradigma de Landau, Bosonização, Pseudospins

Acknowledgements

I would like to thank my advisor, Prof. Rodrigo Pereira, for all the support, guidance and patience during the last two years. I also would like to thank my collaborator Dr. Flávia Ramos, for all the help, and the members of the examination board: Prof. Álvaro and Prof. Francisco for accepting the invitation and asking thought-provoking questions in the thesis defense.

I have learnt a lot at the biweekly meetings of the IIP Quantum Matter group, and the following discussions were of great importance in sharpening my research and knowledge in condensed matter. I am thankful to all participants: Vanuildo, Carlene, Moallison, Fabrizio, Lucas, Hernán, Gabriel and Weslei.

I am forever grateful for my parents, Marcelo and Ana Paula and all my family, for always supporting me in the long path of becoming a scientist. I am also indebted to my friends, in special to Matheus Filipe, for the camaraderie and laughs during those years in the pandemic.

Finally, I would like to thank the financial support by the Conselho Nacional de Desenvolvimento Científico e Tecnológico (CNPq).

Contents

List of Figures

Chapter 1

Introduction

"How many states of matter are there?"

Starting from first principles, one might think that the tools of physics are too simple to deal with such complex questions. In a simple estimate, macroscopic materials have $N \sim 10^{23}$ interacting particles, while only gaseous substances are generally treated in an undergraduate statistical mechanics course.

It is somewhat surprising that only a few physical properties must be taken into account to describe matter around us. A good starting point is given by thermodynamics, whose principles dictate the macroscopic limit of physical systems at equilibrium. The missing ingredient, as shown by Lev Landau in 1937 [7, 8], is the concept of an order parameter: If one can write down a variable(s) ϕ whose value can indicate the presence of some phase, Landau noted that it generally breaks some symmetries of the system. Then, by imposing that the free energy of the system f is a fully well-behaved (analytic) function of this variable, a simple description is obtained by writing down the most general expansion of $f = f(\phi)$, while respecting the symmetries. The minima of this free energy corresponds to the possible values of the order parameter, and, therefore, the possible phases of matter.

A particularly nice example comes from high-school physics: Consider a fluid in a recipient of volume V in which we can measure its density of particles ρ. The common lore is that there are at least three phases of matter: A compressible gas, where the density is uniformly distributed throughout space, a high-density solid state, where particles are pinned in some lattice configuration due to interactions, and a nearly incompressible liquid state, an intermediate state.

The translation symmetry $T : \mathbf{x} \to \mathbf{x} + \mathbf{a}$ plays an important role: While the average position of the molecules of a gas or a liquid can be translated by any vector without changing the phase, this is not the case for a solid, where the positions are fixed periodically, see Fig 1.1(a). Indeed, the translation symmetry is said to be spontaneously broken in a solid, while it is preserved in the liquid/gas. By the Landau prescription, it is necessary to go through a *phase transition* to get from a phase to another. The corresponding order parameter is given by the Fourier transform of the density:

$$\tilde{\rho}(\mathbf{Q}) = \int \mathrm{d}^3\mathbf{x} e^{i\mathbf{Q}\cdot\mathbf{x}} \rho(\mathbf{x}) \ , \tag{1.1}$$

where $\mathbf{Q}$ is a reciprocal lattice vector. If $\tilde{\rho}(\mathbf{Q} \neq 0) \to 0$, translation symemtry is then restored. A sharp conclusion from this analysis is the equivalence of a liquid and a gas under the translation symmetry, since both have uniform density. A commonly found phase diagram of simple fluids is shown in see Fig 1.1(b), where each phase and corresponding transitions are indicated given a pressure and temperature. Note that the liquid/gas transition terminates at a point, known to be the critical point. That is, for high enough temperature and pressure, there is no distinction between a gas and a liquid! Any path starting from the solid phase and ending on any of the other two phases needs to cross a phase transition.

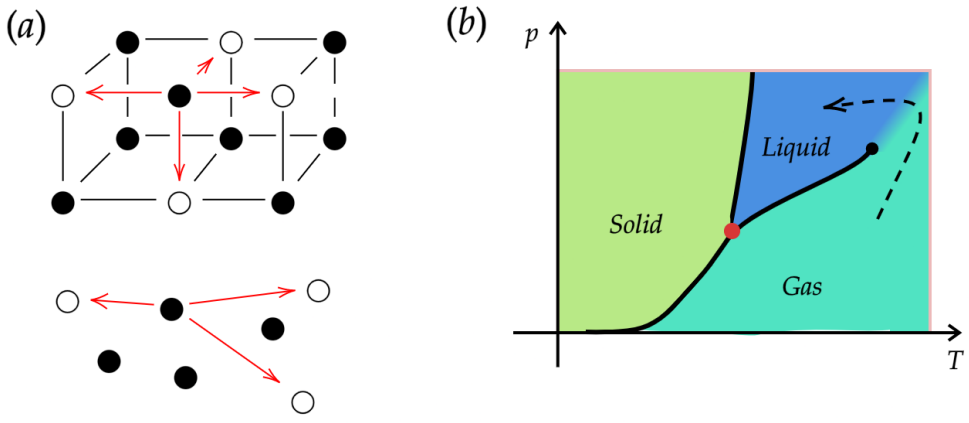

Figure 1.1: (a): Action of the translation symmetry in the solid (gas/liquid) in the top(bottom) figure, pictorially. Note that, for a gas/liquid, the red arrows can move continuously without changing the average properties of the phase. In a solid, allowed translations are locked down to lattice sites. (b): Phenomenological phase diagram of a simple fluid, where the phase transition lines are in black. The red point in the middle is known as the triple point, connecting all three phases. For high enough pressure and temperatures, there are smooth paths connecting the liquid and the gas, as highlighted by the dashed arrow.

However, to properly describe the nature of transitions, the order parameter can behave as a physical degree of freedom and fluctuate in space, $\phi = \phi(\mathbf{x})$. The free energy is then promoted to a functional $\mathcal{F}[\phi(\mathbf{x})]$, known as the Landau-Ginzburg functional [1,3]. Fluctuations are introduced if a partition function is constructed by summing over field configurations, in a framework called statistical field theory (also known as euclidean quantum field theory) [9, 10]. In developments led by Kenneth Wilson [11–14], it was shown that physical observables of statistical field theories depend on which energy scale they are probed: This is the idea of the renormalization group. For example, even if the starting point are atoms interacting in a complicated way microscopically, the physics at long distances (corresponding to low energies) is just described by the order parameter. This procedure can put on qualitative grounds and is used to extract what terms of the Landau expansion are important at long distances. With all principles combined, this framework to describe phases of matter was coined as the Landau-Ginzburg-Wilson (LGW) paradigm [15].

An important prediction from this scheme is the existence of two fundamentally different types of phase transition. A first-order (abrupt) phase transition occurs when discontinuous jumps appear in thermodynamic quantities, such as in the solid-liquid transition, for example. In this case, not much of interesting happens: it can happen in the boundary of two different symmetry-broken phases, with distinct order parameters or in the boundary of two symmetry-equivalent phases [16], and generally symmetries are broken at the transition. It can be understood as a region where both phases coexist, and microscopic details become important.

In a second-order (continuous) phase transition, the order parameter vanishes continuously at the transition, at the boundary between a symmetry-broken phase and a disordered symmetry-preserving phase. Such transitions are the most interesting: Thermodynamic quantities, such as the free energy and specific heat, have power-law divergences in thermodynamic quantities, defining a *universality class*: Two completely different microscopic systems may have the same second-order transition, that is, the divergences are characterized by the same exponents. Moreover, such fixed points generally hold emergent symmetries, since a lot of irrelevant details are "washed out" by the renormalization group. The most significant examples are field theories with conformal symmetry, known as conformal field theories [17].

We are, however, interested in the phases of many-body quantum mechanical systems, which are known to hold phase transitions even at $T = 0$! That is, given a hamiltonian H, the corresponding ground state can have different symmetry-

breaking phases. For quantum spin systems, our main focus, one has a spin degree of freedom on each site σ_i^α, where different components are non-commuting on each site. The following simple-looking hamiltonian already shows the complexity of the quantum ground-state problem:

$$H_{\text{TFIM}} = -\sum_{\langle i,j\rangle} \sigma_i^z \sigma_j^z - g \sum_i \sigma_i^x \ , \tag{1.2}$$

named the transverse field Ising model (TFIM), since there is a magnetic field in the x-direction, whereas the Ising-like interaction is in the z-direction. Intuitively, this is loosely known as "quantum fluctuations": Since one can write local terms which do not commute with each other, the corresponding wavefunctions can "fluctuate" between basis states. In fact, in the above model, this generates a *quantum phase transition* [18]: by taking $g = 0$, the ground state is a ferromagnet in the z-direction, it breaks an internal $\mathbb{Z}_2$ symmetry and is twofold degenerate. For $g \to \infty$, the spins are polarized in the x-direction, without breaking any symmetry. These two phases are, in fact, separated by a continuous phase transition, as predicted by the LGW paradigm, see Fig 1.2(a) and Sec 3.1.

There is a similarity to the finite-temperature classical case, as some kind of fluctuations generates a phase transition following LGW. In fact, one can understand quantum fluctuations acting as thermal fluctuations on a extra dimension: This is known as the *quantum-classical correspondence*. That is, the ground state of a $d-$dimensional quantum system can be mapped to a thermal phase of a $(d+1)-$dimensional classical statistical mechanics problem. In the case of the transverse field Ising model, the classical description is the two-dimensional classical Ising model, solved by Onsager [19]. The quantum and ferromagnetic phases are mapped into each other, while the trivial paramagnet (polarized) phase in the quantum side corresponds to a classical disordered phase.

A solemn conclusion apparently arises from this equivalence: There wouldn't be any true macroscopic manisfestation of quantum mechanics. To put it in another way, every quantum phase would be described by a thermal classical ensemble. This seems implausible, as entangled states do not have any classical description. Indeed, there are phases where no higher-dimensional classical analogs exist, going beyond the LGW paradigm such as topological and fracton phases [20–22]. In particular, we are interested in exotic critical points, encapsulated in what is known

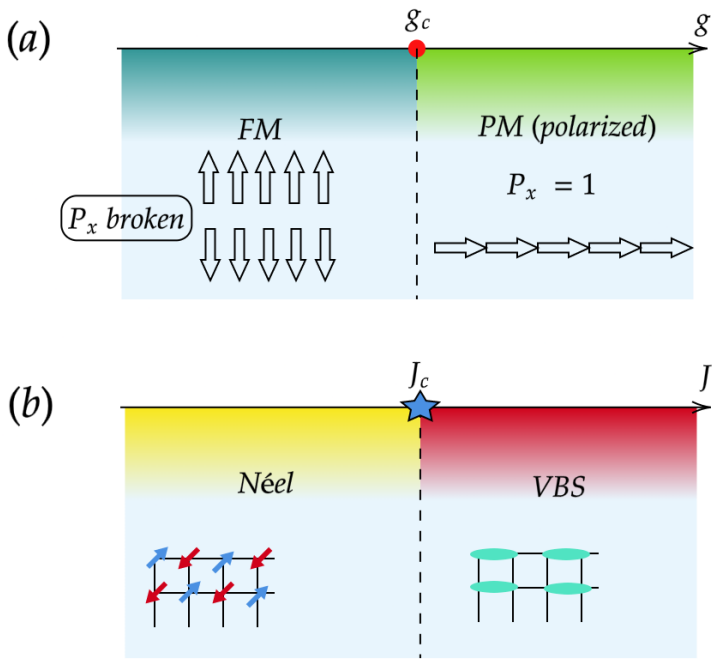

Figure 1.2: Examples of continuous phase transitions. (a) The transverse field Ising model phase transition, between the twofold degenerate ferromagnet and a paramagnet; (b) the deconfined quantum critical point between the Néel phase and the VBS phase, both symmetry-breaking phases.

as deconfined quantum criticality (DQC) [4]: Continuous phase transitions between two symmetry-breaking phases, where the leading fluctuations are not described by the order parameter, but in terms of gapless degrees of freedom probed only at the critical point. It was named in analogy to the confinement/deconfinement transition present in gauge theories, commonly found in particle physics: In such models, there are matter degrees of freedom (electrons, quarks, ...) interacting with gauge bosons (photons, gluons, ...). In the deconfined phase, both excitations can be understood separately, such as photons in electromagnetism. However, in a confined phase, matter bounds to gauge bosons generating new excitations which dominate at low energies. This is what happens in quantum chromodynamics (QCD), where three quarks, bound by gluons, make up protons, seen at low energies at the level of nuclear physics.

The canonical example of DQC is the Néel-VBS transition [15], illustrated in Fig 1.2(b) for the square lattice. On the left side, we have a magnetically ordered antiferromagnetic phase, whereas a valence bond solid (VBS), a phase where spins

form singlet states with their neighbors, resides at the other side of the transition. Pictorially, one can understand the excitations of both ordered states as bound states of a spinon- a chargeless spin-1/2 boson- with a photon, where the spinons are the excitations at the transition. This is surprising, since all operators appearing in the hamiltonian are written in terms of spin operators. This "fractionalization" is responsible for a second-order phase transition, and is a pure quantum effect.

A new landscape emerges: the classification of symmetry-breaking quantum phases and corresponding transitions, which, to our understanding, may follow LGW or be deconfined. In the large zoo of symmetries, our interest lies in a particular one known as time-reversal symmetry: Acting on wavefunctions undergoing time-evolution, the action amounts to an antiunitary operation which inverts the time direction and complex conjugate numbers as $t \to -t, i \to -i$. For spin systems, the action amounts to fully flip the spin operator, as $\mathcal{T} : \boldsymbol{\sigma}_i \to -\boldsymbol{\sigma}_i$. In magnetic phases, for example, $\langle \boldsymbol{\sigma}_i \rangle \neq 0$, and $\mathcal{T}$ is generally broken.

In a seminal paper, Wen, Wilczek and Zee [6] have proven the existence of a non-magnetic, time reversal-breaking phase in two dimensions. Starting from models assuming spin-rotation symmetry, They showed the existence of a *chiral spin state* (CSS), which breaks time-reversal and parity. The corresponding order parameter, defined as a triple product of spin operators, $\boldsymbol{\sigma}_i \cdot (\boldsymbol{\sigma}_j \times \boldsymbol{\sigma}_k)$, is known as *chirality*. This leads to an interesting picture shown in Fig 1.3: Spins are in "entangled triangles" with an internal "current" determined by the sign of the chirality.

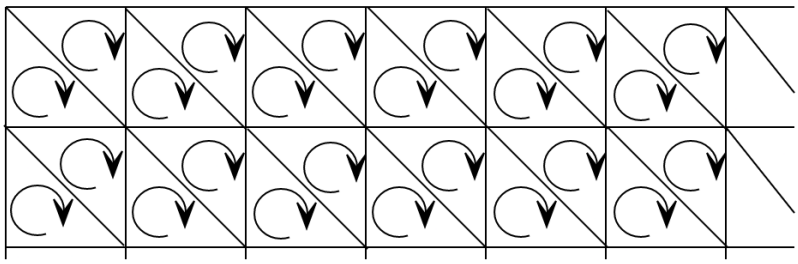

Figure 1.3: Depiction of a chiral spin state of a stripe of the square lattice.

Chiral spin states can host more exotic phases, which was the original inspiration of the three authors. Those are denoted as chiral spin liquids, and are very similar to the celebrated Laughlin state in the fractional quantum Hall effect [23]: Excitations have exotic statistics, and there are robust degeneracies depending on boundary conditions, completely beyond the LGW paradigm. Chiral spin liquids

are an example of phases generally known as quantum spin liquids [24–26]. However, it was only twenty years later that an exactly solvable model in the honeycomb lattice was introduced by Kitaev [27], confirming the possibility of stable spin liquid phases. Henceforth, a new research direction flourished, both in the theoretical study of "Kitaev models" and in the search of materials which may host spin liquid ground states [28, 29].

Going to one dimension lower, quantum phases are known to show a singular behavior: As first shown by Bethe [30], the one dimensional Heisenberg chain, defined as $H = |J| \sum_i \boldsymbol{\sigma}_i \cdot \boldsymbol{\sigma}_{i+1}$, has a gapless ground state, where the excitations are fractionalized spinons. However, in contrast to the deconfined quantum critical point, this is a stable phase, being robust to perturbations [31], and can be considered as an example of a gapless quantum spin liquid. However, as already discussed, there are also LGW-allowed gapped phases, like the transverse-field Ising model. In the midfield, DQC phenomenology was recently found in 1d [5, 32–34]. Previously known transitions, such as Néel-VBS in one dimension, were recast as examples of DQC-like criticality, containing many of the properties of the two-dimensional counterparts.

Vector chiral magnetic phases were found in one dimension [35,36], where parity is broken, while time-reversal is preserved. However, there are few examples of spontaneously-broken time-reversal in a non-magnetic phase [37, 38]. By taking a top-down approach, some questions arise: Is there a stable chiral phase in one dimension ? By perturbing it, what is the nature of the transitions ?

In this thesis, starting from a spin model in a quasi-1D lattice developed in earlier work [39], we construct spontaneously broken chiral spin states in one dimension exactly and discuss phase transitions to other symmetry-broken states, showing the presence of continuous phase transitions between them. In the second and third chapters, we will review the necessary background to understand the main results in the thesis: The second chapter deals with the framework necessary for understanding the LGW paradigm and the phenomenology behind deconfined quantum criticality. The Néel-VBS transition is discussed in detail, since similar aspects of the transition appear in our model and DQC physics is not as standard as other topics in this chapter. The third chapter focuses on one dimension, discussing both the avaliable field theory toolbox and known examples of deconfined-like criticality. In the fourth and fifth chapters, we present the original work (except the first two sections of the fourth chapter), constructing the spin model of interest and the

corresponding chiral phase. In the fifth chapter, various limits of this model are discussed, and phase transitions are analyzed using numerical and field theory arguments. We conclude in the last chapter by reviewing the main results and proposing open questions.

In this thesis, a mix of analytical and numerical results are presented. Analytical work was done by myself with the help of my advisor, Prof. Rodrigo Pereira. The numerical DMRG results were obtained by postdoctoral fellow Flávia Ramos, which also produced the plots in Figs 5.4,4.9, and contributed to parts of other figures in Chapters 4 and 5.

Chapter 2

Quantum phases and transitions

In this chapter, we will put the physics of quantum phases on a qualitative ground. First, the Landau-Ginzburg functional formalism is introduced, along with its general predictions about symmetry-breaking phases and shortcomings about phase transitions. To correctly describe the latter, the tools from field theory and renormalization group are introduced. We will then conclude by expanding the Ising model example and discussing how deconfined quantum critical points violate those principles.

In the first section, we will introduce the Landau-Ginzburg functional and construct some examples, roughly following [1, 16, 40]. For the second session, fluctuations are supplemented and the general ideas from the renormalization group and conformal field theory are introduced. A mix of quantum field theory textbooks are taken as inspiration [2, 3, 18, 41]. In the last section, the physics of deconfined quantum criticality is presented for the most well-studied example: The Néel-VBS transition. We followed closely the presentation of the first two papers written on the subject [4, 15], but will be developed here in detail, including the arguments of fractionalization at the transition.

2.1 Landau-Ginzburg paradigm

As many successful physics frameworks, the LG theory can be constructed from phenomenological inputs (many from experiments), and simple principles are derived.

First, one must define what the order parameter really means. In experiments,

it was found that by cooling off materials, there is a response to external fields appearing at a critical temperature T_c:

$$|\psi| = \begin{cases} 0 & (T > T_c) \\ |\psi_0| > 0 & (T < T_c) \end{cases} . \tag{2.1}$$

This behaviour emerges in seemingly unrelated and different materials, such as a ferromagnet in Fig 2.1(b), where electron spins in a lattice orders in some direction, or a superconductor, depicted in Fig 2.1(c), where electrons pair up in a state where magnetic fields are expelled from the material and have zero resistence. In both this cases, heating up will destroy both properties, see Fig 2.1(a).

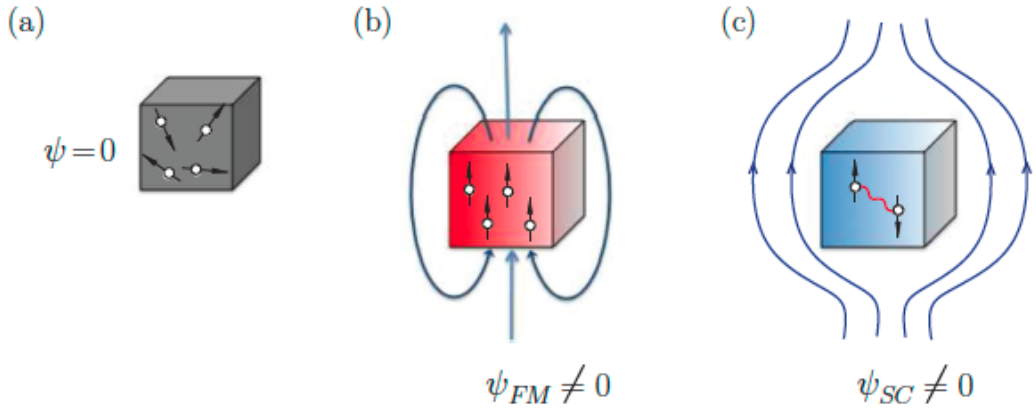

Figure 2.1: Three different examples of macroscopic phases described by order parameters, denoted ψ, ψ_{FM} and ψ_{SC}.(a): A "disordered phase", where the symmetries are preserved, and there is no order parameter; (b) A ferromagnet, where, for low temperatures, the response to magnetic fields as an aligned cluster of spins, which persists up to zero magnetic field ; (c) A superconductor, where the absence of electrical resistance is accompanied by an expulsion of magnetic fields from the material, known as the Meissner effect. Image from [1]

As a side observation, systems can generally be endowed with symmetries: say, for an electron gas, it does not matter if there is a translation is perfomed: in a (sufficiently big) uniform sample, translating each particle leaves the state invariant. Note, however, in the ferromagnet example, it is reasonable to have Heisenberg interactions, where if one rotates both vectors involved a dot product, the answer do not change. However, in a ferromagnet, all spins are pointing in the same direction! This means that this supposed rotational symmetry is broken. This is the intuition of an order parameter: It is a observable which somewhat "feels" the symmetries of a system, which, despite being insignificant at high temperatures, at low temperatures its non-zero values indicates that some symmetry has been broken.

The mathematical definition is as follows. We will focus on vector-like order parameters. Consider a symmetry group G, under which the hamiltonian is invariant. If some d-dimensional phase p breaks the symmetry into a subgroup $G_p \subset G$, we say that there exists an order parameter $\psi : \mathbb{R}^d \to \mathcal{V}$, where $\mathcal{V}$ carries a representation of G, that is:

$$\forall g \in G \quad ; \quad \psi(\mathbf{x}) \xrightarrow{g} \Pi(g) \cdot \psi(\mathbf{x}) \ , \tag{2.2}$$

where $\Pi(g)$ is a linear transformation, and $\cdot$ acts as a matrix-vector multiplication. In the phase p, the order parameter will be locked in some particular configuration: $\langle\psi\rangle = \psi_p(\mathbf{x})$. G_p can be read as the set of transformations leaving ψ_p invariant.

In the classical isotropic ferromagnet, the symmetry group is $G = O(3)$, the group of three-dimensional rotations along with reflections. Ferromagnetism is described by pinning the order parameter in a uniform vector field in some direction $\langle\psi\rangle \sim \mathbf{n}$. Rotations around $\mathbf{n}$ are not broken by this state, concluding that $G_{p=FM} = SO(2)$, the group describing rotations in two dimensions.

Energetics must be given by the microscopic system. That is, ψ must be understood as a "coarse-grained" collective variable, which somehow (1) accounts for the fact that this must be a physical observable, responding to external fields; (2) satisfies thermodynamic constraints. Let us define the order parameter in the lattice scale. If the system is described by a quantum-mechanical hamiltonian H on a lattice, the partition function is given as:

$$Z = \mathrm{Tr}[e^{-\beta H}] \ . \tag{2.3}$$

In principle, if one would have access to all the eigenstates of the hamiltonian, all the thermodynamic properties can be worked out and there would be no need for anything else. However, as already commented in the introduction, this is generally impossible, and some other description is necessary. We will start assuming the existence of an order parameter, and derive the consequences if energetics are governed by such. The order parameter must have a lattice implementation on each site, Ψ_i, which is a (vector) linear operator and acquires a non-zero expectation value. Consider also an external *conjugate field* $h \in \mathcal{V}$ such that $h \cdot \Psi_i$ is a linear operator. We then couple a "response term" to the hamiltonian:

$$Z \to Z[h] = \mathrm{Tr}\left\{\exp\left[-\beta\left(H - h\cdot\sum_i \Psi_i\right)\right]\right\} \ . \tag{2.4}$$

A Gibbs energy functional can be obtained by computing $\mathcal{G}[h] = -\ln Z[h]/\beta$. The expectation value of an *induced* order parameter is:

$$\psi(\mathbf{x}=\mathbf{r}_j; h, N) = \langle\Psi_j\rangle = \frac{1}{Z[h]}\mathrm{Tr}\left\{\Psi_j \exp\left[-\beta\left(H - h\cdot\sum_i \Psi_i\right)\right]\right\} = -\frac{1}{N}\frac{\partial\mathcal{G}}{\partial h} \ , \tag{2.5}$$

generally, for any $h > 0$, this order parameter must be non-zero, since this source term explicitly breaks the symmetry. In order to study true spontaneous symmetry breaking, one must take the thermodynamic limit and then turn off the external field, thus giving a definition of the order parameter:

$$\psi(\mathbf{x}) = \lim_{h\to 0}\lim_{N\to\infty}\psi(\mathbf{x}; h, N) \ . \tag{2.6}$$

However, it is not clear how to compute it. By inspection of eq. (2.5), this definition is only useful with the full information of the spectrum of the hamiltonian, which is exactly what we are trying to avoid. To proceed, consider the free energy functional known as *Landau function*, which is a Legendre transform of the Gibbs functional:

$$\mathcal{F}[\psi] = \mathcal{G}[h] + Nh\psi \ . \tag{2.7}$$

Noting that $h = N^{-1}\delta\mathcal{F}/\delta\psi$, for zero magnetic field, the dominant field configurations satisfy:

$$\frac{\delta\mathcal{F}[\psi]}{\delta\psi(\mathbf{x})} = 0 \ . \tag{2.8}$$

This can be understood as a functional equation. By minimizing the free energy, the solutions describes the behaviour of the order parameter. With this insight, symmetry can now be invoked: If G is a symmetry, one must consider only G-invariant functionals:

$$\mathcal{F}[\psi] = \mathcal{F}[\Pi(g) \cdot \psi] \ . \tag{2.9}$$

Of course, there is an infinite number of solutions for the above equation. The first approximation, known as the Landau expansion, is to consider both uniform configurations $\psi(x) = \psi_0$, and Taylor-expand $\mathcal{F}$ for small $|\psi_0|$, hoping to capture the essential physics. The first non-trivial example is $G = \mathbb{Z}_2$, acting on a real order parameter by flipping a sign $\psi \xrightarrow{\mathbb{Z}_2} -\psi$. The Landau expansion is given as:

$$f(\psi_0) \equiv \frac{1}{N}\mathcal{F}[\psi(\mathbf{x}) = \psi_0] = \frac{r}{2}\psi_0^2 + \frac{u}{4}\psi_0^4 + \cdots \ , \tag{2.10}$$

where the constant $\mathcal{O}(\psi_0^0)$ term was dropped. Truncating at fourth order, the minima may be analyzed as a function of the phenomenological parameters (r, u). For $u < 0$, there is a thermodynamical instability, corresponding to unphysical $\psi \to \pm\infty$ solutions. For $r > 0, u > 0$, the minimum is $\psi = 0$. This is a disordered phase, where the symmetry is preserved. For $r < 0, u > 0$, there are two minima, located at $\psi_0^{\pm} = \pm\sqrt{-r/u}$: an ordered symmetry-breaking phase. Indeed, both minima are connected by the symmetry, and this describes a continuous (since the minima disappear smoothly) ordered-disordered transition for $r \to 0^{\pm}$. This is also known as a second-order phase transition, since the second order derivative of the free energy has a discontinuity in this limit.

Symmetry rules it all: by only assuming that the order parameter can be written (locally) microscopically, the above computation predicts that all $\mathbb{Z}_2$-invariant systems must have this transition at $r = 0$, which may correspond to a condition involving only the microscopic parameters of the hamiltonian and the temperature. Case in point, Landau was interested in finite-temperature classical transitions, where r, measuring the distance to the critical point, can be understood as a temperature scale:

$$r \equiv a(T - T_c) \ , \tag{2.11}$$

the free energy profile is shown as a function of temperature in Fig 2.2(a). The easiest example occurs in the classical Ising model $H = -J\sum_{\langle i,j\rangle}\sigma_i\sigma_j$ at finite temperature, where the order parameter is the local magnetization σ_i, and the relevant symmetry is spin inversion $P : \sigma_i \to -\sigma_i$. At high temperatures, spins are pointing in random

directions, averaging out to zero: $\langle \sigma_i \rangle = 0$. Cooling the system, suddenly a magnet emerges below the critical temperature, breaking P spontaneously.

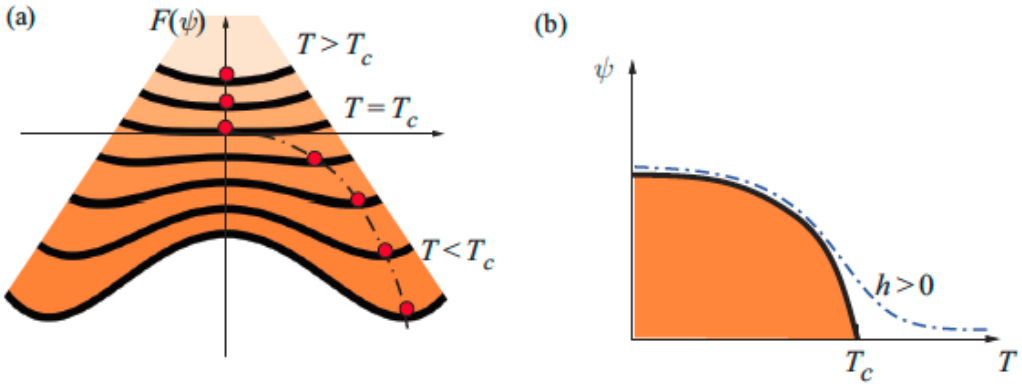

Figure 2.2: Landau theory of $\mathbb{Z}_2$ ordered-disordered transitions. (a) The free energy profile as a function of temperature. For $T > T_c$, the system is at the $\psi_0 = 0$ minimum. By cooling off the system, the symmetry is spontaneously broken, and one of the two ordered minima is chosen as the macroscopic state; (b) The order parameter as a function of temperature. For zero magnetic field, it is not a differentiable function at $T = T_c$. If an external field is applied, say, favoring ψ^+, the ordered and disordered phases are "mixed" together, since the order parameter vanishes smoothly. Image from [1].

A comment is warranted in the case of quantum phases, where $T \to 0$. Entropic fluctuations disappear and the free energy is now an energy density $f(\psi_0) \sim \varepsilon(\psi_0)$, otherwise, one has the same analysis. The transition is now driven due to some parameter(s) in the hamiltonian $H = H(\lambda)$ reaching a critical value, and the r parameter is introduced as $r \sim \lambda - \lambda_c$. Indeed, the above Landau expansion is a good first approximation to the transition of the transverse field Ising model in eq. (1.2) [18]. The physics of quantum phase transitions will be further explored in the next section.

Let us add back the source field as a physical probe field. The additional term in the free energy is $\delta f(\psi_0) = h\psi_0$. Notice that the symmetry is now explicitly broken, and there is an energy difference between ψ_0^+ and ψ_0^-. It means that, at low temperatures, by smoothly varying the field from negative to positive values, the order parameter will jump discontinuously from ψ_0^+ to ψ_0^-. This is a first-order phase transition, and is somewhat featureless: there is no symmetry left to distinguish between the polarized phase and the disordered phase, See Fig 2.2(b).

The Landau expansion has some glaring problems on its assumptions. In eq. (2.10), the supposed thermodynamic instability for $u < 0$ is actually cured if one would add the $\mathcal{O}(\psi_0^6)$ term. In this case, the free energy develops three minima, and

the transition becomes of first order, similar to the effect of an external field. This illustrates a larger issue: After truncation, there is no guarantee that higher order terms can affect the structure of the phase diagram in the Landau expansion. This is due of its phenomenological nature: The order is truncated when the corresponding physics matches experiment/the model in question.

A second problem are at excitations: In the macroscopic regime, non-uniform configurations of the order parameter can occur, and those can both be probed in experiments and play an important role in the phase transitions. Examples include domain walls in magnetic systems, and vortices in superconductors, which was the aspiration of Vitaly Ginzburg and Lev Landau to extend the uniform expansion to add spatial fluctuations of the order parameter [42]. In the $\mathbb{Z}_2$ example, one promotes eq. (2.10) to:

$$\mathcal{F}[\psi(\mathbf{x})] = \int_{\mathrm{R}^d} \mathrm{d}^d\mathrm{x} \left[\frac{v}{2}(\nabla\psi)^2 + \frac{r}{2}\psi^2 + \frac{u}{4}\psi^4 + \cdots\right] , \tag{2.12}$$

where there is a new "kinetic term" which weighs fluctuations of the order parameter. In $\cdots$, there are terms that also involve higher order gradients and fields, such as $\mathcal{O}(\nabla^2\psi^2)$, along with the terms previously discarded in the uniform expansion. The r and u terms now act as an energy potential for the order parameter, which we will call $V(\psi)$. This becomes a (classical) field theory problem [43] : By interpreting $\mathcal{F}$ as an action, the corresponding minima must satisfy some differential equation. By computing directly eq. (2.8):

$$(-v\nabla^2 + r + u\psi^2 + \cdots)\psi = 0 . \tag{2.13}$$

To solve this equation, it is necessary to provide the order parameter at the boundary, that is, $\psi(|\mathbf{x}| \to \infty)$. Since $\mathcal{F}[\psi(\mathbf{x})] \geq V(\psi_0)$, note that the minima of the potential still corresponds to the uniform configurations. For simplicity and later interest, consider $d = 1$. In the ordered phase, for $r < 0$, we can study solutions with "twisted" boundary conditions:

$$\psi_0(x = -\infty) = \psi_0^- \quad ; \quad \psi_0(x = \infty) = \psi_0^+ . \tag{2.14}$$

The solution, shown schematically in Fig 2.3, is known as a soliton:

$$\psi_{\mathrm{dw}}(x) = \sqrt{-\frac{r}{u}} \tanh\left(\frac{x - x_0}{\xi}\right) , \tag{2.15}$$

where x_0 is the position of the domain wall and $\xi = \sqrt{-v/r}$ is the correlation length, which measures how broad the overlapping region is, and therefore, the size of the domain wall. They cost a finite energy $\Delta_{\mathrm{dw}} \sim \xi^{-1}$. In a lattice model, ψ_{dw} corresponds to domain wall excitations in one-dimensional $\mathbb{Z}_2$-breaking phases. Indeed, this is the case for the transverse field Ising chain, for example [18]. In some sense, this is a counterintuitive result, since configurations which stay in the same vacuum, for example $\psi(x \to \pm\infty) = \psi_0^+$ costs twice the energy, since it is necessary to create a soliton and an "anti-soliton"- a soliton with the boundary conditions in eq.(2.14) reversed- pair. Upon quantization, domain walls give us interesting relations between boson and fermion fields in one dimension, discussed in the next chapter.

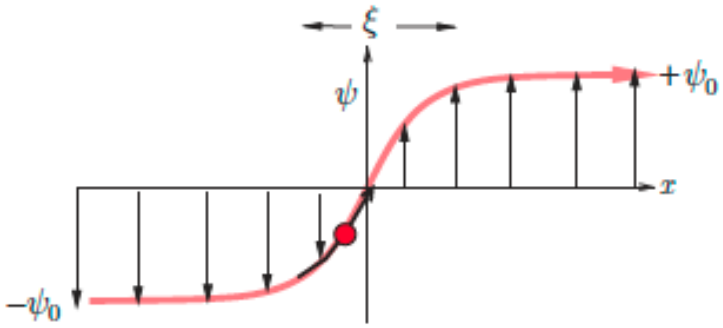

Figure 2.3: A soliton configuration tunneling between two different vacua in the ordered phase. ξ is the correlation length, identified as the length of a domain wall. Image from [1].

However, rarely one has both a single order parameter and just a single $\mathbb{Z}_2$ symmetry. In general, one can have multiple competing symmetry-breaking phases in a single system. Let us study the predictions for a two-component real order parameter $\psi = (\psi_1, \psi_2)$, transforming under a $G = (\mathbb{Z}_2)_1 \times (\mathbb{Z}_2)_2$ symmetry, where the subscripts indicate which component the symmetry acts, e.g.: $(\psi_1, \psi_2) \xrightarrow{(\mathbb{Z}_2)_1} (-\psi_1, \psi_2)$. The corresponding energy potential is given as:

$$V(\psi_1, \psi_2) = \frac{r_1}{2}\psi_1^2 + \frac{u_1}{4}\psi_1^4 + \frac{r_2}{2}\psi_2^2 + \frac{u_2}{4}\psi_2^4 + \frac{v}{4}\psi_1^2\psi_2^2 + \cdots , \tag{2.16}$$

a phase diagram is again computed by minimizing V. The calculation is similar to

the simple $\mathbb{Z}_2$ case, although more involved and not particularly illuminating [40]. Here we will state the results. Four phases are found: a disordered phase with $(\psi_1 = 0, \psi_2 = 0)$, two individually-ordered phases with $(\psi_1 \neq 0, \psi_2 = 0)$ and $(\psi_1 = 0, \psi_2 \neq 0)$ (which we will call phase 1 and 2, respectively), and a mixed phase $(\psi_1 \neq 0, \psi_2 \neq 0)$. In the 5-dimensional phase diagram (cutting out thermodynamic unstable regions), our interest lies in what happens between the phases 1 and 2: For the ordered-disordered transitions, there is a continuous phase transition, as already discussed.

Two situations can generally occur, as illustrated in Fig 2.4(a): It may have a first order transition between the two phases, or both are separated by the mixed phase. Continuous phase transitions are fine-tuned ! One must tune the parameters to kill off the mixed phase between ordered phases, see Fig 2.4(b). This is not the case for the ordered-disordered transition, where the smooth vanishing of an order parameter is generic.

The intuition behind this result comes from a higher-dimensional generalization of the picture of a second-order phase transition in Fig 2.2(a): Let us start from some point in the phase diagram where the minima of the free energy corresponds to the phase 1 pair. To have a continuous phase transition, one must pick a path in the parameter space where both minima fuse exactly in $(\psi_1 = 0, \psi_2 = 0)$. On general grounds, this must also correspond to a point in the phase diagram. Indeed, there are tricritical points, connecting the mixed and both phases 1/2, of continuous character.

Thus, in order to have robust second-order phase transitions between ordered phases, it is necessary to have some sort of protection not captured in this analysis. Otherwise, the transition just becomes of first order. However, there is a notable exception: Consider two symmetry-breaking phases 1 and 2 preserving $G_{p,1}, G_{p,2} \subset G$, respectively. If $G_1 \lhd G_2$, that is, one group is a *normal subgroup*[1] of the other, a continuous phase transition is allowed: Starting in the phase 2, one can write a G_2-invariant free energy functional. One can then understand the phase transition from phase 2 to phase 1 as an order-disorder transition, where the symmetry breaking pattern $G_2 \to G_1$ appears as classical vacua in this free energy. Examples will be presented in the fifth chapter.

[1] A normal subgroup is a subgroup where its elements are invariant under the adjoint action of the full group [44]

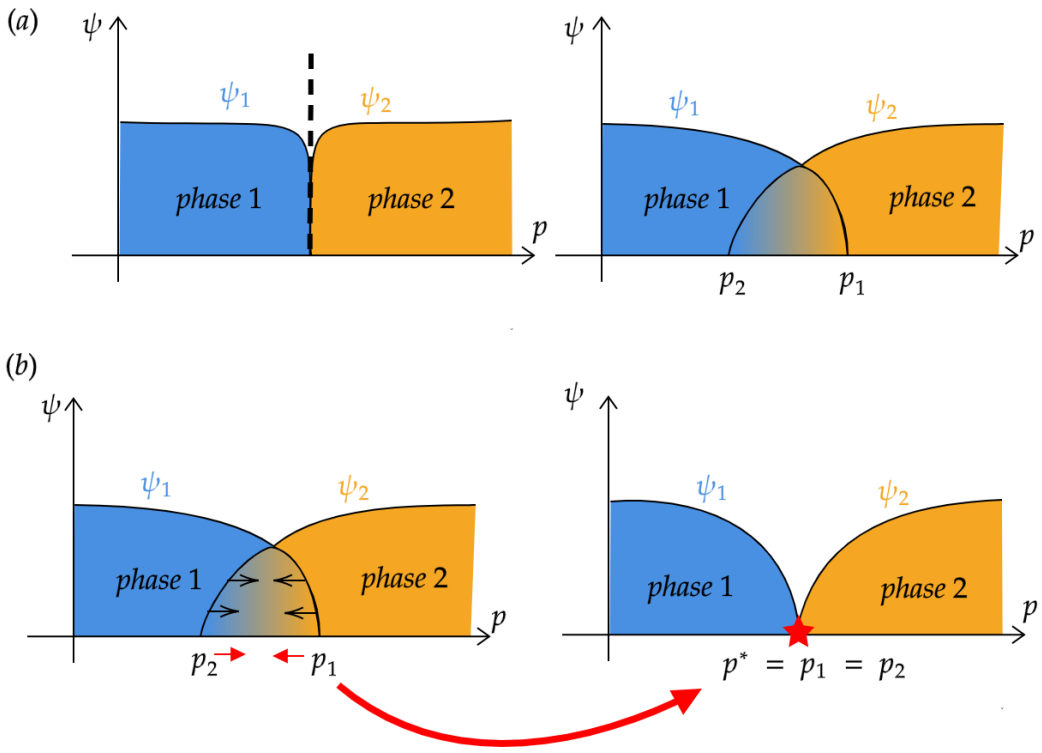

Figure 2.4: A one-dimensional cut in direction p of the phase diagram obtained by minizing eq.(2.16). (a): The two expected scenarios for an ordered-ordered phase transition. In the left, a first order transition occurs, where the minima of the free energy is changed abruptly. In the right, a second scenario where there is an intermediate region where both phases coexist. p_1, p_2 are some values of the parameters where the order parameter of each phase vanishes; (b) To get a proper continuous phase transition, one must fine-tune $p_1 = p_2 = p^*$.

However, the above framework treats continuous phase transitions and first-order phase transitions in the same physical ground: Even if there is a thermodynamic distinction, what actually happens to the degrees of freedom in the system in both cases, for example, such as the domain wall excitations in the transition? Classical field configurations do not capture such fluctuations correctly. We will tackle such questions in the next section.

2.2 The renormalization group and the Landau-Ginzburg-Wilson paradigm

So far, we have been ignoring the question of observables beyond the order parameter. One might ask about thermodynamics, which shows signs of the interesting

properties of second-order phase transitions [1]. Since our interest lies in quantum phases, a different approach will be taken, probing another class of observables: correlation functions.

Since the classical case is a limit of the quantum case, let us consider again a microscopic system on the lattice and an operator A_i defined on the lattice site $\mathbf{r}_i$. The corresponding correlation function is given as:

$$G(\mathbf{r}_i, \mathbf{r}_j) \equiv \langle A_i A_j \rangle \ . \tag{2.17}$$

The average $\langle \cdots \rangle$ can be taken on a ground or thermal state. This object measures how correlated different degrees of freedom are as the distance is changed. In ground states, a quite general result is avaliable due to Hastings and Koma [45,46]: Let ΔE be the energy difference between a ground state and the rest of the spectrum in the thermodynamic limit, known as the energy gap. The result is the presence of exponential decay of correlations:

$$G(\mathbf{r}_i, \mathbf{r}_j) \xrightarrow[|\mathbf{r}_i - \mathbf{r}_j| \to \infty]{} \text{const.} \times \exp\left(-\frac{|\mathbf{r}_i - \mathbf{r}_j|}{\xi} \right) \ , \tag{2.18}$$

where ξ is also known as the correlation length. Intuitively, this corresponds to disordered states, since there is no degeneracy. Otherwise, for ordered states, by letting $\mathcal{A}_i = \Psi_i$ be the order parameter, the correlation factorizes at long distances:

$$G(\mathbf{r}_i, \mathbf{r}_j) \xrightarrow[|\mathbf{r}_i - \mathbf{r}_j| \to \infty]{} \langle \Psi_i \rangle \langle \Psi_j \rangle + \text{const.} \times \exp\left(-\frac{|\mathbf{r}_i - \mathbf{r}_j|}{\xi} \right) \ , \tag{2.19}$$

which saturates to a constant at very long distances due to the first term. We have already encountered the correlation length in the analysis of excitations of ordered phases. One can then interpret that eqs. (2.18),(2.19) are the result of *fluctuations*: Even if the average is taken in the ground state, this exponential decay occurs due to the creation of finite energy cost "particles", such as the previously studied domain walls, or localized excitations in the disordered phase. Exactly due to this finite cost, they have a finite length. Those are *gapped* excitations.

A few remarks on terminology: In quantum phase transitions, the main observable is the energy gap from the ground state: If excited states above the ground

state costs finite energy (in the thermodynamic limit), we say that the corresponding phase is *gapped*. Otherwise, the system is *gapless*: Excitations can be created to a continuum of states, without energy cost. This is a very important distinction because there are a plethora of rigorous arguments for the stability of gapped phases [47], mainly around the adiabatic principle: For a gapped ground state, one can generally change the parameters of the Hamiltonian "slowly" without creating excitations, and therefore leaving the state invariant. In the gapless case, perturbations can generate excitations arbitrarily, and it is quite hard to prove stability on general grounds. A continuous quantum phase transition between two gapped phases, generally can be understood by the process of "condensation": The excitations of the ordered phase become gapless at the transition.

For zero temperature, the LG functional can be understood as an energy density. Consider a quantum hamiltonian $H = H(\lambda)$, where λ represents the microscopic parameters. In second-order phase transitions, the energy gap scales as:

$$\Delta E \sim |\lambda - \lambda_c|^{-\nu} \,, \tag{2.20}$$

where ν is known as a critical exponent, and λ_c parametrizes the critical region. For the $\mathbb{Z}_2$ example, $\Delta E \sim |r|^{-\nu}$. In fact, one can associate a correlation length ξ by introducing a dynamical exponent $z > 0$, such that $\Delta E \sim \xi^{-z}$. This means a diverging correlation length at the transition. This is a striking feature: We say that the *gapless* excitations of a continuous phase transitions have slow decay of correlations. Indeed this can be encoded in a *emergent symmetry* which is present only at the transition, which is one of scaling, written at the continuum as $D : \mathbf{x} \to \mathbf{x}/b$. Under this operation, eq. (2.19) is only invariant if the correlation length is transformed in the same way. In fact, scaling invariant systems, in general, are described by slow-decaying power law correlations $G \sim |\mathbf{r}_i - \mathbf{r}_j|^{-\delta}$, where δ is an exponent determined by the operators whose correlations are measured, as will be explained later.

Such features shine light on the incompleteness of the LG functional. It needs to be accompained by fluctuations of the order parameter. We can associate Boltzmann weights to each field configuration as $\exp(-\mathcal{F}[\psi])$, and sum over all field configurations as any statistical mechanics problem. This is known as a path integral, and a partition function can be formally defined:

$$\mathcal{Z} \equiv \int D\phi \ \exp(-\mathcal{S}[\phi]) \ , \tag{2.21}$$

where $\mathcal{S}[\phi]$ is the action, which is classically the same as the LG functional. This measure integrates over field values in all points in space $D\phi \propto \prod_{\mathbf{x}} d\phi(\mathbf{x})$. Until now, there is no clear connection between the lattice degrees of freedom and the LG construction in terms of continuum fields, beyond the symmetry group. In fact, the order parameter viewpoint has some "coarse-graining" attached to it, that is, physically it can be understood as the average of the lattice order parameter in some region. For example, for the classical Ising case:

$$\phi(\mathbf{x}) \sim \sum_{j \in M_{\mathbf{x}}} \langle \sigma_j \rangle \ , \tag{2.22}$$

that is, the field represents a magnetization average around some region in the lattice $M_{\mathbf{x}}$ near $\mathbf{x}$. This is an actual starting point for the original Landau theory from the microscopic hamiltonian H, where the interactions are decomposed in terms of the fields. (The pure Landau theory is also known as mean-field theory). This indicates that, if the lattice is d_L-dimensional, $d_L = d$, the dimension of the action. This is indeed what happens in classical systems. In quantum systems, fluctuations do generate an effective extra dimension, and so $d = d_L + 1$. This is due to the fact that, in classical statistical mechanics, the field action in the Boltzmann weight corresponds to the hamiltonian. However, in the quantum system, the microscopic partition function in eq.(2.3) must be computed on a basis, and because states are constructed from a non-commuting algebra, it is necessary to consider the action from the Legendre transform of the hamiltonian, which adds an extra dimension. The simplest case is for a quantum particle and is worked out in detail in [48]. For a hamiltonian which has a clear continuum limit, $H = \int \mathrm{d}^{d_L}\mathrm{x} \ \mathcal{H}$, where $\mathcal{H}$ is the corresponding hamiltonian density, one can compute the partition function written in eq. (2.3):

$$Z = \mathrm{Tr}[e^{-\beta H}] = \sum_i \langle i| \exp(-\beta H)|i\rangle = \int_{\mathrm{PBC}} \mathcal{D}[\mathrm{d.o.f}] \ \exp\left(-\mathcal{S}[\mathrm{d.o.f}]\right) \ , \tag{2.23}$$

reduced to eq. (2.21) from scalar fields. We now have an "euclidean action" of the type $\mathcal{S} = \int \mathrm{d}\tau \mathrm{d}^{d_L}\mathrm{x}(\cdots)$,where we have defined $\tau = it$, dubbed imaginary time.

We refer to $(\tau, \mathbf{x})$ as a point of "spacetime". A subtle detail is that only periodic boundary conditions are considered in imaginary time. Locally in the lagrangian, this imaginary time direction can just be incorporated as another coordinate. However, for "global" considerations, such periodic boundary conditions can have non-trivial effects. Note that this result indeed reduces to the form of eq. (2.21), with $d = d_L + 1$. This is also sometimes called the *quantum-classical* correspondence, where a quantum-mechanical partition function is written as a statistical average of a classical action. Specifically in the field theory context, this is referred to as statistical field theory or (euclidean) quantum field theory. Correlation functions are now defined in this formalism as:

$$G(\mathbf{x}, \mathbf{y}) = \langle \mathcal{O}(\mathbf{x}) \mathcal{O}(\mathbf{y}) \rangle = \frac{1}{\mathcal{Z}} \int D\phi \, O(\mathbf{x}) \mathcal{O}(\mathbf{y}) \exp(-\mathcal{S}[\phi]) \, , \tag{2.24}$$

as any statistical mechanics problem. Given some action, computing field theory observables is something of an art in theoretical physics, and is well-developed in many references [1,3,10,41,49,50]. We will be brief and focus on the physical insights of statistical/quantum field theory related to the renormalization group.

The quoted results on correlation functions reveal a deeper connection between length and energy scales. As discussed, the physics of quantum phases is the physics of ground states and the corresponding low-energy excitations. In a lattice, there is a minimum length scale, a, which is the distance between lattice sites. The idea is that all the relevant properties of a macroscopic phase must be encoded in long distance correlations, in distances way larger than a lattice scale. Henceforth, low energies corresponds to long distances (and high energies, with short distances). In a partition function defined on the lattice, one can then only consider states which, as one "zooms out", become significant. This procedure is known as the *renormalization group* (RG).

Let us revisit our $\mathbb{Z}_2$ example. It is useful to isolate the kinetic and potential part of eq.(2.12), by using the action notation:

$$\mathcal{S} = \mathcal{S}_0 + \mathcal{S}_\mathrm{V} \ , \tag{2.25}$$

$$\mathcal{S}_0 = \int_{\mathrm{R}^d} \mathrm{d}^d\mathrm{x} \ \frac{1}{2}(\nabla\phi)^2 \ , \tag{2.26}$$

$$\mathcal{S}_V = \int_{\mathrm{R}^d} \mathrm{d}^d\mathrm{x} \left[\frac{r}{2}\phi^2 + \frac{u}{4}\phi^4 + \cdots\right] \ , \tag{2.27}$$

where we have redefined the parameters such that $v = 1$. Note that the pure kinetic term action $\mathcal{S}_0$ is invariant under D, if the field is redefined as:

$$\phi \xrightarrow{D} \phi' = b^{(D-2)/2}\phi; \, , \tag{2.28}$$

which is a physical transformation: By eq.(2.21), the action must be dimensionless. Therefore, due to eq.(2.26), the field must have dimensions $[\phi] = (\text{length})^{-(D-2)/2}$, explaining the above transformation law under scaling. Therefore, if $\mathcal{S}_V$ is ignored, we are sitting in a critical point! This is known as the *Gaussian fixed point*. The correlation function of two fields can be computed for long distances under this action, giving a power law behaviour:

$$\langle\phi(\mathbf{x})\phi(\mathbf{y})\rangle_{\text{Gaussian}} \sim \frac{1}{|\mathbf{x}-\mathbf{y}|^{d-2}} \ , \tag{2.29}$$

which can be understood as the proper $\xi/a \to \infty$ limit of correlation functions, while manifesting scale invariance. Due to the absence of scales in the critical point, note that correlations only depend on the dimension present in the exponent. We say that the terms in $\mathcal{S}_V$ are "dimensionful", due to the nontrivial field dimensions. To study how such terms behave at long distances, we will study the properties of the Gaussian theory and study the other terms as proper perturbations. $\mathcal{S}_0$ also has three additional symmetries:

- Translations: $T : \mathbf{x} \to \mathbf{x} + \mathbf{a}$;
- Rotations: $SO(d) : \mathbf{x} \to R \cdot \mathbf{x}$ such that $\det R = 1$;
- Special conformal transformations, whose action is rather involved and not very important to our present discussion;

Those three symmetries combined generate the *conformal group* in d-dimensions, and field theories with this symmetry are known as conformal field theories (CFTs)[2]. This is also a huge topic on its own right [17], and we will only go through the results which are needed in our further analysis in the next chapters. Reason being, the symmetry group is so large that it constrains much of the physics, and a lot of results can be proven, a rare case in quantum field theory overall. Field theory, as defined, is the study of fluctuating fields given some classical action. One can then ask about observables. Well, we can allow anything of the form $\langle f(\phi)\rangle$. It turns out that, in CFTs, one can classify what is known as the "operators" of the theory (referring to the canonical form of field quantization, opposed to the path integrals studied here) by just analyzing how they transform under the conformal group. In practice, this generally means a (infinite) list of fields (or a simple function thereof), defined on a point of spacetime such as $\{\phi, \phi^2, \phi^3\nabla\phi, \cdots\}$.

Let $\{\mathcal{O}_i(\mathbf{x})\}$ be the set of operators of a theory (the index i here denotes some ordering in this set, there is no connection to a lattice), and consider the two-point correlation functions $G_{ij}(\mathbf{x},\mathbf{y}) \equiv \langle \mathcal{O}_i(\mathbf{x})\mathcal{O}_j(\mathbf{y})\rangle$. Invariance under translations imposes $G_{ij}(\mathbf{x},\mathbf{y}) \to G_{ij}(\mathbf{x}-\mathbf{y})$, and rotations imposes $G_{ij}(\mathbf{x}-\mathbf{y}) \to G_{ij}(|\mathbf{x}-\mathbf{y}|)$. Scale invariance, as discussed, acts both on field operators and space. Consistency under D requires [3]:

$$\mathcal{O}_i \xrightarrow{D} \mathcal{O}'_i = b^{\Delta_i}\mathcal{O}_i \ , \tag{2.30}$$

as the field ϕ in our previous example. $\Delta_i \in \mathbb{R}$ is known as the scaling dimension of the operator $\mathcal{O}_i$. Therefore, since:

$$G_{ij}(|\mathbf{x}-\mathbf{y}|) = \langle \mathcal{O}_i(\mathbf{x})\mathcal{O}_j(\mathbf{y})\rangle \xrightarrow{D} G_{ij}(|\mathbf{x}/b-\mathbf{y}/b|) = b^{\Delta_i+\Delta_j}G_{ij}(|\mathbf{x}-\mathbf{y}|) \ , \tag{2.31}$$

G_{ij} is a homogeneous function of degree $-\Delta_i-\Delta_j$. Due to Euler's theorem, the solution must follow a power law:

[2] Obligatory remark: Not all RG fixed points are CFTs (but scale and rotational invariance implies conformal invariance under local interactions [51]). However, there are a lot of examples where this is indeed the case, and certainly all treated on this thesis are.

[3] Mathematically, this action under D implies that $\mathcal{O}_i$ transforms irreducibly under dilatations [17, 41]

$$G_{ij}(|\mathbf{x}-\mathbf{y}|) \sim \frac{1}{|\mathbf{x}-\mathbf{y}|^{\Delta_i+\Delta_j}} , \tag{2.32}$$

agreeing with the result computed for the gaussian theory for $d > 4$ in eq.(2.29), for $\Delta_i = \Delta_j = (d-2)/2$. This is the slow decay of the correlations of continuous phase transitions, and it can be probed on the lattice, by evaluating correlations of well-separated operators. Consider now multi-point correlation functions of the form $\langle \mathcal{O}_i(\mathbf{x}_i)\, \mathcal{O}_j(\mathbf{x}_j)\, \Phi(\mathbf{x}_1, \cdots, \mathbf{x}_n)\rangle$ in the situation depicted in Fig. 2.5: the first two operators are near each other far away from the operators defined at Φ. At long distances, operators at $\mathbf{x}_1, \mathbf{x}_2, \cdots$ "see" the effects of $\mathcal{O}_i$ and $\mathcal{O}_j$ at the midpoint. This means that, under correlation functions one can expand the product $\mathcal{O}_i\mathcal{O}_j$ in the set of scaling operators of the CFT evaluated at the midpoint:

$$\mathcal{O}_i(\mathbf{x}_i) \cdot \mathcal{O}_j(\mathbf{x}_j) \sim \sum_k \frac{c_{ijk}}{|\mathbf{x}_i - \mathbf{x}_j|^{\Delta_i+\Delta_j-\Delta_k}} \mathcal{O}_k\left(\frac{\mathbf{x}_i + \mathbf{x}_j}{2}\right) . \tag{2.33}$$

This is known as the *operator product expansion* (OPE), and describes the leading singularities which describe the theory. The power-law exponent is fixed by conformal symmetry, balancing the mismatch of scaling dimensions for each term. Constants c_{ijk} are called structure constants, and encode how the operators are generated in correlation functions.

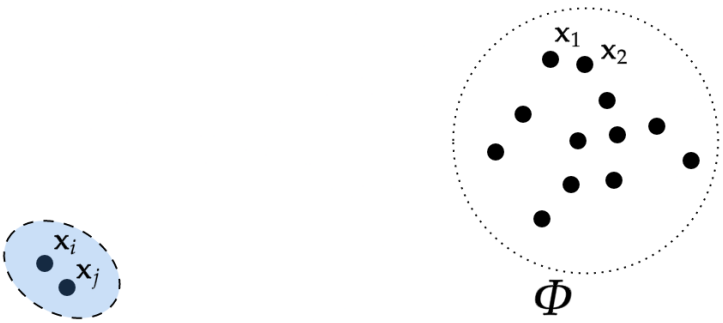

Figure 2.5: Pictorial representation of the operator product expansion: Operators defined on Φ are far away from the $\mathbf{x}_i$ and $\mathbf{x}_j$ points. As both points get closer together, correlations between those points with Φ may well be described by single operators defined in $\mathbf{x}_k$ near both points. Adapted from [2].

We are now ready to state the main principle behind the renormalization group. Consider perturbing any conformally invariant action with a subset of scaling operators:

$$\mathcal{S} = \mathcal{S}_0 + \sum_{j \in S} g_j \int \mathrm{d}^d \mathrm{x}\ \mathcal{O}_j(\mathbf{x}) \ , \tag{2.34}$$

If one starts with a field theory described by couplings $\{g_j\}$ and a partition function $\mathcal{Z}(g)$, after a scaling transformation we impose the invariance of the theory by redefining the coupling

$$\mathcal{Z} \xrightarrow{D} \mathcal{Z}'(g'(b)) = \mathcal{Z}(g) \ . \tag{2.35}$$

Note that the new couplings depend on the scale on which the physics is now probed. For an infinitesimal scale transformation, define $b = e^{d\ell} \simeq 1 + d\ell$, $g' \simeq g + dg/d\ell d\ell$. It can be shown that the renormalization group equations must be satisfied:

$$\frac{d\tilde{g}_k}{d\ell} \equiv \beta_{g_k}(g) = (\Delta_k - d)\tilde{g}_k - \frac{S_d}{2} \sum_{i,j \in S} c_{ijk} \tilde{g}_i \tilde{g}_j + \cdots \ . \tag{2.36}$$

where dimensionless variables are defined: $\tilde{g}_i = g_i a^{\Delta_i - d}$. S_d is is the surface area of the hypersphere in d dimensions. β_{g_k} is known as the *beta function* of g_k, and is responsible for the RG flow. The first order term could be derived only from dimensional grounds by studying how the perturbation scales under D. The second order term captures correlations from the OPE. In fact, the derivation above shows a perturbative nature in the construction of the couplings g. To go beyond $\sim g^2$ (also known as "one-loop" order), it is necessary to probe a next layer of singularities not captured by OPEs, and use techniques from quantum field-theoretic renormalization [49]. For our purposes, the RG equations at one loop already suffices.

Note that we have a "trivial" fixed point where $\beta_{g_i}(g = 0) = 0 \ , \ \forall g_i$: In our example, this is just the Gaussian fixed point. Now that we are acquainted with the general structure of the renormalization group, there are roughly three different destinies for some coupling g_i, given some initial condition at $\ell = 0$:

- $\beta_{g_i} > 0$: The coupling grows with the length scale, and is said to become *relevant*;

- $\beta_{g_i} = 0$: The coupling doesn't change with the length scale, denoted as *marginal*;
- $\beta_{g_i} < 0$: The coupling decreases with the length scale, and becomes *irrelevant*.

Generally, only marginal and relevant terms needs to be studied to understand the long-distance physics. Relevant terms are generally responsible for the gapped excitations and phases, and marginal terms renormalizes the operators defined on the fixed point. Irrelevant operators are "washed away" at long distances, and generally do not affect the physics. However, an exception sometimes occurs in symmetry-breaking phases, where new vacua are generated. In this case, the leading irrelevant operators may strongly influence the low energy states; known as *dangerously irrelevant operators*. This is the case for the $u\phi^4$ operator in eq. (2.27) [3].

Beyond gapped phases, the RG flow may reveal new fixed points, defined by $\beta_{g_i}(g^* \neq 0) = 0 \ , \ \forall g_i$. In this case, something interesting can happen: the phase transition may be described by a different fixed point than the initially perturbed one. It is said to have another *universality class*: Power law exponents of correlations, for example, may be different, since it is a different CFT.

For completeness, we will state the results found for the $\mathbb{Z}_2$ example. It is useful to define the parameter $\varepsilon = 4 - d$, and we will define $\lambda = 6u$. The general behaviour of the beta function of λ is shown in Fig 2.6(a). For $\varepsilon < 0$, the previous analysis holds even with the one-loop corrections: The transition between disordered and ordered phases is Gaussian. For $\varepsilon > 0$, there is a new, non-trivial fixed point, which appears at order ε. The phase diagram emerging from the RG flow is shown in Fig 2.6(b): There is a separatrix between the Gaussian and the non-trivial fixed point. The effects of fluctuations have non-trivial effects: For example, If $r_0 < 0$ but small, the theory flows to the disordered (paramagnet) phase, instead of the ordered (ferromagnet) phase predicted by the LG functional.

This new fixed point is known as the Wilson-Fisher (WF) fixed point, also named the Ising CFT. One can compute the thermodynamic exponents from a $\varepsilon \ll 1$ expansion, and compare to the results of numerical simulations of Ising models: There is amazing agreement even for $\varepsilon = 2$, well out of bounds of the convergence radius in the solution [3]. However, the physics at the transition and corresponding degrees of freedom is only well understood analytically for $d = 2$, explored in the next chapter.

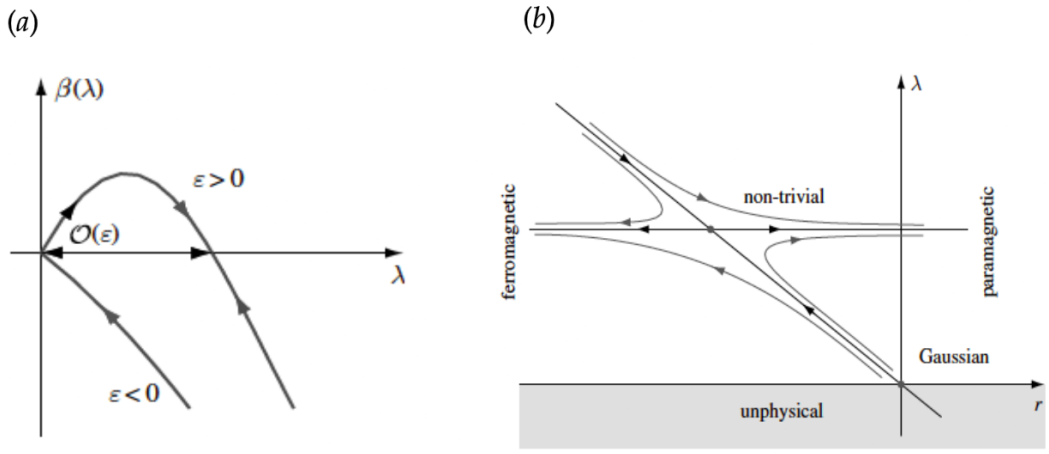

Figure 2.6: Infrared behaviour of the RG flow of $\mathbb{Z}_2$ action. (a): Beta function profile of the λ coupling: A new zero emerges as long that $d < 4$, or $\epsilon > 0$; (b) The RG flow solution for $d < 4$. The flow direction is pointed out in the lines: Starting from the Gaussian fixed point, one can see that it is in fact unstable, and the flow in the separatrix goes to the Wilson-Fisher fixed point. Any small perturbation of the relevant operator r will generate both ordered (ferromagnetic) and disordered (paramagnetic) phases. Images from [3].

On the $\mathbb{Z}_2 \times \mathbb{Z}_2$ example with the potential shown in eq. (2.16), a similar result occurs. If $v = 0$, the phase diagram would be just "two copies" of Fig 2.6(b), with two different WF fixed points. By taking $v \neq 0$, perturbatively, there is no expectation of new fixed points, only a change in the flow: Case in point, one can then flow from the phase 1 to the phase 2, without necessarily hitting the fixed points. This is a first order phase transition microscopically, but it is a process that holds no special place in the long distance physics.

The symmetry-respecting expansion of the action and corresponding renormalization group analysis around a gaussian fixed point is the theoretical trademark of the Landau-Ginzburg-Wilson paradigm. It is indeed very successful in classical models [9], and in the study of symmetry-breaking quantum phases [18]. However, in the latter, there is a class of transitions in which the local order parameter viewpoint breaks down, studied in the next and last section of this chapter.

2.3 Deconfined quantum criticality

We will be interested in quantum spin-1/2 models in two dimensions. We will show, by working a specific example, that it is indeed possible to have a continuous phase

transition between ordered phases. Furthermore, at the transition, the corresponding field theory is now described by any of the two order parameters, but by a new "deconfined" excitation defined only at the transition. We will also show that this behaviour is of a gauge theory, generally used in particle physics to describe interactions. Since we are in a dimension lower than our universe, the physics can change drastically even with the simple-looking Maxwell electrodynamics [4, 15].

Quantum spin models can be defined on any lattice by just stating that there is a spin-1/2 Pauli degree of freedom on each site i, $\boldsymbol{\sigma}_i = (\sigma_i^x, \sigma_i^y, \sigma_i^z)$, satisfying:

$$[\sigma_i^\alpha, \sigma_j^\beta] = i\delta_{ij}\epsilon^{\alpha\beta\gamma}\sigma_i^\gamma \ , \tag{2.37}$$

where the index γ is summed over. In particular, let us consider a hamiltonian with the following symmetries:

- Spin rotation symmetry $SO(3)$: Every spin is rotated globally in the fundamental representation: $\sigma_i^\alpha \to U^\dagger(R)\sigma_i^\alpha U(R) = R_\beta^\alpha \sigma_i^\beta$, given a rotation matrix R ;
- Translations T_x, T_y: Translation of unit length ($a = 1$) in the cartesian x and y directions, respectively: $\boldsymbol{\sigma}_i \xrightarrow{T_x} \boldsymbol{\sigma}_{\boldsymbol{i}+\hat{\boldsymbol{x}}}$,$\boldsymbol{\sigma}_i \xrightarrow{T_y} \boldsymbol{\sigma}_{\boldsymbol{i}+\hat{\boldsymbol{y}}}$;
- Lattice rotations $R_{\pi/2}$: $\pi/2$ rotations of the lattice sites;
- Time reversal: An anti-unitary symmetry whose action flips the sign of spin operators, $\boldsymbol{\sigma} \to -\boldsymbol{\sigma}$.

The lattice symmetries span the square lattice. It is useful to picture a hamiltonian with Heisenberg-like interactions:

$$H = J\sum_{\langle i,j\rangle} \boldsymbol{\sigma}_i \cdot \boldsymbol{\sigma}_j + \cdots \ , \tag{2.38}$$

where $\langle i, j\rangle$ indicates sum over nearest neighbours. We will limit ourselves to antiferromagnetic couplings, that is, $J > 0$. We will now suppose that there exists then a Néel phase, where the spins are ordered antiferromagnetically in some direction in space, as depicted in Fig.2.7.

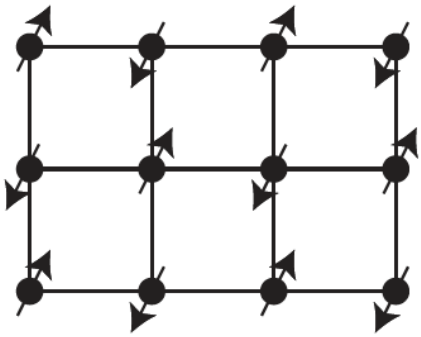

Figure 2.7: The Néel state in the square lattice. The spins are pointing in a staggered configuration defined by some direction $\mathbf{n}$, drawn pointing in the plane of the lattice for simplicity.

The order parameter is the staggered magnetization, defined as:

$$\langle \sigma_i \rangle = (-1)^{P(\mathbf{r}_i)} \mathbf{n} \ , \tag{2.39}$$

where $P(\mathbf{r}_i) = \pm 1$ is $+1$, -1 for even and odd sublattices, respectively.

There is a distinct continuous description of such ordered phases, which are not directly given by the LG functional, but in a similar sprit. For now, let us ignore the role of lattice symmetries. The relevant group is then $SU(2)$ with time reversal, both broken by the Néel state. There is a subgroup of the broken symmetry which is still present: rotations around $\mathbf{n}$ (as occuring in the ferromagnetic state), defined by $G_p = U(1)$. Then, one can understand the degeneracy by evaluating the coset $SU(2)/U(1) \simeq S^2$, that is, the number of configurations on the two sphere. A proposed (infrared) partition function is given as:

$$\mathcal{Z}_0 = \int_{\mathbf{n}^2=1} D\mathbf{n} \ \exp\left(-\mathcal{S}_0\right) = \int D\mathbf{n} \ \delta(\mathbf{n}^2 - 1) \exp\left(-\frac{1}{2g} \int \mathrm{d}^3\mathrm{x} \ (\nabla \mathbf{n})^2\right) \ , \tag{2.40}$$

where $\mathbf{n}$ is now promoted to a (vector) field which can fluctuate in space, constrained to have unit length, by summing configurations which satisfy the functional delta. This is known as the non-linear sigma model (NLσM) in the target manifold $\Sigma = S^2$. Note that, in some sense, eq. (2.40) is already a theory at long distances, describing the vector fluctuations of the macroscopically observed Néel state. As is commonly the case for non-linear sigma models, it comes from a high-energy theory, and indeed, for our case, it comes from a LGW scheme. The order parameter field

is $O(3)$-covariant, written as $\mathbf{\Phi}(\mathbf{x})$. Then, in the potential expansion written as $V(\mathbf{\Phi}) = r\mathbf{\Phi}^2 + u(\mathbf{\Phi}^2)^2 + \cdots$, the ordered state have minima at $\mathbf{\Phi}(\mathbf{x}) \sim |\Phi_0|\mathbf{n}(\mathbf{x})$, where $\mathbf{n}$ is a unit vector. By flowing in this limit and ignoring (safe) irrelevant terms, eq. (2.40) is obtained. However, note that this generally describes a ferromagnetic phase. The correct Néel vacua must involve two fields, such as $\mathcal{S}_{\text{LGW}}[\mathbf{\Phi}_1, \mathbf{\Phi}_2]$, in order to correctly describe both sublattices with minima $\mathbf{\Phi}_1 = -\mathbf{\Phi}_2 \sim |\Phi_0|\mathbf{n}(\mathbf{x})$. In this representation, lattice translation operators permute the sublattices 1 and 2. This means that the expectation of ignoring lattice symmetries in the continuum is short lived. However, in the end, this procedure leads to the same infrared NLσM. Is there a difference between antiferromagnetic and ferromagnetic excitations?

The surprising feature is that, in this model, there is a "hidden" symmetry-allowed term:

$$\mathcal{S}_B = \frac{i}{2}\sum_j (-1)^{P(\mathbf{r}_j)}\mathcal{A}(\mathbf{r}_j) = \frac{i}{2}\sum_j \int \mathrm{d}\tau\ (-1)^{P(\mathbf{r}_j)}\mathbf{A}(\mathbf{n})\cdot\partial_\tau \mathbf{n}(\mathbf{r}_j)\ . \tag{2.41}$$

This is known as the *Berry phase* term, and $\mathbf{A}$ is a vector field such that, for any closed path P on S^2, $\int_P \mathrm{d}\mathbf{n}\cdot\mathbf{A} = \Omega_P$, where Ω_P is the solid angle encircled by such orbit. $\mathbf{A}$ can be interpreted as a vector potential of a monopole on each lattice site. A naive continuum limit would not have this term in the action, since it oscillates on the lattice, and is linear on $\mathbf{n}$. To properly explain why this term is present, it is necessary to go through the proof of path integral quantization of quantum spins, which is nicely exposed in Auerbach's book [52].

For the overall properties of the Néel phase, this term indeed does not matter, but it plays an important role in a transition to a distinct symmetry-breaking phase: The Berry phase affect non-perturbative *instanton* effects [53, 54]. They occur in ordered phases, and represent the tunneling between different vacua. Manifested at the imaginary times, one may write a instanton configuration by considering a particular vacuum in $\tau \to -\infty$ to another vacuum in $\tau \to \infty$. Most of the time, the instanton itself can be represented as a particle, that is, a localized excitation sandwiched between the two low-energy backgrounds. They contribute to the path integral by summing over all distinct instanton configurations.

In the most simple example, consider a one-dimensional quantum mechanical particle in a double well, that is, a potential of the form $V(x) = ax^2 + bx^4$.

The symmetry is a $\mathbb{Z}_2$ symmetry, the spatial parity $P : x \to -x$. Indeed, in the imaginary-time path integral, this is equivalent to our Ising-like example, with $d = 1$, and $x = x(\tau)$ playing the role of the order parameter. We have already found such instanton configurations: They are the solitons/domain walls[4] studied in the last section. Summing over instantons give an "instanton gas" picture: Such configurations are equivalent to putting instanton/anti-instanton pairs on a circle, since imaginary time is periodic [3].

Note however, that they are "heavy" excitations: to tunnel between minima of the potential, there is an energy barrier between then. Therefore, deep in an ordered phase, it may be that the leading (lightest) excitations of the spectrum are around a fixed minima: We want to investigate the properties of the Néel phase and possible phase transitions if we consider the effects of instantons and Berry phases.

On the other hand, in classical magnets, there are configurations known as *skyrmions*. They are robust due to the presence of a topological invariant $Q \in \mathbb{Z}$, which counts the number of skyrmions, which can be written in terms of the Néel vector:

$$Q = \frac{1}{4\pi} \int \mathrm{d}^2\mathrm{x}\, \mathbf{n} \cdot (\partial_x \mathbf{n} \times \partial_y \mathbf{n}) \,. \tag{2.42}$$

This is known as the skyrmion charge, and is zero for uniform spin configurations. The quantization implies that it is impossible to destroy a skyrmion by smoothly varying $\mathbf{n}$[5]. An illustration of a $Q = +1$ skyrmion in the (x, y) plane is shown in Fig 2.8.

Such configurations may be included in the path integral. Since their origin comes from a topological current, classically conserved, indeed it reflects a topological $U(1)_T$ symmetry. However, they can also be manifested as instantons, tunneling between the classical vacua of the Néel phase. To see that, interpret Fig 2.8 as the (x, τ) plane in the horizontal and vertical directions, respectively (while maintaining y as a constant). Comparing the top and bottom part of the figure, corresponding to $\tau \to \pm\infty$, one can see that the spin directions are interchanged. Instantons itself are created adding non-local terms in the lagrangian in terms of "monopole

[4]Solitons is the name reserved for configurations which tunnel in different vacua in real space, while instantons refer to tunneling processes in imaginary time.

[5]Those arguments are mathematically rigorous. The existence of such quantized invariants emerge from considerations of homotopy theory [55].

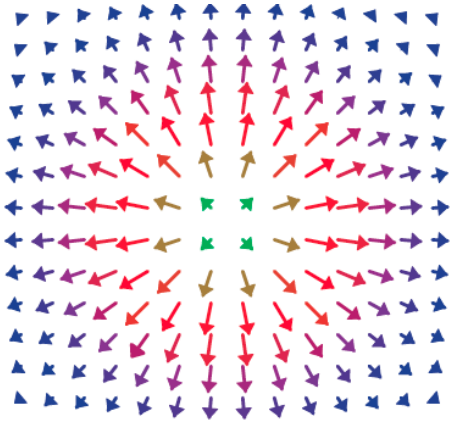

Figure 2.8: A skyrmion in $\mathbf{n}$. The arrows show the projection of $\mathbf{n}$ in the (x, y) plane, and we are ignoring the sublattice oscillation $(-1)^P$ which happens in the physical lattice spins. Image from [4].

operators" [54]:

$$\mathcal{L}_m = \sum_{n=1}^{\infty} \lambda_n(x,y) \left([\mathcal{M}(\mathbf{x})]^n + \left[\mathcal{M}^\dagger(\mathbf{x})\right]^n \right) , \tag{2.43}$$

where the couplings $\{\lambda_n\}$ are noted as "monopole fugacities". Those terms spoils this $U(1)_T$ symmetry, since $\mathcal{M}$ creates and destroys skyrmions in spacetime. This is where the Berry phase term becomes important: As shown by Haldane [53], configurations which change the charge Q in spacetime contribute to the sum:

$$\mathcal{S}_B = \frac{i\pi}{2} \sum_m \zeta_m \Delta Q_m , \tag{2.44}$$

Given a spin configuration $\mathbf{n}$, this action is computed as follows: m is the position of the instantons of a given configuration (also called monopoles) which create or destroy a Skyrmion on some plaquette of the square lattice, and $\zeta_m = 0, 1, 2, 3$ is an integer field which depends on the dual lattice parity of the plaquette. Due to periodic boundary conditions in the time direction, configurations must have instanton ($\Delta Q = 1$) and anti-instanton ($\Delta Q = -1$) pairs such that $\sum_m \Delta Q_m = 0$.

Note the imaginary nature of this action. Since it will be exponentiated in the partition function, it is only defined modulo 2π, and thus each ζ_m is only defined modulo 4, as is the case. Each configuration $\mathbf{n}$ contributes with $\exp(-i\mathcal{S}_B)$. Let us evaluate the effect of the terms in (2.43). For $n = 1$, this term creates configurations

where there is a instanton/anti-instanton pair, contributing with a phase:

$$\exp(-i\mathcal{S}_B) = \exp\left(-i\frac{\pi}{2}(\zeta_f - \zeta_i)\right) \ , \tag{2.45}$$

where ζ_f and ζ_i are the integers labelling the final and initial plaquettes. However, for any such configuration, one can just take another configuration with ζ_f and ζ_i shifted by one plaquette, the phase picks up a minus sign. Therefore, there is a destructive interference in the path integral, and single instanton configurations do not contribute. This argument also follows for $n = 2, 3$. However, for $n = 4$, $e^{i\mathcal{S}_B} = 1$, and there is constructive interference. Therefore, the lowest order terms are fourth-order monopole operators:

$$\mathcal{L}_m \sim \lambda_4(x, y)\left([\mathcal{M}(\mathbf{x})]^4 + \left[\mathcal{M}^\dagger(\mathbf{x})\right]^4\right) \ . \tag{2.46}$$

Still, the physical nature of such operators is not clear from this argument. That is, starting from the Néel phase, and considering the instanton effects, in eq. (2.46), what happens? Is there a phase where $\langle\mathcal{M}\rangle \neq 0$?

Instantons, from their definition, involve fluctuating from different vacua and are therefore non-perturbative: The physics at long distances can be hard to evaluate, in contrast to the LG-expansion discussed previously. However, one may point out the similarity of this problem to the celebrated Kosterlitz–Thouless transition [56], where two-dimensional vortex-antivortex pairs can generate a transition to a disordered phase. This is indeed what is expected from a high-energy LGW theory, where a continuous phase transition would occur from the ordered state to $\mathbf{\Phi} = 0$. However, the result here is surprising.

The physical lattice operators corresponding to the monopoles can be obtained from symmetry principles. However, it is a subtle calculation, since one must respect the covariance under the symmetries of the lattice. For example, $\mathbf{n}$ is odd under lattice translation T_x, T_y, since it corresponds to a alternating antiferromagnetic vector. Therefore, $T_{x,t}^{-1} Q T_{x,y} = -Q$, and skyrmions and antiskyrmions are interchanged. Therefore:

$$\mathcal{M}^\dagger(\mathbf{x}) \xrightarrow{T_x} -i\mathcal{M}(\mathbf{x}+x\hat{x}) \,, \tag{2.47}$$

$$\mathcal{M}^\dagger(\mathbf{x}) \xrightarrow{T_y} +i\mathcal{M}(\mathbf{x}+y\hat{y}) \,, \tag{2.48}$$

where $\hat{x}, \hat{y}$ are unit vectors in the spatial x and y directions. The $e^{i\pi/2} = i$ factor is the Berry phase difference of the monopole placed in two different neighboring plaquettes. Similar considerations also lead to the transformation law under $\pi/2$ lattice rotations:

$$\mathcal{M}^\dagger(\mathbf{x}) \xrightarrow{R_{\pi/2}} i\mathcal{M}^\dagger(\mathbf{x}) \,. \tag{2.49}$$

Finally, $\mathcal{M}$ must be invariant under the $SU(2)$ spin symmetry. The simplest lattice operator satisfying such transformation law are the following spin bilinears:

$$\mathcal{M}(\mathbf{x}=\mathbf{r}_j) \sim e^{i\pi/4}\left[(-1)^{x_j}\boldsymbol{\sigma}_j \cdot \boldsymbol{\sigma}_{j+\hat{x}} + i(-1)^{y_j}\boldsymbol{\sigma}_j \cdot \boldsymbol{\sigma}_{j+\hat{y}}\right] \equiv e^{i\pi/4}\psi_{\text{VBS}}(\mathbf{r}_j) \,. \tag{2.50}$$

A lattice site is written as $\mathbf{r}_j = x_j\hat{x} + y_j\hat{y}$. The field ψ_{VBS} describes the order parameter of a new phase completely distinct from the Néel phase, known as the *Valence Bond Solid* (VBS), pictured in Fig 2.9. The ideia is that the bolded bonds are spin singlets, and the phase of ψ_{VBS} describes the overlap between "columnar" VBS or "plaquette" VBS. By decomposing $\psi_{\text{VBS}} = |\psi_{\text{VBS}}|e^{i\phi}$, note that eq. (2.46) is written:

$$\mathcal{L}_m \sim \lambda_4 |\psi_{\text{VBS}}|^4 \cos(4\phi + \pi) \,, \tag{2.51}$$

where the monopole fugacity λ_4 is taken to be uniform. Suppose λ_4 is a relevant coupling: For either sign of λ_4, there are four distinct vacua (for example, for $\lambda_4 < 0$, we have $\phi = -\pi/4, \pi/4, 3\pi/4, 5\pi/4$), breaking the highlighted lattice symmetries: Translations T_x, T_y and $R_{\pi/2}$. Since spin singlets are $SU(2)$-invariant, the spin rotation symmetry is preserved.

Therefore, instanton "condensation" is the VBS order:

$$\langle \mathcal{M} \rangle \sim \langle \psi_{\text{VBS}} \rangle \neq 0 \,. \tag{2.52}$$

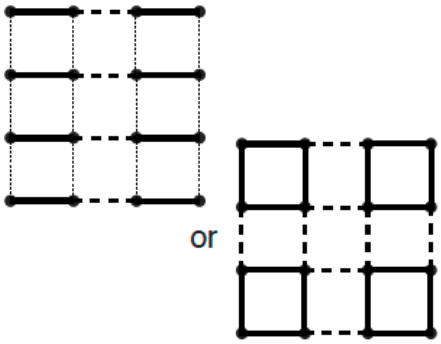

Figure 2.9: Two examples of valence bond solid states. In both cases, the highlighted bonds depict spin singlets. In the left figure, there is "columnar" order, where the singlets are formed in the horizontal direction. In the right, an example of a "plaquette" order is shown, where there is a mix between horizontal and vertical singlets. Image from [4].

This challenges the LGW paradigm, if a continuous transition arises between the two ordered phases. The expected, as shown in Fig 2.4, is a first-order phase transition, or an intermediary VBS-Néel state. This can be proven by constructing an action $\mathcal{S}_{\rm LGW}[\mathbf{n}, \psi_{\rm VBS}]$. A similar phenomenology would be found as the simple $\mathcal{S}_{\rm LGW}[\psi_1, \psi_2]$ in Sec. 2.2. With the monopole constraints in operators involving $\psi_{\rm VBS}$, the picture is less clear. To clarify those results, it is useful to use a different theory. Let us decompose the Néel vector in what are known as bosonic *spinons*:

$$n^a(\mathbf{x}) = z^*_\alpha(\mathbf{x})\sigma^a_{\alpha\beta}z_\beta(\mathbf{x}) \ , \tag{2.53}$$

where $\alpha, \beta = 1, 2$ is summed over. This is known as the $\mathbb{CP}^1$ map, since it is spanned by z due to the fact $\mathbf{n}^2 = 1 \ \rightarrow \ |z|^2 \equiv |z_1|^2 + |z_2|^2 = 1$. This decomposition is far from unique. There is an invariance under a local $U(1)$ gauge transformation $z_\alpha \rightarrow e^{i\theta(\mathbf{x})}z_\alpha$. This shows that any local theory involving spinons must be a gauge theory, that is, a gauge field must be introduced to enforce this symmetry and take care of the redundancy in writing the spinons. We can show that the partition function in eq. (2.40) can be rewritten as [57, 58]:

$$\mathcal{Z}_0 = \int_{|z|^2=1} D\mathbf{a}Dz \exp\left(-\frac{1}{g}\int \mathrm{d}^3\mathrm{x}\ |(\nabla - i\mathbf{a})z|^2\right) \ . \tag{2.54}$$

This can be proven by "integrating" out over the dummy variable $\mathbf{a}$, reducing to solve its equation of motion from the action, holding $\mathbf{a} = i(z^*_\alpha\nabla z_\alpha - \text{complex conjugate})$. By then substituting back this expression, one can reduce to the original non-linear

sigma model action. $\mathbf{a}$ indeed transforms as a $U(1)$ gauge field: $\mathbf{a} \to \mathbf{a} + \nabla\theta$.

Note the presence of a topological current $\mathbf{j} = \nabla \times \mathbf{a}$ (remember here that ∇ is a spacetime gradient). Violations of the conservation equation, $\nabla \cdot \mathbf{j} \neq 0$, indicates the presence of singularities in the gauge field. However, does that correspond to physical configurations? Consider the charge Q, which corresponds to the flux of the gauge field:

$$Q = \frac{1}{2\pi} \int \mathrm{d}^2\mathrm{x} (\nabla \times \mathbf{a})_\tau = \frac{1}{2\pi} \int \mathrm{d}^2\mathrm{x} (\partial_x a_y - \partial_y a_x) \ , \tag{2.55}$$

which is gauge invariant, and it does correspond to the skyrmion charge.

The monopole physics enters in this gauge theory as actual monopoles for the gauge field $\mathbf{a}$. A $\Delta Q = \pm 1$ flux violation corresponds to $(\nabla \times \mathbf{a})_\tau \to (\nabla \times \mathbf{a})_\tau + 2\pi$. This means that in the path integral, the flux is only defined modulo 2π, referred to as a *compact* $U(1)$ gauge field [59].

We will now deform the action describing eq. (2.54), in hope of describing a transition away from the Néel state. Consider the lagrangian:

$$\mathcal{L} = |(\nabla - i\mathbf{a})z|^2 + r(|z|^2) + u(|z|^2)^2 + \mathcal{L}_m - \frac{1}{e^2} \sum_{\square} \mathcal{W}_{\square} \ , \tag{2.56}$$

where the constraint $|z|^2 = 1$ was softened, using again the "high-energy" completion trick to write down a potential for the bosonic *spinon* field z_α, and introduced some dynamics for the gauge field, in terms of Wilson lines, defined as:

$$\mathcal{W}_{\square} = \exp\left(i \oint_{\square} \mathrm{d}\mathbf{x} \cdot \mathbf{a} \right) \ , \tag{2.57}$$

where $\square$ are elementary plaquettes on spacetime. This is the standard procedure in order to define gauge fields dynamics on a lattice [60]. Regularizing space-time as a cubic lattice with spacing 1,

$$\sum_{\square} \mathcal{W}_{\square} = \frac{1}{2} \sum_{a,b=\tau,x,y} \cos\left(\partial_a a_b - \partial_b a_a\right) = \sum_{b=\tau,x,y} \cos\left[(\nabla \times \mathbf{a})_b\right] \ , \tag{2.58}$$

where constants were ignored in the last equality. Note that, due to compactness, the kinetic term for the $U(1)$ gauge field must be 2π periodic.

The Néel phase now corresponds to condensing the spinon field $\langle z_\alpha \rangle \neq 0$ [6]. If monopole operators are absent in the action, the Q charge is conserved, and there is an emergent $U(1)_T$ symmetry. The gauge field is now non-compact, and eq. (2.58) can now be safely expanded, generating a $(\nabla \times \mathbf{a})^2$ term in the lagrangian, which is the usual Maxwell action for electrodynamics. Expanding and writing eq. (2.56) in this approximation:

$$\mathcal{L}_{\text{DQC}} \equiv |(\nabla - i\mathbf{a})z|^2 + r^*(|z|^2) + u(|z|^2)^2 + \frac{1}{2e^2}(\nabla \times \mathbf{a})^2 \,. \tag{2.59}$$

Straightforward quantization of the gauge field gives rise to photon-like gapless mode! Indeed, as argued below, the above action does describe the phase transition between the Néel-VBS states. $r = r^*$ is tuned in order to have a scale-invariant critical point. The spinon field has charge 1 under the gauge field, and transforms as a spinor under the $SU(2)$ symmetry: It carries a spin 1/2 degree of freedom. This is not expected for any excitation in the LGW expansion: The Néel vector $\mathbf{n}$ transforms as a vector, which is a spin 1 representation. As eq. (2.53) suggests, the Néel vector excitations are described by a pair of spinons. This means that at criticality, there is *fractionalization*: Even if physical states must have integer spin, the excitations are said to be fractionalized if they can separated in half-integer spin particles.

Notice that the spinons are charged under a gauge field and therefore feel a force between then. This is where the non-compactness argument becomes important: For compact gauge fields, Polyakov [59] showed that instantons (monopole effects) in and dominate the spectrum of the theory, resulting in confinement. At low energy, charges are bound together, and there is an energy cost proportional to the distance separating them. This is what happens in the confined phase of quantum chromodynamics where the low-energy excitations are mesons, bound states of quarks interacting with gluons, and this also *should* happen in the VBS phase,

[6] Some words of caution on terminology and "condensing" operators: Both the monopole and spinon operators are charged under the $U(1)$ gauge field, and, therefore, are not gauge invariant. In order to construct gauge-invariant states of such excitations, it is necessary to add Wilson lines $e^{i\int a}$. In the condensed matter literature, such Wilson lines are omitted, however they are important if Chern-Simmons terms are present [61,62]. We will proceed without adding the Wilson lines, which are not important otherwise, following the usual discussion of the Anderson-Higgs mechanism [63].

identified as monopole condensation. In a deconfined phase of a gauge theory, there is a fixed energy cost to separate charges, independent of the distance. This is what happens in the usual quantum electrodynamics of electrons and photons.

In the Néel phase, the condensation of the spinon field means that, due to the Anderson-Higgs mechanism [49], the photon adquires a mass. To see why, in eq. (2.59), just replace $z = z_0 = \text{const}$, the previous kinetic term generates a term $\sim |z_0|^2\mathbf{a}^2$, which is the mass term for vector fields. Therefore, in the gauge field language, the Néel phase corresponds to the Higgs phase, the VBS is the confined phase, while right at the critical point there is deconfinement of excitations. Hence, the transition is dubbed as *deconfined quantum criticality* (DQC). In the confined/Higgs phases, there are LGW-allowed excitations, which break down at the critical point.

However, it is still necessary to show some evidence that eq. (2.56) does in fact flow to a fixed point of the form of eq. (2.59), rendering monopoles irrelevant in the process. There are a number of different arguments: One is from the analysis of the Sachdev-Jalabert (SJ) model, a lattice regularization of a $\mathbb{CP}^{N-1}$ model with Berry phase effects [64]. The large-N and the $N = 1$ cases agree concerning the existence of a critical point with deconfined excitations [15]. We will take a different route.

We will break the full spin rotation symmetry to a $U(1)$ subgroup, while maintaining other symmetries. In the lattice, this means the presence of anisotropic interactions such as $\sigma_i^z\sigma_j^z$. In the NLσM action, this amounts to adding a term such as $\mathcal{L}_w = w(n^z)^2$, with $w < 0$. The resulting $\mathbb{CP}^1$ action is then written as:

$$\mathcal{L}_{\text{e.p}} = |(\nabla - i\mathbf{a})z|^2 + w(|z_1|^2 - |z_2|^2)^2 + \mathcal{L}_m \ , \tag{2.60}$$

where the constraint $|z|^2 = 1$ is considered exactly in the partition function, and the λ_4 monopole operators are added. The resulting Néel order has "easy-plane anisotropy": by ordering $\langle z_\alpha\rangle \neq 0$, energetically favored $|\langle z_1\rangle| = |\langle z_2\rangle|$ states means that only $n^\pm = n^x \pm in^y$ orders, while $n^z = 0$. By combining $|z_1|^2 - |z_2|^2 \simeq 0$ and $|z_1|^2 + |z_2|^2 = 1$, we conclude that low energy spinon fields have fixed magnitude, $|z_0| = \text{const.}$. Therefore, we introduce a phase field $\varphi_\alpha(\mathbf{x})$:

$$z_\alpha(\mathbf{x}) \sim \frac{|z_0|}{\sqrt{2}} \exp[i\varphi_\alpha(\mathbf{x})] \ , \tag{2.61}$$

where the phase field is defined modulo 2π, that is, one can interpret its existence as two NLσM with a circle as the target manifold, $\Sigma = S^1$. The lagrangian is written as:

$$\mathcal{L}_{\text{e.p}} \sim \frac{|z_0|^2}{2}(\nabla\varphi - \mathbf{a})^2 + \mathcal{L}_m \ , \tag{2.62}$$

where $\varphi = (\varphi_1, \varphi_2)$ was defined. The components of the Néel vector in plane are written as:

$$n^{\pm} \sim \frac{|z_0|}{2}\exp[\pm i(\varphi_2 - \varphi_1)] \ , \tag{2.63}$$

and there is no Skyrmion number in this case. The topological charge which can be defined is the winding numbers of the phases:

$$q_\alpha = \frac{1}{2\pi}\oint d\mathbf{x}\cdot\nabla\varphi_\alpha \quad ; \quad \alpha = 1, 2 \ , \tag{2.64}$$

defined on closed curves on each (imaginary-)timeslice. However, in the easy plane case, the gauge field flux only couples to the *sum* of the charges:

$$q_1 + q_2 = \frac{1}{2\pi}\oint d\mathbf{x}\cdot\nabla(\varphi_1 + \varphi_2) = \frac{1}{2\pi}\oint d\mathbf{x}\cdot\mathbf{a} = \frac{1}{2\pi}\oint \mathrm{d}^2\mathbf{x}\cdot(\nabla\times\mathbf{a}) \ , \tag{2.65}$$

which can be seen from the equations of motion for the gauge field in eq.(2.62). Monopole operators cannot be ignored, which can be seen from the above equation: By taking a space-like surface in the last equality, they create vortices /anti-vortices in the phase field, and, therefore, $n^{\pm}$. Physically, a 2π vortex in the φ_1 field ($\varphi_1 \to \varphi_1 + 2\pi$) is the same as an antivortex in the φ_2 field ($\varphi_2 \to \varphi_2 - 2\pi$), since they appear in opposite signs in the argument of eq. (2.63). Note also that we can define "meron" fields which shift the phase angles by π. Let $\psi_{1,2}$ be the field creating each of the merons, that is, by acting on a semiclassical state, $\varphi_{1,2} \xrightarrow{\psi^*_{1,2}} \varphi_{1,2} + \pi$. Therefore, one can construct a monopole, manifested as a vortex creation operator, as:

$$\mathcal{M}^\dagger \sim e^{i\pi/4}\psi^*_{\text{VBS}} \sim \psi_1^*\psi_2 \ . \tag{2.66}$$

This identity can be proven also by consistency of symmetry principles in the meron field [15,65]. Suppose now w negative, but small. Acting with ψ_1, the vortex core will have $n^z < 0$, and for ψ_2, $n^z > 0$, as each z_1, z_2 must vanish near the core. Therefore, the meron field charge corresponds to the easy-plane $U(1)$ charge. We are now ready to make a change of variables in our description. We write, by again softnening the $|z|^2 = 1$ constraint in a potential:

$$\mathcal{L}_{\text{e.p}} = |(\nabla - i\mathbf{a})z|^2 + V(z_1, z_2) + \mathcal{L}_m \ , \tag{2.67}$$

where the potential is of the form $V(z_1, z_2) = r|z|^2 + u(|z|^2)^2 + w'|z_1|^2|z_2|^2$. In $2+1$ dimensions, there is a duality between bosonic "particle" operators (such as $z_{1,2}$), charged under a gauge field with flux creation operators ($\psi_{1,2}$), known as *particle-vortex* duality [61,66–68]: It states that given an action for the particle operator, in our case given by $\mathcal{L}_{\text{e.p}}$, there is a dual action describing $\psi_{1,2}$, however coupled to a distinct $U(1)$ non-compact gauge field. For the case in question, we have:

$$\tilde{\mathcal{L}}_{\text{e.p}} = |(\nabla - i\mathbf{b})\psi|^2 + \tilde{V}(\psi_1, \psi_2) + \frac{1}{2e_v^2}(\nabla \times \mathbf{b})^2 + \mathcal{L}_m \ , \tag{2.68}$$

where $\tilde{V}(\psi_1, \psi_2) = r_v|\psi|^2 + u_v(|\psi|^2)^2 + w_v'|\psi_1|^2|\psi_2|^2$ is the potential for the meron fields. The monopole lagrangian is now local, by substituting eq. (2.66) in eq. (2.46):

$$\mathcal{L}_m = \lambda_4 \left[(\psi_1^* \psi_2)^4 + (\psi_2^* \psi_1)^4\right] \ . \tag{2.69}$$

There is an overall $U(1)$ gauge symmetry, with the standard action $\psi_{1,2} \to e^{i\theta(\mathbf{x})}\psi_{1,2}$, and $\mathbf{b} \to \mathbf{b} + \nabla\theta$. The corresponding current is $\mathbf{j} = \nabla \times b$. In fact, this is a manifestation of the global $U(1)$ spin symmetry in $\mathcal{L}_{\text{e.p.}}$, since it is dual to the spin current $z^\dagger(\nabla - i\mathbf{a})z$. However, there is a distinct global $U(1)_T$ symmetry for $\lambda_4 = 0$,$\psi_\alpha \to e^{-i(-1)^\alpha \rho}\psi_\alpha$, where $\rho \in mathbbR$, corresponding to the conservation of the "skyrmion number", now associated with the total winding number:

$$Q = \int \mathrm{d}^2\mathrm{x}\ \psi^\dagger \sigma^z \psi = q_1 - (-q_2) \ , \tag{2.70}$$

where the extra minus sign from q_2 comes from the fact that monopoles are created

with a ψ_2 anti-particle. Indeed, for $\lambda_4 \neq 0$, this symmetry is broken down to $\mathbb{Z}_4$, due to Berry phase effects. In this description, if:

$$\langle \psi_{1,2} \rangle \neq 0 \, , \tag{2.71}$$

due to the Anderson-Higgs, the gauge field $\mathbf{b}$ is gapped. This corresponds to the Néel phase, since $U(1)$ spin symmetry is the gauge symmetry. However, if the composite monopole operator is relevant, we have a paramagnet phase, equivalent to the VBS phase:

$$\langle \psi_{\text{VBS}} \rangle \sim \langle \psi_1^* \psi_2 \rangle \neq 0 \, . \tag{2.72}$$

This is indeed the phenomenology found in the original $\mathbb{CP}^1$ model, however with the role of monopoles as a correction to the potential breaking the $U(1)_T$ symmetry. It can be further argued, as done in Appendix C of [15], that indeed, the scaling dimension of the monopole operator is irrelevant at the transition between those two regimes. Therefore, $\mathcal{L}_m$ can be safely discarded, and by again invoking this duality, eq. (2.59) is a good description, at least in the easy-plane anisotropic limit.

For the isotropic case, numerical Monte-Carlo results do suggest that by forbidding monopoles in the partition function of the NLσM in eq.(2.40), a continuous phase transition emerges with some evidence of a gapless photon [69, 70]. Numerical evidence for this transition also shows a diverging correlation length [71, 72]. After this first incarnation, deconfined quantum criticality is now a umbrella term for exotic, continuous phase transitions without order parameter excitations at low energies, where several examples were found [73–76]. See [16] for a review of some of such transitions.

In the next chapter, we will discuss the physics of spin chains. First, some extra field theoretic tools in 1+1 dimensions are reviewed, such as the restraining dynamics of two dimensional conformal field theories and bosonization. After doing so, we will also review continuous transitions between symmetry-broken phases found in spin chains.

Chapter 3

Tools and examples in one dimension

As commonly is the case in physics, problems get easier as dimensions are lowered. In this chapter, we will explore some extra properties of conformal field theories in $1+1$ dimensions, which can be classified by a number known as *central charge*. As a consequence, we will also comment on the equivalence of fermions and bosons which occur, including how to map bosonic to fermionic operators and virse versa. Examples will be provided, commenting on the connection to the LGW paradigm and/or the deconfined quantum criticality phenomenology.

The discussion on conformal field theory is based on [17,41,51]. The conventions used with dual bosons are similar to the expressions in [77] in the thermodynamic limit. The field-theoretic perspective discussion on bosonization is based on [78]. Both the transverse field Ising model and the XY chain are treated with considerable detail in [18], while the discussion of the phases and transitions of the $J_1 - J_2$ XYZ chain is based on [5].

3.1 Conformal Field Theory in two dimensions and bosonization

As presented in the last chapter, the way to fully characterize CFTs are by computing scaling dimensions and the structure constants. We will now show that, in two spacetime dimensions, there are two numbers which can classify degrees of freedom in a CFT. This will be useful to classify phase transitions in lattice models.

Consider the two-dimensional plane spanned by two coordinates (x_1, x_2), and

define the complex coordinates $z = x_1 + ix_2$ and $\bar{z} = x_1 - ix_2$. Assume that a CFT has an action given by $\mathcal{S}_0$. Classically, due to Noether's theorem [41], it is known that every symmetry corresponds to a conservation of a corresponding spacetime current. Since the conformal group is constructed from spacetime symmetries, we introduce the energy-momentum tensor. If $\mathbf{x} \to \mathbf{x} + \boldsymbol{\epsilon}(\mathbf{x})$ is some infinitesimal transformation, T^{ab} represents the corresponding change in degrees of freedom:

$$\delta\mathcal{S}_0 \equiv -\frac{1}{2\pi}\int \mathrm{d}^2\mathrm{x}\; T^{ab}\partial_a\epsilon_b = \frac{1}{2\pi}\int \mathrm{d}^2\mathrm{x}\; \partial_a T^{ab}\epsilon_b \;, \tag{3.1}$$

where $a, b = 1, 2$. To each of the subgroups of the conformal group, one can evaluate the symmetry consequences of the energy-momentum tensor. Invariance under translations and rotations implies that T^{ab} is symmetric and conserved. Furthermore, scale invariance imposes that it is also traceless. In complex coordinates, this basically means that it decomposes into holomorphic and antiholomorphic parts:

$$T_{zz}(z,\bar{z}) \to T(z) \quad ; \quad T_{\bar{z}\bar{z}}(z,\bar{z}) \to \bar{T}(\bar{z}) \;, \tag{3.2}$$

and $T_{z\bar{z}} = T_{\bar{z}z} = 0$. By the use of Ward identities [1], one can show that these features follow to the quantum case (that is, when the energy-momentum tensor is probed inside correlation functions) with the exception of the traceless condition in curved manifolds [17]: If R is the curvature of some two-dimensional Riemannian manifold,

$$\langle \mathrm{tr}T \rangle = \langle T^a_a \rangle = \frac{c}{24\pi}R \;, \tag{3.3}$$

where c is known as the central charge, and is a property of the conformal field theory. It is also noted as *conformal anomaly*, since it indicates a quantum violation of scale symmetry in curved space. What is non-trivial is that it is also related to the number of degrees of freedom of the system, even in flat spacetime. In fact, for example, if the theory is defined on $\mathbb{R} \times S^1$ (a cylinder, and the manifold in which we are most interested, since τ, the imaginary time, is periodic), the leading contribution to the ground state energy, if L is the length of the periodic direction, and we set the velocity of propagation to $v = 1$, is given as:

[1] Ward identities basically state that if there is a classical Noether-type conservation equation $\nabla \cdot \mathbf{j} = 0$, in the quantum theory it is manifested in correlation functions, as $\langle \nabla \cdot \mathbf{j} \cdots \rangle = 0$, where $\cdots$ indicates other operators of the theory. Violations of the Ward indenties are known as *quantum anomalies*.

$$E_{\rm gnd} = -\frac{\pi c}{6L} \,. \tag{3.4}$$

Since diagonal components of the stress-energy tensor can be interpreted as energy density, it is perhaps unsurprising that the central charge can be computed as the coefficient for the TT correlator:

$$\langle T(z)T(0)\rangle = \frac{c/2}{z^4} \quad ; \quad \langle \bar{T}(\bar{z})\bar{T}(0)\rangle = \frac{c/2}{\bar{z}^4} \,. \tag{3.5}$$

The central charge depends on the short-distance content of the theory, and cannot be fixed only by symmetries. However, an important property is that the central charge is additive: If one consider two CFTs described by $\mathcal{S}_0^{(1)}$ and $\mathcal{S}_0^{(2)}$, with central charges c_1 and c_2, say, by computing the above correlator, it easy to see that if one consider $\mathcal{S}_0 = \mathcal{S}_0^{(1)} + \mathcal{S}_0^{(2)}$ (two decoupled CFTs), the total central charge is given as: $c = c_1 + c_2$.

At first sight, this procedure may seem not very useful in classifying CFTs: If one constructs, for example, a $c = 0.548$ CFT, how to really distinguish its physics to a $c = 0.549$ one? Universality saves the day: Recall that the main appeal of RG fixed points is the fact that different lattice systems may flow to the same universality class at the transition at low energies. Thus, one may not expect a continuous spectrum of central charges to classify conformal field theories which happens at phase transitions. Indeed that is the case, and physical phase transitions are described by *minimal models*, where conformal charges are rational.

For our discussion, we will only need two examples: $c = 1$ and $c = 1/2$. The former was already mentioned in the last chapter, albeit in two dimensions, it is the free boson:

$$\mathcal{S}_0^{(1)} = \frac{1}{2}\int \mathrm{d}^2\mathrm{x}\, (\nabla\phi)^2 \,. \tag{3.6}$$

When fully endowed with the $U(1)$ shift symmetry, where $\phi \to \phi + \text{const}$, this was referred to as the Gaussian fixed point. Note that two-point correlation functions in eq. (2.29) are singular for $d \to 2$. This is due to the Mermim-Wagner theorem, which states that infrared correlation functions of "Goldstone bosons" (for the $U(1)$ case, equivalent to bosons with shift symmetry) are divergent at long distances.

Indeed, a careful computation removing a short distance singularity shows that $\langle\phi(\mathbf{x})\phi(\mathbf{y})\rangle \sim -\ln|\mathbf{x}-\mathbf{y}|^2$: There is no finite physical result in the infrared! This is due to the fact the shift symmetry implies that ϕ is not a physical operator of the theory, since its value is arbritary. Note however, this is not the case for the current $\mathbf{j}(\mathbf{x}) = \nabla\phi(\mathbf{x})$, which is well-defined. Further operators are constructed by adding higher order derivatives, etc. For example, the holomorphic part of the energy-momentum tensor is written as $T(z) = -(\partial_z\phi)^2/2$. With proper normalization, the TT correlator yields unit central charge. There are also special operators dubbed *vertex operators*:

$$V_\alpha(\mathbf{x}) = \exp\left[i\alpha\varphi(\mathbf{x})\right] \ , \tag{3.7}$$

if $\phi \to \phi + a$, $V_\alpha = e^{i\alpha\phi} \to e^{i\alpha a}V_\alpha$. This implies that correlation functions must be "charge-neutral" to respect this symmetry: That is, $\langle V_{\alpha_1}\cdots V_{\alpha_n}\rangle \neq 0$ only if $\sum_i \alpha_i = 0$. By looking at the two-point correlations, one concludes that they are indeed scaling operators which can be classified by $|\alpha|$ (expression shown in App. B):

$$\langle V_\alpha(\mathbf{x})\, V_{-\alpha}(\mathbf{y})\rangle \sim \frac{1}{|\mathbf{x}-\mathbf{y}|^{\alpha^2/2\pi}} \ , \tag{3.8}$$

and, therefore, will flow non-trivally if added in the action. For our purposes, we will consider *compact bosons*, that is:

$$\phi(\mathbf{x}) \in \mathbb{R} \to \varphi(\mathbf{x}) \in [0, R) \simeq S^1 \ , \tag{3.9}$$

as the phase field in the easy-plane Néel phase studied in the last chapter. In this case, we define some R such that only $\varphi \mod R$ corresponds to physical configurations. Note that the compactification restricts the well-defined operators of the theory, since they must be invariant under $\varphi \to \varphi + R$. This means that there is a discrete spectrum of vertex operators:

$$V_n(\mathbf{x}) = \exp\left[i\frac{2\pi n}{R}\varphi(\mathbf{x})\right] \quad ; \quad n = 0, 1, \cdots \ , \tag{3.10}$$

Those operators will play a big role in constructing symmetry-breaking phases in

one dimension.

We are using the terms bosonic and scalar fields interchangeably: In the LGW field theories, the scalar field, which represents the continuum limit of order parameters, must carry integer spin, as explained for the Néel case. Bosons, in quantum mechanics, are defined as integer spin particles which are symmetric under exchange, and therefore the definitions match. We will now consider fermionic fields, manifested as spinors.

As shown by Dirac, there is a way to construct relativistic fermions by "taking the square root" of the relativistic boson [49]. We will take a different route, since we want to define fermions in a euclidean action, and the original derivation concerns the invariance of the full Lorentz group. Here the structure is simpler. Consider the operator:

$$-\nabla^2 = -\partial_\tau^2 - \partial_x^2 \,, \tag{3.11}$$

where $\tau = x_1, x = x_2$. Note that $\mathcal{S}_0^{(1)} = 1/2 \int \phi(-\nabla^2)\phi$. Now, define a set of matrices $\boldsymbol{\gamma} = (\gamma_1, \gamma_2)$ such that:

$$\{\gamma_a, \gamma_b\} = 2\delta_{ab} \,, \tag{3.12}$$

therefore, $(\boldsymbol{\gamma} \cdot \nabla)^2 = -\nabla^2$. Our case of interest, as highlighted in the next sections, is the case where this algebra is realized by 2×2 matrices. In fact, we can just take the Pauli matrices $\gamma_1 = \sigma^x$ and $\gamma_2 = -i\sigma^y$. We can define then two-dimensional Dirac fermions, as two component fields:

$$\psi(\mathbf{x}) \equiv \begin{pmatrix} \psi_L(\mathbf{x}) \\ \psi_R(\mathbf{x}) \end{pmatrix} \,. \tag{3.13}$$

(not to be confused by the previous instances of the letter ψ, where it was used to denote scalar fields) We define then the Dirac action, by also defining the Dirac adjoint $\bar{\psi} = \psi^\dagger \gamma_1$:

$$\mathcal{S}_0^{(D)} = i \int \mathrm{d}^2\mathrm{x}\, \bar{\psi}(\boldsymbol{\gamma} \cdot \nabla)\psi \,. \tag{3.14}$$

We will later show that those fermions arise in lattice models at long distances. However, we need to be more specific to construct a partition function. Dirac fermions are complex, which means $\psi_\alpha^\dagger \neq \psi_\alpha$, and they anticommute, that is $\psi_\alpha^\dagger \psi_\beta = -\psi_\beta \psi_\alpha^\dagger$, where each field is evaluated on a different point. This property allows to construct a proper anti-symmetric fermionic Hilbert Space. Again omitting the details of the stress tensor and its correlation, it can be shown that $c^{(D)} = 1$. That is the same result as the free boson! In this theory, the two point correlation is written as:

$$\langle \psi_L^\dagger(\mathbf{x}) \psi_L(\mathbf{x}') \rangle \sim -\frac{1}{(\tau - \tau') + i(x - x')} , \tag{3.15}$$

$$\langle \psi_R^\dagger(\mathbf{x}) \psi_R(\mathbf{x}') \rangle \sim -\frac{1}{(\tau - \tau') - i(x - x')} , \tag{3.16}$$

clearly different from the logarithmically divergent correlations of free bosons. If central charges indeed provide a classification of CFTs, it is necessary to have some operator in the free boson theory on which the fermionic fields are mapped. This is known as *bosonization*. One may ask also about symmetries, which apparently do not match: A free fermion has a $U(1)_R \times U(1)_L \simeq U(1)_V \times U(1)_A$ symmetry, corresponding to the conservation of the current of the right and left moving fermions. They can be written as the axial and vector currents:

$$\mathbf{j}_V = \bar{\psi} \boldsymbol{\gamma} \psi \quad ; \quad Q_V = \int \mathrm{dx} \, (\psi_R^\dagger \psi_R + \psi_L^\dagger \psi_L) , \tag{3.17}$$

$$\mathbf{j}_A = \bar{\psi} \boldsymbol{\gamma} \gamma_3 \psi \quad ; \quad Q_V = \int \mathrm{dx} \, (\psi_R^\dagger \psi_R - \psi_L^\dagger \psi_L) , \tag{3.18}$$

where $\gamma_3 = \gamma_1 \gamma_2$. Their separate conservation law has a physical meaning, already manifested in the correlation functions: One can interpret massless Dirac fermions as two propagating "left-moving" and "right-moving" fermions. We now consider a compact boson. The shift symmetry, denoted as $U(1)_s$, is manifested as the current $\mathbf{j}_s = \nabla \varphi$. However, there is an extra $U(1)_w$ symmetry, of topological nature. Its current is given as:

$$\mathbf{j}_w \equiv \frac{1}{R} \hat{z} \times \nabla \varphi , \tag{3.19}$$

that is, it corresponds to the "winding" of the boson, as the charge is $Q_w = \int \mathrm{dx}\, j^0_w/R = \int \mathrm{dx}\partial_x\varphi/R \in \mathbb{Z}$. Indeed it is topological in nature, as was the case for the Skyrmion number and the vortex winding. The quantization works if we take periodic boundary conditions in the spatial direction, $\varphi(-L/2) = \varphi(L/2)$, effectively putting the system on a torus $\mathbb{T}^2 = \mathbb{S}^1 \times \mathbb{S}^1$ (remember that the time direction is always periodic). If one is interested only in local processes, choosing $\varphi(\pm\infty) = 0$ will make this charge vanish. However, for singular configurations where there is winding, this expression can be non-trivial. Naturally we now have a $U(1)_s \times U(1)_w$ symmetry. We can then conjecture that fermions and bosons in $1+1$ dimensions are equivalent descriptions in the torus, where currents $(\mathbf{j}_V, \mathbf{j}_A)$ match to $(\mathbf{j}_s, \mathbf{j}_w)$.

Indeed, we will show that is the case and construct the operators that map the fermion fields into the bosonic theory. Before doing so, it is useful to rewrite the compactified boson theory. The partition function of a compact boson is given as:

$$\mathcal{Z}_0^{(B)} = \int_{\varphi \mod R} D\varphi \exp\left\{-\frac{K}{2}\int \mathrm{d^2x}\ \left[(\partial_\tau\varphi)^2 + (\partial_x\varphi)^2\right]\right\} . \tag{3.20}$$

where we have introduced an extra parameter K. We will use the following identity of gaussian integrals:

$$e^{-b^2/2a} = \int_{-\infty}^{\infty} \mathrm{dx}\, e^{-\frac{a}{2}x^2 - ibx} , \tag{3.21}$$

to rewrite:

$$\exp\left[-\frac{K}{2}\int \mathrm{d^2x}\ (\partial_\tau\varphi)^2\right] = \int D(\partial_x\theta)\ \exp\left\{-\int \mathrm{d^2x}\ \left[\frac{1}{2K}(\partial_x\theta)^2 - i\partial_x\theta\partial_\tau\varphi\right]\right\} , \tag{3.22}$$

renaming $D(\partial_x\theta) \to D\theta$, the partition function is rewritten as:

$$\mathcal{Z}_0^{(B)} = \int_{\varphi \mod R} D\varphi \int_{\theta \mod R} D\theta \exp\left\{-\int \mathrm{d^2x}\ \left[\frac{1}{2K}(\partial_x\theta)^2 + \frac{K}{2}(\partial_x\varphi)^2 - i\partial_x\theta\partial_\tau\varphi\right]\right\} . \tag{3.23}$$

Note that we have imposed $R-$periodicity in the field $\theta = \theta(\mathbf{x})$. This is due to the

fact one can further integrate in the φ field, by exchanging the ∂_x and ∂_τ derivatives in the last term to arrive at:

$$\mathcal{Z}_0^{(B)} = \int_{\theta \mod R} D\theta \exp\left\{-\frac{1}{2K}\int \mathrm{d}^2\mathrm{x}\ \left[(\partial_\tau\theta)^2 + (\partial_x\theta)^2\right]\right\}\ , \tag{3.24}$$

which is the same as the original theory with $K \to K^{-1}$! This is what is sometimes called $T-$duality. θ must be compact to hold the same vertex operator spectrum as the original theory. θ and φ are known as *dual bosons*. The corresponding currents are, in fact, exchanged:

$$\mathbf{j}_s^\theta \equiv \nabla\theta \quad \leftrightarrow \quad \mathbf{j}_w^\varphi \equiv \frac{1}{R}\hat{z}\times\nabla\varphi\ , \tag{3.25}$$

$$\mathbf{j}_w^\theta \equiv \frac{1}{R}\hat{z}\times\nabla\theta \quad \leftrightarrow \quad \mathbf{j}_s^\varphi \equiv \nabla\varphi\ . \tag{3.26}$$

The physical interpretation is that bosonic particles in one side of the duality correspond to winding modes in the another side of the duality. In fact, θ is related to the canonical momentum of φ. It will be useful to discuss a hamiltonian formulation, since, in one dimension, one can generally derive the continuum dynamics directly from some low-energy approximation in the lattice hamiltonian. The K-parameter theory is known as a Luttinger liquid [79]. Consider the action in eq. (3.23), defined in real time:

$$\mathcal{S}_{\mathrm{LL}} \equiv \int \mathrm{dtdx}\ \left[-\frac{1}{2K}(\partial_x\theta)^2 - \frac{K}{2}(\partial_x\varphi)^2 + \partial_x\theta\partial_t\varphi\right]\ , \tag{3.27}$$

the canonical momentum to φ is $\Pi_\varphi = \partial\mathcal{L}_{LL}/\partial(\dot{\varphi}) = \partial_x\theta$. A hamiltonian in a time-slice is then constructed from a density $H_{\mathrm{LL}} = \int \mathrm{dx}\ \mathcal{H}_{\mathrm{LL}}$, where:

$$\mathcal{H}_{\mathrm{LL}} = \Pi_\varphi\partial_t\varphi - \mathcal{L}_{LL} = \frac{1}{2K}(\partial_x\theta)^2 + \frac{K}{2}(\partial_x\varphi)^2\ . \tag{3.28}$$

Canonical quantization, an alternative to a path integral formulation of φ, Π_φ is given by the operators satisfying $[\varphi(x), \Pi_\varphi(y)] = i\delta(x-y)$. Then, since one can write:

$$\theta(x) = \int_{-\infty}^{x} \mathrm{dy}\ \Pi_{\varphi}(y)\ , \tag{3.29}$$

one may then impose:

$$[\varphi(x), \theta(y)] = iH(x-y)\ , \tag{3.30}$$

where H is the Heaviside theta function. This gives a "topological" interpretation for the dual fields: If $x > y$, the non-commutativity reflects a non-local correlation between the fields. For general K, the Luttinger liquid has two types of physical vertex operators:

$$V_{\alpha}(x) = \exp\left[i\alpha\ \varphi(x)\right]\ , \tag{3.31}$$
$$\tilde{V}_{\beta}(x) = \exp\left[i\beta\ \theta(x)\right]\ , \tag{3.32}$$

where both α, β are quantized as integer multiples of $2\pi/R$. The $\tilde{V}$ operators are then charged with the shift symmetry for the dual boson θ/winding symmetry of φ. Furthermore, correlations have a $K-$dependence on the exponents, modifying eq.(3.8), see App. B:

$$\langle V_{\alpha}(x) V_{-\alpha}(y)\rangle \sim \frac{1}{|x-y|^{\alpha^2/2\pi K}}\ , \tag{3.33}$$
$$\langle \tilde{V}_{\beta}(x) \tilde{V}_{-\beta}(y)\rangle \sim \frac{1}{|x-y|^{\beta^2 K/2\pi}}\ . \tag{3.34}$$

We now present the main result: Since the dual bosons are compact, the K parameter can be used to redefine the compactification radius to $\sqrt{K}R$. At $K = 1$, we introduce the fermion fields as:

$$\psi_{L,R}(\mathbf{x}) \sim \frac{1}{\sqrt{2\pi}} \exp[-i\sqrt{\pi}(\theta \mp \varphi)]\ , \tag{3.35}$$

where we have chosen $R = 2\sqrt{\pi}$. The proof for this equation requires constructing the Hilbert space for the free bosons and fermions, computing the corresponding

spectrum, and showing that, in both cases, the states can be mapped to each other if a (more complicated version of) the above equation is identified. Since we are dealing with spinless fermions and long-distance physics, such details do not matter much and are well described in [77, 80]. To get a physical interpretation of this result, one can identify fermionic excitations as soliton configurations in $1+1$, as explained in an example in the last section.

Also, since both theories are free, one can directly check by computing both partition functions on a torus, that the result indeed agree with each other, $\mathcal{Z}_0^{(B)} = \mathcal{Z}_0^{(D)}$ [17]. We will refer to the mapping in eq. (3.35) as *bosonization*. Operators can be mapped from one side to another, and the following dictionary will be used in the rest of this thesis:

$$\rho_L = \psi_L^\dagger \psi_L \sim \frac{1}{2\sqrt{\pi}}(\partial_x \varphi + \partial_x \theta) \ , \tag{3.36}$$

$$\rho_R = \psi_R^\dagger \psi_R \sim \frac{1}{2\sqrt{\pi}}(\partial_x \varphi - \partial_x \theta) \ , \tag{3.37}$$

$$\psi_R^\dagger \psi_L \sim \frac{1}{2\pi} \exp(-i\sqrt{4\pi}\varphi) \ , \tag{3.38}$$

$$\psi_L \psi_R \sim \frac{1}{2\pi} \exp(-i\sqrt{4\pi}\theta) \ . \tag{3.39}$$

Note that the last two operators are identified with vertex operators in the bosonic theory. Furthermore, if we refer to the symmetry of the free boson as the winding symmetries of each dual boson as $U(1)_\varphi \times U(1)_\theta$ (think of the action in the form written in eq. (3.27)), one can see that the vector and axial currents of the fermions indeed map to the winding currents of φ and θ, respectively. Remember that the gapped phases can be obtained by perturbing fixed points. The ideia and usufulness of this duality is that we can perturb from the $c = 1$ fixed point in two different ways. Therefore, perturbations which can be hard to analyze in one side may be easy in another. This also will be shown in examples.

We will investigate a case where fermionic excitations arise in gapped phases in spin chains, while discovering the $c = 1/2$ CFT. Consider again the transverse field Ising model (TFIM), which we rewrite here:

$$H_{\text{TFIM}} = -\sum_i \left(\sigma_i^z \sigma_{i+1}^z + g\ \sigma_i^x\right) \ . \tag{3.40}$$

Now equipped with the LGW story, we have a proper starting point. For $g \to 0$, the ground state must be two degenerate ferromagnetic states, eigenstates of the classical Ising hamiltonian $\sum_i \sigma_i^z \sigma_{i+1}^z$. For $g \to \infty$, the spins are polarized in the x direction, with a unique ground state. This is an ordered-disordered transition: In the ferromagnetic phase, the symmetry $P_x : \sigma_i^{y,z} \to -\sigma_i^{y,z}$ is broken, while preserved in the polarized phase. Since $P_x^2 = 1$, we indeed are working with a $\mathbb{Z}_2$ symmetry. As discussed in the last chapter, this is the Wilson-Fisher fixed point.

In one dimension, this problem can be solved exactly: There is a map from spin-1/2 degrees of freedom to spinless fermions, similar to the bosonization mapping. This is the Jordan-Wigner transformation:

$$\sigma_i^x = 2c_i^\dagger c_i - 1 \,, \tag{3.41}$$

$$\sigma_i^{x,-} \equiv \frac{1}{2}(\sigma_i^z + i\sigma_i^y) = B_i c_i \quad ; \quad B_i = \exp\left(i\pi \sum_{j=1}^{i-1} c_j^\dagger c_j \right) \,, \tag{3.42}$$

$$\sigma_i^{x,+} \equiv \frac{1}{2}(\sigma_i^z - i\sigma_i^y) = B_i c_i^\dagger \,, \tag{3.43}$$

The intuition is as follows: Spinless fermions, on each site, can be in two states: $|0\rangle$, empty, and $c^\dagger|0\rangle = |1\rangle$, full. We can identify those as eigenstates of the σ^x operator, $\sigma^x|\leftarrow\rangle = -|\leftarrow\rangle$ and $\sigma^x|\rightarrow\rangle = |\rightarrow\rangle$, respectively. Then, the spin flip operators (in this basis) $\sigma^{x,-}$ and $\sigma^{x,+}$ now destroy/create fermionic particles, $\sigma^{x,-} \sim c$ and $\sigma^{x,+} \sim c^\dagger$. However, since this is defined on the lattice, we need to be careful about the operators and states. The fermionic operators must satisfy the already foreshadowed fermionic algebra:

$$\{c_i, c_j^\dagger\} = \delta_{ij} \quad ; \quad \{c_i, c_j\} = \{c_i^\dagger, c_j^\dagger\} = 0 \tag{3.44}$$

(the fermion fields $\psi_{L/R}$ satisfy a similar version in the continuum). Thus, to construct proper fermionic states out of the "bosonic" nature of spin states, we add the non-local "string" operator B_i, involving a sequence of fermion operators in other sites. It can be checked that the spin algebra in eq. (2.37) and eq. (3.44) are satisfied concurrently.

Therefore, we rewrite the hamiltonian in terms of fermions, where periodic boundary conditions are considered:

$$H_{\text{TFIM}} = -\sum_i \left[(c_i^\dagger - c_i)(c_{i+1}^\dagger + c_{i+1}) + 2g\, c_i^\dagger c_i - g\right] \tag{3.45}$$

$$= -\sum_i \left[c_i^\dagger c_{i+1} + c_{i+1}^\dagger c_i + (c_i^\dagger c_{i+1}^\dagger + c_{i+1} c_i) + 2g\, c_i^\dagger c_i\right] , \tag{3.46}$$

where the g constant term is dropped out in the second line, since we are not interested in the exact expression for the ground state energy, but excitations. This is a "free fermion" hamiltonian, where all operators are quadratic. The terms in the parentheses are called "pairing terms", and are similar to the BCS pairing $c_{i,\uparrow}^\dagger c_{i,\downarrow}^\dagger +$ h.c in superconductors. Indeed, a similar effect occurs here. But, for pedagogical purposes, let us drop such terms and call this simplified hamiltonian $\bar{H}_{\text{TFIM}}$. we have:

$$\bar{H} = -\sum_i \left[c_i^\dagger c_{i+1} + c_{i+1}^\dagger c_i + 2g\, c_i^\dagger c_i\right] . \tag{3.47}$$

This is a tight-binding chain, where the fermions feel an on-site potential $V_0 = 2g$, and hop around nearest neighbors with an energy scale $t = 1$. Due to periodic boundary conditions and translational invariance, we can introduce momentum modes:

$$c_j = \frac{1}{\sqrt{N}} \sum_{k=-\pi/a}^{\pi/a} e^{ikaj} c_k , \tag{3.48}$$

By choosing $a = 1$, we have:

$$\bar{H} = \sum_{-\pi<k\pi} \bar{\varepsilon}(k)\, c_k^\dagger c_k , \tag{3.49}$$

where $\bar{\varepsilon}(k) = -2\cos(k) - 2g$. Ground state properties are obtained by filling the negative energy modes on this band. For $g < 1$, as depicted in Fig. 3.1, we have, at two points $k = \pm k_F$, gapless excitations. This is very different from the expected gapped domain walls, studied in Sec. 2.1. This already shows that the pairing terms cannot be ignored. Before tackling the full problem, let us try to extract the low energy degrees of freedom of eq. (3.49). By expanding $\bar{\varepsilon}$:

$$\bar{\varepsilon}(k) \simeq \pm v_F(k \mp k_F) + \cdots \ , \tag{3.50}$$

where we have used that $\bar{\varepsilon}(k_F) = 0$, and $v_F = 2\sin(k_F)$. In the above equation, we are expanding around both $\pm k_F$ points. Therefore, both contributions must be accounted in the hamiltonian:

$$\bar{H} \simeq \sum_{k=-\pi}^{\pi} v_F(k - k_F)\ c_k^\dagger c_k - \sum_{k=-\pi}^{\pi} v_F(k + k_F)\ c_k^\dagger c_k \tag{3.51}$$

$$\simeq \sum_k v_F k(c_{k,R}^\dagger c_{k,R} - c_{k,L}^\dagger c_{k,L}) \ . \tag{3.52}$$

In the last line, the momenta were redefined to $-\infty < k < \infty$, since only the k modes which are relevant are near the $\pm k_F$ points, and relabelled $c_{k+k_F} \sim c_{k,L}$ and $c_{k-k_F} \sim c_{k,R}$. As already implicit in the notation, this is a relativistic Dirac fermion: In real space, one can take $k \to -i\partial_x$ as the quantum mechanical operator, and define $\psi_{L,R}(\mathbf{x})$ as the Fourier transform of $c_{k,L/R}$ operators. We then get the Dirac hamiltonian:

$$\bar{H} \simeq \int \mathrm{dx}\ i v_F(\psi_L^\dagger \partial_x \psi_L - \psi_R^\dagger \partial_x \psi_R) = \int \mathrm{dx}\ i v_F \psi^\dagger \sigma^3 \partial_x \psi \ , \tag{3.53}$$

which is the hamiltonian derived from the action in eq. (3.14). This means this gapless phase of $\bar{H}$ is the $c = 1$ CFT, which, by bosonization, is the gaussian fixed point. We will show in the next section that there is a distinct quantum spin chain with gaussian criticality.

Consider then again the pairing terms. In retrospect, a symmetry analysis show that those terms need to be there. In eq. (3.47), there is a continuous $U(1)$ symmetry, corresponding to the conservation of the total fermion number $N = \sum_i c_i^\dagger c_i$, labelling the states counting how many fermions they are. At low energies, this symmetry is promoted to a $U(1)_L \times U(1)_R$ symmetry. However, the original H_{TFIM} does not possess any continuous symmetry at the lattice. Indeed, the effect of the pairing term is breaking the $U(1)$ down to a $\mathbb{Z}_2$ fermion parity symmetry, which is the fermionic form of P_x. The exact solution invokes what are known as *Majorana fermions*:

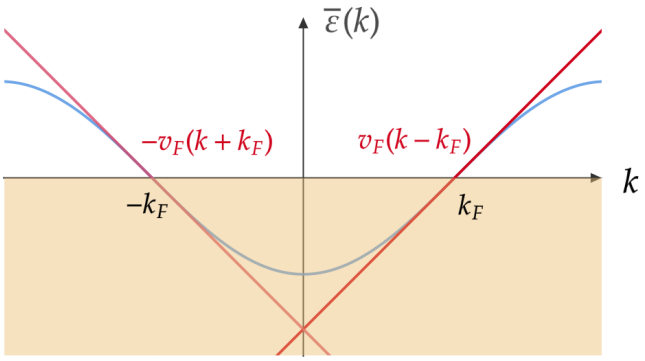

Figure 3.1: Linearization of the dispersion around $\pm k_F$. In blue, it is plotted $\bar{\varepsilon}(k)$. In red, we have the Dirac branches corresponding to left and right-moving fermions. This approximation is justified, since all negative energy states are filled (depicted in light orange), and low-energy fluctuations are well-approximated by considering only linear contributions at $\pm k_F$.

$$c_i = \frac{1}{2}(a_i + ib_i) \ , \tag{3.54}$$

where it can be shown that $a_i^\dagger = a_i$ and $b_i^\dagger = b_i$, and both satisfy $\{a_i, a_j\} = \{b_i, b_j\} = 2\delta_{ij}$, $\{a_i, b_j\} = 0$. They are also called "real fermions", since particles and holes are identified. The hamiltonian is then written as:

$$H_{\text{TFIM}} = i \sum_j \left(a_{j+1} b_j + g b_j a_j\right) \ . \tag{3.55}$$

Introducing momentum modes a_k and b_k by following eq. (3.48), the Brillouin zone is cut by half: The "reality conditions" on the Majoranas impose $a_k^\dagger = a_{-k}$ and $b_k^\dagger = b_{-k}$. Defining $a_k = (\chi_{k,L} + \chi_{k,R})/\sqrt{2}$ and $b_k = (\chi_{k,L} - \chi_{k,R})/\sqrt{2}$ and expanding near a gapless point, we arrive at:

$$H_{\text{TFIM}} \simeq \int \mathrm{dx}\, i \left[v_F(\chi_L \partial_x \chi_L - \chi_R \partial_x \chi_R) + m \chi_R \chi_L\right] \ , \tag{3.56}$$

where $\chi_R(\mathbf{x})$ and $\chi_L(\mathbf{x})$ are the Majorana fields in the continuum, and $m \propto |g-1|$ is a fermion mass: This generates a mass gap in the spectrum, which, due to relativistic invariance, is of the form $\varepsilon(k) = \sqrt{k^2 + m^2}$. At $m = 0$, we obtain a pair of massless chiral Majorana fermions, which we claim is the CFT which describes the WF fixed point in $1+1$ dimensions.

This is also known as the Ising CFT. There is no need to compute its central charge: One can build two copies of chiral Majorana fermions from a chiral Dirac pair by introducing $\psi_{L/R} = (\chi_{L/R} + i\xi_{L/R})/2$, where χ and ξ are Majorana fields. By direct computation, eq. (3.53) reduces to the above equation with $m = 0$. Therefore, by the addition property of the central charge, $c^{(M)} = c^{(D)}/2 = 1/2$.

The Ising CFT has interesting properties and operators. For example, even if the lattice spin operators are non-local in terms of the fermions, the corresponding scaling dimensions can, in fact, be computed. It is well-described by the LGW paradigm: Even if the theory has a "fractionalized" description in terms of fermionic degrees of freedom, it lives on an ordered-disordered phase transition.

3.2 Ordered-ordered transitions in one dimension

Due to the singular nature of quantum phases in one dimension, it is maybe unsurprising to find out that there are universal continuous phase transitions between ordered phases. A canonical example is the XY chain:

$$H_{\mathrm{XY}} = -\sum_i (\sigma_i^y \sigma_{i+1}^y + J\sigma_i^z \sigma_{i+1}^z) \,, \tag{3.57}$$

taking $J > 0$. A straightforward analysis shows a $y-$ferromagnetic phase for $J \to 0$ with $\langle \sigma_i^y \rangle \neq 0$, breaking $P_z : \sigma_i^{x,y} \to -\sigma_i^{x,y}$ and $P_x : \sigma_i^{y,z} \to -\sigma_i^{y,z}$, and a $z-$ferromagnetic phase, at $J \to \infty$ with $\langle \sigma_i^z \rangle \neq 0$, breaking $P_y : \sigma_i^{x,z} \to -\sigma_i^{x,z}$ and $P_x : \sigma_i^{y,z} \to -\sigma_i^{y,z}$. Both phases break time reversal. By the LGW analysis, this falls into the two-order parameter example with a $\mathbb{Z}_2 \times \mathbb{Z}_2$ group structure, since $P_z = P_x P_y$. Henceforth, it predicts a first-order transition generically. This model can also be solved exactly with the Jordan-Wigner transformation and Majorana fermions. We will only be interested in the physics near the transition. By doing the same steps as the TFIM, the corresponding fermionic hamiltonian is written as:

$$H_{\mathrm{XY}} = -\sum_i \left[(J+1)(c_i^\dagger c_{i+1} + c_{i+1}^\dagger c_i) + (J-1)(c_i^\dagger c_{i+1}^\dagger + c_{i+1} c_i) \right] \,, \tag{3.58}$$

For $J = 1$, the pairing terms disappear and we have the same model as eq. (3.47) with $g = 0$. The low energy limit is identical, and we have gapless Dirac fermions

at $\pm k_F = \pm\pi/2$. To compute the effect of the pairing term at the transition, there is a standard trick to construct low-energy operators from the lattice expression: In eq. (3.48), all momenta in the Brillouin zone contribute equally. However, since the Dirac modes $\psi_{L/R}$ dominate at low energies, one may consider the contributions at $k = \pm k_F$. In real space, this means:

$$c_j \sim e^{ik_F x_j}\psi_R(x_j) + e^{-ik_F x_j}\psi_L(x_j)\ . \tag{3.59}$$

Therefore, in the continuum, there is an induced pairing between right and left-moving fermions:

$$H_{\rm XY} \simeq \int \mathrm{dx}\ \left[iv_F\psi^\dagger\sigma^z\partial_x\psi + i\delta\ \left(\psi_R^\dagger\psi_L^\dagger - \psi_L\psi_R\right)\right]\ , \tag{3.60}$$

where $\delta \propto (J-1)\sin k_F$ and $v_F \propto (J+1)\sin k_F$. By taking $\delta < 0$ or $\delta > 0$, the pairing generates a mass for the fermions, entering the gapped ordered phases. Using bosonization clarifies the physical interpretation. In App. A, the Jordan-Wigner transformation and bosonization formulas are combined to write the lattice spin operators in terms of the compact bosons (φ, θ) (ignoring oscillating terms which are not relevant for this model):

$$\sigma_j^x \sim \frac{2}{\sqrt{\pi}}\partial_x\varphi \tag{3.61}$$

$$\sigma_j^y \sim -\sqrt{\frac{2}{\pi}}\sin\left[\sqrt{\pi}\left(\theta - \frac{\sqrt{\pi}}{4}\right)\right] \tag{3.62}$$

$$\sigma_j^z \sim \sqrt{\frac{2}{\pi}}\cos\left[\sqrt{\pi}\left(\theta - \frac{\sqrt{\pi}}{4}\right)\right]\ . \tag{3.63}$$

By using the bosonization dictionary, eq. (3.60) is rewritten as:

$$H_{\rm XY} \simeq \int \mathrm{dx}\ \left\{\frac{v_F}{2}\left[(\partial_x\theta)^2 + (\partial_x\varphi)^2\right] - \frac{\delta}{\pi}\ \sin\left(\sqrt{4\pi}\theta\right)\right\}\ . \tag{3.64}$$

The corresponding euclidean action can be obtained, by invoking $T-$duality to remove the φ boson:

$$\mathcal{S}_{\rm XY} = \int \mathrm{d}^2\mathrm{x} \left[\frac{v_F}{2}(\nabla\theta)^2 - g_0 \cos\left(\sqrt{4\pi}\theta\right)\right] , \tag{3.65}$$

where $g_0 = \delta/\pi = (J-1)/\pi$. This action is of the form of a sine-gordon model [79], and appear quite frequently in the long-distance physics of spin chains. In general, one proceeds to also consider symmetry-allowed higher order vertex operators which are not generated on the lattice, and then the renormalization group equations are computed. Since $\sin\left(\sqrt{4\pi}\theta\right) = (\tilde{V}_{\sqrt{4\pi}} - \text{h.c})/2i$, the corresponding scaling dimension can be read from eq. (3.8): $(\sqrt{4\pi})^2/4\pi = 1 < 2$. Therefore, the first-order term in the beta function is $\beta(g) = g$. In this example, the results agrees with the naive expectation from a semiclassical analysis: Interpret $-g_0 \sin\left(\sqrt{4\pi}\theta\right)$ as a potential for the compact boson. For $g_0 < 0$, $J < 1$, the minima for $\theta \in [0, 2\sqrt{\pi})$ are $\theta_0 = 3\sqrt{\pi}/4, 7\sqrt{\pi}/4$, which yields the $y-$ordered ferromagnetic phase $\langle\sigma^y\rangle \neq 0$, $\langle\sigma^z\rangle = 0$. On the other hand, for $g_0 > 0$, one has $\theta_0 = \sqrt{\pi}/4, 5\sqrt{\pi}/4$, corresponding to the $z-$ordered phase $\langle\sigma^y\rangle = 0$, $\langle\sigma^z\rangle \neq 0$. For $\delta = 0$, a continuous phase transition then emerges, with central charge $c = 1$. We will refer to this transition as a $\mathrm{FM}_y - \mathrm{FM}_z$ transition. By changing the overall sign in eq. (3.57), both phases transform into Néel antiferromagnetic phases in the y and z directions, breaking also translation symmetry. The overall conclusion stays the same, and in the $\mathrm{Neel}_y - \mathrm{Neel}_z$, there is a Dirac cone in the spectrum.

Stating that this transition is beyond the LGW paradigm is premature, since its stability must be proven to discard a fine-tuned transition. Fortunately, it was recently shown that such transitions occur in much more general quantum spin chains [5, 32, 33], both with field theory arguments and strong numerical evidence. We can encapsulate the general form as the $J_1 - J_2$ XYZ spin chain :

$$H_{J_1-J_2\ \mathrm{XYZ}} = \sum_{l=1,2}\sum_j J_l[\sigma^x_j\sigma^x_{j+l} + \Delta_y\sigma^y_j\sigma^y_{j+l} + \Delta_z\sigma^z_j\sigma^z_{j+l}] , \tag{3.66}$$

where J_1, J_2 are the energy scales for first and second neighbor interactions, respectively. Using the tools that we have been developing, we will discuss the phases and transitions which emerge in this model and how the DQC phenomenology emerges in those models.

Let us state the phase diagram results. Let $\mathcal{J} = J_2/J_1$, and take all parameters $\mathcal{J}, \Delta_y, \Delta_z$ as positive. The XYZ hamiltonian is recovered for $\mathcal{J} = 0$, which has

an exact solution using the Bethe ansatz [81]. The corresponding phase diagram is shown at the $\Delta_y - \Delta_z$ plane in Fig. 3.2: There are three Néel phases, pointing on each of the three spin directions, depending on the dominant coupling in eq. (3.66). It must be symmetric under Δ_y and Δ_z, since a spin rotation around the $x-$axis can map each point to another. The transitions are all $c = 1$ with the emergent $U(1) \times U(1)$ symmetry structure. However, at $\Delta_y = \Delta_z = 1$, this is promoted to a $SU(2) \times SU(2)$ symmetry, described by the WZW theory of the Heisenberg chain [82]. In all such transitions, a lattice spin rotation symmetry is "doubled" to a larger emergent symmetry. This indeed already shows that the LGW-evading conclusion in the XY chain is robust, corresponding to any of the $\text{Neel}_\alpha/\text{Neel}_\beta$ transitions.

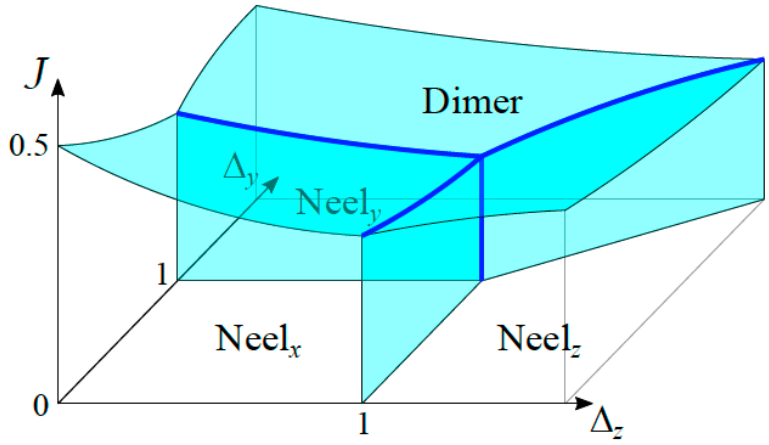

Figure 3.2: Phase diagram of the $J_1 - J_2$ XYZ chain defined in eq.(3.66). The light blue planes indicate the $c = 1$ transitions, with a $U(1) \times U(1)$ symmetry. At the isotropic point $\Delta_y = \Delta_z = 1$, this is promoted to a $SU(2) \times SU(2)$ symmetry. Image from [5].

More interesting is the case where second neighbor interactions are considered, $\mathcal{J} > 0$. For $\mathcal{J} \gg 1$, in the rotationally symmetric limit where $\Delta_y = \Delta_z = 1$, singlets are formed on every two sites, forming a dimerized phase, a one-dimensional valence bond solid [31]. Away from this limit, the dimers may not be perfect singlets anymore (not perfectly rotation-invariant), but are stable. In the phase diagram in Fig. 3.2, the dimerized phase emerges near $\mathcal{J} \simeq 0.5$. In the $\text{Neel}_{x,y,z}$ to VBS transitions, there is a $U(1) \times U(1)$ $c = 1$ theory. This is quite special: A whole plane in this phase diagram has a fully emergent continuous symmetry, since there is only $\mathbb{Z}_2 \times \mathbb{Z}_2$ in general. All transitions are indeed LGW-forbidden, being continuous at the boundary of ordered phases.

We will sketch the field theory construction. Consider then the XYZ hamilto-

nian, for $J_2 = 0$:

$$H_{\rm XYZ} = J_1 \sum_j [-\tilde{\sigma}^x_j \tilde{\sigma}^x_{j+1} - \Delta_y \ \tilde{\sigma}^y_j \tilde{\sigma}^y_{j+1} + \Delta_z \ \sigma^z_j \sigma^z_{j+1}] \ , \tag{3.67}$$

where we have defined $\tilde{\sigma}^{x,y}_j = (-1)^j \sigma^{x,y}_j$. Consider now $\Delta_z \ll \Delta_y$. In the Jordan Wigner transformation, we can consider the quantization axis on the $z-$direction, where $\sigma^z = 2c^\dagger_j c_j - 1$, and the spin flip operators are $\tilde{\sigma}^\pm = (\tilde{\sigma}^x \pm i\tilde{\sigma}^y)/2$.

The XYZ hamiltonian is then written as:

$$H_{\rm XYZ} = -J_1 \sum_j [(1+\Delta_y)(c^\dagger_i c_{i+1} + c^\dagger_{i+1} c_i) + (1-\Delta_y)(c^\dagger_i c^\dagger_{i+1} + c_{i+1} c_i) - \Delta_z \sigma^z_i \sigma^z_{i+1}] \ . \tag{3.68}$$

The first two terms reduce to the XY chain with $\Delta_y = J$. The continuum limit of the last term can be computed from the bosonized version of σ^z, adding the contribution from the oscillating term:

$$\sigma^z_i \sigma^z_{i+1} \sim \frac{4}{\pi} (\partial_x \varphi)^2 - \frac{4}{\pi^2} \cos\left(\sqrt{16\pi}\varphi\right) \ . \tag{3.69}$$

The first term renormalizes the Gaussian part, and the second term is another deformation to the fixed point. Writing $H_{\rm XYZ} = \int {\rm dx} \ \mathcal{H}_{\rm XYZ}$, the corresponding hamiltonian density is written:

$$\mathcal{H}_{\rm XYZ} = \frac{v}{2} \left[K(\partial_x \theta)^2 + K^{-1} (\partial_x \varphi)^2\right] - g_0 \ \sin\left(\sqrt{4\pi}\theta\right) - \lambda_0 \ \cos\left(\sqrt{16\pi}\varphi\right) \ , \tag{3.70}$$

where $g_0 \propto (\Delta_y - 1)$, and:

$$\frac{vK}{2} \simeq J_1 v_F \ , \tag{3.71}$$

$$\frac{v}{2K} \simeq J_1 \left(v_F + \frac{8\Delta_z}{\pi^2}\right) \ , \tag{3.72}$$

$$\lambda_0 = J_1 \frac{4\Delta_z}{\pi^2} \ . \tag{3.73}$$

There are three order parameters:

$$\langle \sigma_j^x \rangle \sim (-1)^j \left\langle \sin\left(\sqrt{\pi}\tilde{\theta}\right) \right\rangle \ , \tag{3.74}$$

$$\langle \sigma_j^y \rangle \sim (-1)^j \left\langle \cos\left(\sqrt{\pi}\tilde{\theta}\right) \right\rangle \ , \tag{3.75}$$

$$\langle \sigma_j^z \rangle \sim (-1)^j \left\langle \cos\left(\sqrt{4\pi}\varphi\right) \right\rangle \ , \tag{3.76}$$

where we have defined $\tilde{\theta} = -\theta + \sqrt{\pi}/4$. The competition between deformations coming from $\tilde{V}_{\sqrt{4\pi}}$ and $V_{\sqrt{16\pi}}$, with scaling dimensions $1/K, 4K$ respectively, generates all three Néel phases. For small Δ_z, $K \leq 1$, the λ_0 term is irrelevant, and there is a $\text{Neel}_x/\text{Neel}_y$ phase transition due to the g_0 term, which is relevant. However, the K-parameter also flows in a Luttinger liquid. If one starts in the transition line in $\Delta_y = 1$, there is a critical value of Δ_z beyond which $K \to 0$ at long distances. In this limit, λ_0 flows to positive values and the Neel_z phase appears in the vacua $\varphi = 0, \sqrt{\pi}/2$. Since the same phenomenology must be found by perturbing the $\text{Neel}_z/\text{Neel}_x$ phase transition by switching $\Delta_y \leftrightarrow \Delta_z$, there is also a $c = 1$ transition line in this case. Moreover, we find the special point where $\Delta_y = \Delta_z = 1$, which fixes $K = 1/2$: For a spin-rotation symmetric ground state, $\langle \sigma_i^x \sigma_j^x \rangle = \langle \sigma_i^y \sigma_j^y \rangle = \langle \sigma_i^z \sigma_j^z \rangle$. Since $\langle \tilde{V}_{\sqrt{\pi}}(x) \tilde{V}_{-\sqrt{\pi}}(0) \rangle \sim |x|^{-1/(4K)}$ and $\langle V_{\sqrt{4\pi}}(x) V_{-\sqrt{4\pi}}(0) \rangle \sim |x|^{-K}$, equating the exponents enforce the condition on the Luttinger parameter.

With suitable renormalizations, eq. (3.70) also can describe the physics for $J_2 \neq 0$. To show this carefully, it is necessary to expand all four-fermion terms into chiral fermions and then use the bosonization formulas, we will just state the results. The second neighbor interactions renormalizes K, g_0, λ_0 as:

$$\frac{1}{2}\delta(vK) \simeq -J_1 \frac{8}{\pi^2}\mathcal{J} \ , \tag{3.77}$$

$$\frac{1}{2}\delta\left(\frac{v}{K}\right) \simeq J_1 \frac{8}{\pi^2}\mathcal{J} \ , \tag{3.78}$$

$$\delta\lambda_0 \simeq -J_1 \frac{4(\Delta_z + b)\mathcal{J}}{\pi^2} \ . \tag{3.79}$$

Where b is a non-universal coefficient which depends on lattice details. The main difference from this equations is that now one can have $\lambda_0 < 0$. For sufficient large $\mathcal{J}$, $K \to 0$, and λ_0 becomes negative and large, while the g_0 becomes irrelevant.

This occurs generically, and kills off all three Néel phases. The vacua correspond to $\varphi = \sqrt{\pi}/4, 3\sqrt{\pi}/4$. By expanding into bosonic operators, it can be shown that this corresponds to the VBS phase, where:

$$(-1)^j \langle \boldsymbol{\sigma}_j \cdot \boldsymbol{\sigma}_{j+1} \rangle \sim \left\langle \sin\left(\sqrt{4\pi}\varphi\right) \right\rangle \neq 0 \ . \tag{3.80}$$

The phase transition occurs in a plane in the phase diagram, and occurs also for $J_1 < 0$, where $\text{Neel}_\alpha \to \text{FM}_\alpha$ [32]. It was numerically found to be described by the $U(1) \times U(1)$ $c = 1$ theory where $g_0, \lambda_0 = 0$ written in eq. (3.70) [5, 33]. This is the dimerized phase referred in Fig. 3.2. To investigate how this emergent symmetry may arise, consider the Neel_z/VBS transition. At low energies, each order parameter is written in terms of chiral fermions bilinears (ignoring oscillating terms):

$$N(x) = (-1)^j \sigma^z_j \sim \psi^\dagger_R \psi_L(x) + \text{h.c} = \psi^\dagger \sigma^1 \psi \ , \tag{3.81}$$

$$D(x) = (-1)^j \boldsymbol{\sigma}_j \cdot \boldsymbol{\sigma}_{j+1} \sim -i\psi^\dagger_L \psi_R + \text{h.c} = \psi^\dagger \sigma^2 \psi \ . \tag{3.82}$$

Both order parameters behave as a mass term for the chiral fermions. Indeed, interactions between chiral fermions in the hamiltonian are of the form $\mathcal{H}_{\text{int}} \sim D(x)N(x)$. Therefore, one can consider a trial mean-field hamiltonian given by:

$$\mathcal{H}_{\text{M.F}} = iv\psi^\dagger \sigma^3 \partial_x \psi + N(x)\ \psi^\dagger \sigma^2 \psi + D(x)\ \psi^\dagger \sigma^1 \psi \ . \tag{3.83}$$

Notice that this procedure still mantains the $U(1)_V : \psi \to e^{i\lambda}\psi$ symmetry of chiral fermions, enhanced to the full $U(1)_V \times U(1)_A$ symmetry if $N = D = 0$, which corresponds to the phase transition. Consider a regime deep into any of the two phases, where $N \neq 0$ or $D \neq 0$. For concreteness, consider the dimer (VBS) phase. The low energy states are such that $D(x) = \text{const.}$. Excitations corresponds to deformations of $\varphi(x)$. Invoking the results of Sec. 2.1, we know that it must be domain walls between the two degenerate VBS states. Jackiw and Rebbi solved the two-dimensional Dirac equation with a domain wall mass term [83], and found that there exist zero modes (i.e: Localized solutions with no energy cost) of the form:

$$\psi(x) = e^{-\int_{-\infty}^{x} \mathrm{dx}'\ D(x')} \psi_0 \ , \tag{3.84}$$

for $D(-\infty) \to 0$. Therefore, this domain wall can be considered as a Dirac fermion wavepacket: Another manifestation of bosonization. Take the soliton to connect $\varphi(-\infty) = \sqrt{\pi}/4$ and $\varphi(\infty) = 3\sqrt{\pi}/4$. Near the origin, $\varphi(0) \simeq \sqrt{\pi}/2$, nucleating one of the degenerate Néel states, see Fig. 3.3. Similar behaviour occurs if a domain wall is constructed in the Néel phase. This "dual description" is notoriously similar to what we have found in the two-dimensional Néel/VBS transition: Defects of the Néel phase (monopoles) host the order parameter of the VBS on their core. It also works in the other way around: A careful analysis of a vortex constructed at the boundary of the fourfold degenerate VBS phases nucleates a spinon [84].

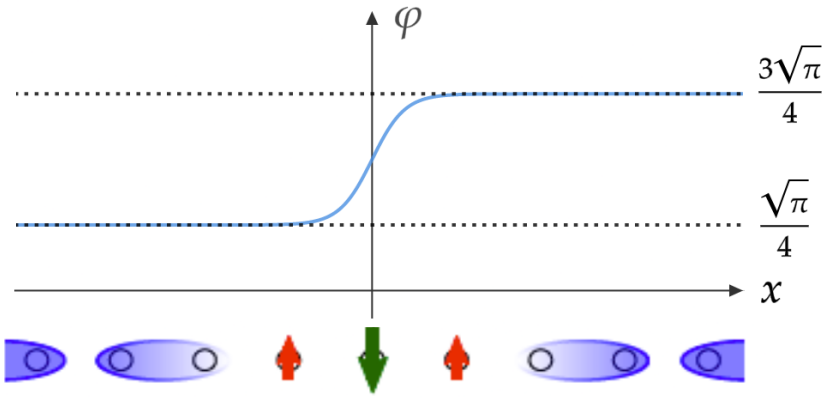

Figure 3.3: Solitons/Domain walls deep in the VBS phase. As the field tunnels between degenerate states, the order parameter of the Néel state is non-zero. Image adapted from [5].

In one dimension, there are a simpler incarnation of monopole operators, local in the original variables. In this model, those can be constructed explicitly [5], alas must be redefined for the Neel$_{x,y}$/VBS transitions, since they involve pinning the dual boson θ on a side of the transition, and φ in another. A unified description is then complicated, since the dual bosons are the shift generators of each other. Jiang and Motrunich [32] discussed this issue at length for the FM$_z$/VBS transitions, and discussed how to construct different effective theories where the duality is manifested.

In the next chapter, we will switch gears to discuss the role of time-reversal symmetry in spin models, and construct a quasi-1D model realizing novel gapped phases. All the properties discussed here, such as the emergent symmetries, deconfined transitions and the corresponding field theoretic discussion will appear in the field theory treatment in Chapter 5.

Chapter 4

The zigzag chain and the chiral state

In this chapter, our focus will be on the construction of chiral phases, non-magnetic time-reversal breaking in one dimension. First, we will present an exactly solvable model with a exponentially degenerate ground state. In the second section, after an interlude discussing the construction of chiral spin states, we show that there is a class of deformations of the solvable model which generates a chiral spin state as the ground state. We then conclude by showing that this phase is stable to perturbations, and the corresponding excitations can condense to generate a distinct symmetry-breaking phase.

In the first section, [6] is followed. The results in the second section were already derived in [39], albeit using different methods. The last two sections constitute original work.

4.1 Chiral Spin State

Time-reversal is, in some sense, a special symmetry. Consider a spin-1/2 degree of freedom.Intuitively defined to be generated by $\left(\prod_i e^{-i\frac{\pi}{2}\sigma_i^y}\right) K$, where K denotes complex conjugation, it flips the sign of the spin operator in any basis. Its antiunitary nature aided by the fact that the generator squares to -1 for a single spin, leads to the Kramers theorem [85, 86]: Let $|E\rangle$ be a eigenstate with energy E constructed from a $\mathcal{T}$-invariant hamiltonian H. It follows not only that $\mathcal{T}|E\rangle$ is also an energy E eigenstate, but also that $\langle E|\mathcal{T}|E\rangle = 0$: The energy spectrum must then be at least doubly degenerate.

For a many-body spin systems, time-reversal breaking can be seen in the simplest example of a doubly-degenerate ferromagnet: In order to split up the degeneracy, the intuitive perturbation is a magnetic field, which breaks time-reversal explicitly. Clearly all magnetic phases have this property, since $\langle \boldsymbol{\sigma}_i \rangle \neq 0$ breaks $\mathcal{T}$. However, one may ask if non-magnetic phases also realizes $\mathcal{T}$-breaking. In a two-dimensional square lattice, consider a spin hamiltonian which has $SU(2)$ spin symmetry, a lattice parity and time-reversal. Let us define the *scalar spin chirality* operator on three lattice sites defined by i, j, k:

$$\chi_{ijk} = \boldsymbol{\sigma}_i \cdot (\boldsymbol{\sigma}_j \times \boldsymbol{\sigma}_k) \ . \tag{4.1}$$

If probed on three spins of a square plaquette, one can see that this operator is odd under a lattice inversion. Furthermore, it is odd under time-reversal, since it involves an odd number of spins. However, it is a scalar under $SU(2)$ spin rotations. The given task is to find a hamiltonian with such symmetries, whose ground state is simultaneously non-magnetic $\langle \boldsymbol{\sigma} \rangle = 0$ and chiral $\langle \chi \rangle \neq 0$. The construction given by Wen *et al.* [6] is as follows: Consider first the following hamiltonian on the square lattice:

$$H = J[(\boldsymbol{\sigma}_1 + \boldsymbol{\sigma}_2 + \boldsymbol{\sigma}_3 + \boldsymbol{\sigma}_4)^2 + (\boldsymbol{\sigma}_5 + \boldsymbol{\sigma}_6 + \boldsymbol{\sigma}_7 + \boldsymbol{\sigma}_8)^2 + \cdots] \ , \tag{4.2}$$

for $J > 0$. Such exchange terms are spatially separated plaquettes, see Fig 4.1. The above expression is then a sum of decoupled four spin hamiltonians, and therefore can be solved exactly. The ground state on each plaquette are then singlets formed from the four spins. It can be shown there are two degenerate ground states per plaquette. One has then an exponential degeneracy of $2^{N/4}$ states, where N is the number of spins on the lattice.

By construction, such states are also chirality eigenstates for any triangle defined on the unit cell. That is, they can be labelled by $\{|\chi_0\rangle, |-\chi_0\rangle\}$, where $\chi_0 = 2\sqrt{3}$. One can then think of each plaquette as effective Ising variables for the chiralities. Thus, they can be coupled to construct a chiral state:

$$H' = -Q[\chi_{123}\chi_{567} + \chi_{123}\chi_{9,10,11} + \cdots] = -Q \sum_{\langle I,J \rangle} \chi_I \chi_J \ , \tag{4.3}$$

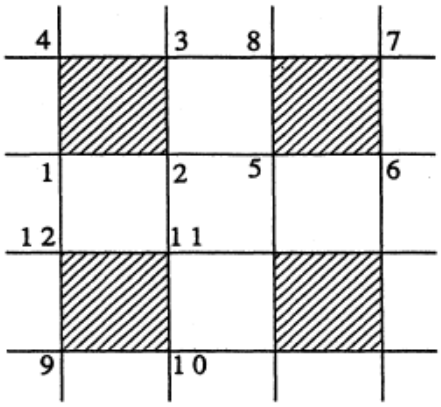

Figure 4.1: Shaded plaquettes indicating the four spin terms in the square lattice. Figure from [6].

where $Q > 0$ and I, J labels the triangular plaquettes. For $H + H'$, the exponential degeneracy is lifted, and we have a twofold degenerate ground state, spanned by: $\otimes_p |\chi_0\rangle_p$ and $\otimes_p |-\chi_0\rangle_p$, where p labels each plaquette. This is the two dimensional chiral spin state.

4.2 Kitaev tetrahedral Chain

We will introduce a one dimensional model, where our interest lies. This is a compass model [87], where each bond on the chain has an Ising-like interaction $\sigma_i^\alpha \sigma_j^\alpha$ in a definite spin direction α

$$H_{\text{tet}} = \sum_{\alpha=x,y,z} J_\alpha \sum_{\langle ij \rangle_\alpha} \sigma_i^\alpha \sigma_j^\alpha \ , \tag{4.4}$$

where $J_\alpha > 0$, pictorially shown in Fig. 4.2. The geometry is coined as the tetrahedral chain, since unit cells form a tetrahedral shape.

Let us list the symmetries present in this hamiltonian: There is time reversal $\mathcal{T} : \boldsymbol{\sigma} \to -\boldsymbol{\sigma}$, present in any Ising-type hamiltonian with bilinear interactions $\sigma_i^\alpha \sigma_j^\beta$, a lattice C_2 rotation symmetry $\mathcal{R} : \{\boldsymbol{\sigma}_{1,A} \leftrightarrow \boldsymbol{\sigma}_{2,B} \ ; \ \boldsymbol{\sigma}_{1,B} \leftrightarrow \boldsymbol{\sigma}_{2,A} \ ; \ j \to -j\}$, and a set of spin π rotation symmetries which we will call Klein rotations $\mathcal{K}_1$ and $\mathcal{K}_2$, since $\mathcal{K}_1 \times \mathcal{K}_2 \simeq \mathbb{Z}_2 \times \mathbb{Z}_2$, the Klein group. Acting on a unit cell, the explicit action is given as:

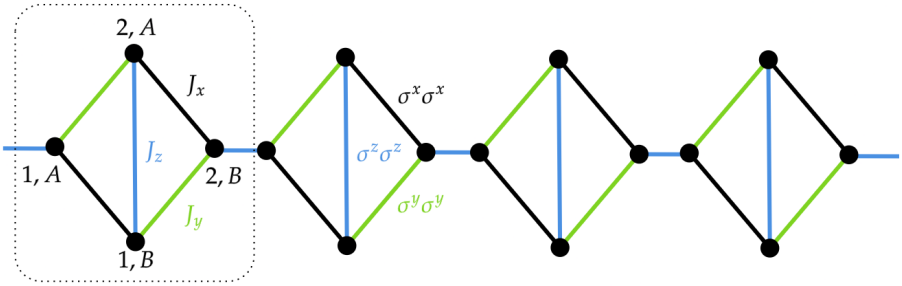

Figure 4.2: Figure of the tetrahedral chain, where the unit cell is highlighted, along with the four sublattices $(1,A),(2,A),(1,B),(2,B)$. A color scheme is adopted: black, green and blue bonds corresponds to the presence of x, y, z Ising interactions, respectively.

$$\mathcal{K}_1 : \begin{cases} \left(\sigma^x_{1,A}, \sigma^y_{1,A}, \sigma^z_{1,A}\right) \to \left(-\sigma^x_{1,A}, -\sigma^y_{1,A}, \sigma^z_{1,A}\right) \\ \left(\sigma^x_{1,B}, \sigma^y_{1,B}, \sigma^z_{1,B}\right) \to \left(-\sigma^x_{1,B}, \sigma^y_{1,B}, -\sigma^z_{1,B}\right) \\ \left(\sigma^x_{2,A}, \sigma^y_{2,A}, \sigma^z_{2,A}\right) \to \left(\sigma^x_{2,A}, -\sigma^y_{2,A}, -\sigma^z_{2,A}\right) \\ \boldsymbol{\sigma}_{2,B} \to \boldsymbol{\sigma}_{2,B} \end{cases}$$
$$\mathcal{K}_2 : \begin{cases} \boldsymbol{\sigma}_{1,A} \to \boldsymbol{\sigma}_{1,A} \\ \left(\sigma^x_{1,B}, \sigma^y_{1,B}, \sigma^z_{1,B}\right) \to \left(\sigma^x_{1,B}, -\sigma^y_{1,B}, -\sigma^z_{1,B}\right) \\ \left(\sigma^x_{2,A}, \sigma^y_{2,A}, \sigma^z_{2,A}\right) \to \left(-\sigma^x_{2,A}, \sigma^y_{2,A}, -\sigma^z_{2,A}\right) \\ \left(\sigma^x_{2,B}, \sigma^y_{2,B}, \sigma^z_{2,B}\right) \to \left(-\sigma^x_{2,B}, -\sigma^y_{2,B}, \sigma^z_{2,B}\right) \end{cases} \tag{4.5}$$

The idea behind this action is to construct spin rotations preserving each bilinear on the bonds. Kimchi and Vishwanath [88] discussed this group in detail in the context of Kitaev-Heisenberg model, where $\mathcal{K}$ acts as a duality, mixing Kitaev and Heisenberg couplings. If the hamiltonian is defined on a finite general lattices, it was found that the duality exists if the number of x, y and z bonds are all even or odd. Indeed, it can be checked that the tetrahedral chain satisfies this condition. Furthermore, in the choice of parameters where the Klein group becomes a symmetry, it was conjectured that there might be a phase where it is spontaneously broken down to $\mathbb{Z}_2$, without breaking any other symmetries.

Note the quantum nature of the ground state of eq. (4.4): Each bond favors a different Ising direction, thus frustrating the spins on the lattice sites: For general $J_{x,y,z}$, there is no clear semi-classical description. However, it is exactly solvable. In the original paper, the authors introduced Jordan-Wigner fermions, in similar sprit to what was done in the last chapter. We will adopt an alternative description, where four Majorana flavors are introduced:

$$\sigma_j^\alpha = i b_j^\alpha a_j \quad ; \quad \alpha = x, y, z \ . \tag{4.6}$$

The four operators b^x, b^y, b^z, a satisfy the Majorana fermionic algebra discussed in the context of the transverse field Ising model. This mapping was first introduced by Kitaev [27], in a different two-dimensional honeycomb model with the same structure of a trivalent lattice with each bond containing the x, y and z interactions. We will then denote eq. (4.4) as the Kitaev tetrahedral model or the tetrahedral chain.

There is a "doubling" of degrees of freedom: For Jordan Wigner fermions, the decomposition holds two Majorana modes, referred as b_j, a_j in the last chapter. This means that states constructed from this four-Majorana construction must satisfy some constraint: mappings of spin operators into fermion or bosonic modes of this sort, are called *partons* [24], and generally have some occupation constraint. Indeed, in this case, physical states must satisfy $D = b^x b^y b^z a = 1$ [27]. By combining this relation with the fermionic algebra, one can check that the spin operators satisfy the defining algebra. By substituting (4.6) in (4.4), one can write:

$$H_{\text{tet}} = \sum_{\alpha=x,y,z} J_\alpha \sum_{\langle i,j\rangle_\alpha} \left(-i b_i^\alpha b_j^\alpha\right) i a_i a_j = \sum_{\alpha=x,y,z} J_\alpha \sum_{\langle ,ij\rangle_\alpha} u_{ij}^\alpha i a_i a_j \ , \tag{4.7}$$

where we have defined $u_{jk}^\alpha \equiv -i b_j^\alpha b_k^\alpha$. At first sight, this looks like a quartic hamiltonian, describing how the Majorana modes scatter, and, therefore, not solvable. However, one can check that $[u_{ij}^\alpha, H_{\text{tet}}] = 0$. Thus, this fermion bilinear is conserved on each bond. Henceforth, the fermion spectrum is divided into $u_{ij}^\alpha = \pm 1$ sectors. The excess of degrees of freedom causes a redundancy, manifested as a $\mathbb{Z}_2$ gauge symmetry: letting $u_{ij}^\alpha \to \zeta_i u_{ij}^\alpha \zeta_j$ and $a_i \to \zeta_i a_i$ for $\zeta_i = \pm 1$, leaves the hamiltonian invariant. Physically, this means that one can think of this problem as a Majorana fermion a_i hopping around a background defined by a $\mathbb{Z}_2$ gauge field. To evaluate the physical spin configurations, we must identify what spin operators commute with the hamiltonian to establish the gauge invariant states. On every unit cell, there are two *flux operators* (also called Wilson loops) defined on the triangular plaquettes, see Fig. 4.3. Those are written as:

$$W_{j,1} = \prod_{\langle i,j\rangle_\alpha \in \triangleleft} u_{ij}^\alpha = \sigma_{j,1,A}^z \sigma_{j,1,B}^y \sigma_{j,2,A}^x \quad ; \quad W_{j,2} = \prod_{\langle i,j\rangle_\alpha \in \triangleright} u_{ij}^\alpha = \sigma_{j,1,B}^x \sigma_{j,2,B}^z \sigma_{j,2,A}^y \ . \tag{4.8}$$

It can be verified that $[W_{j,1}, H_{\text{tet}}] = [W_{j,2}, H_{\text{tet}}] = 0$. Those are the operators on which the physical spectrum is classified. The unitary generators of the Klein symmetry can also be expressed in terms of the flux:

$$U_1 = \prod_j W_{j,1} \quad ; \quad U_2 = \prod_j W_{j,2} \ , \tag{4.9}$$

which can be verified by direct computation of $U_{1,2}^\dagger \boldsymbol{\sigma} U_{1,2}$. The Klein generators then measures the "flux parity".

Finding a ground state corresponds to minimizing the ground state energy with respect to $\{W_{j,1}, W_{j,2}\}_j$. That is, given some flux configuration, in eq. (4.7), define the hamiltonian matrix:

$$h_{ij} = \begin{cases} J_\alpha u_{ij}^\alpha & \text{if } \langle i,j \rangle \text{ is a type } \alpha \text{ bond} \ , \\ 0 & \text{otherwise} \ . \end{cases} \tag{4.10}$$

One can show on general grounds that a quadratic Majorana hamiltonian can be brought to the usual form of free complex fermions with $H_{\text{tet}} = \sum_k \varepsilon_k (c_k^\dagger c_k - 1/2)$, where ε_k are the eigenvalues of h_{ij} [27]. The ground state energy is then $E = -1/2 \sum_k \varepsilon_k$. Then, by fixing the lattice structure with N sites, and picking a gauge field configuration to match a flux distribution, eq. (4.10) can be diagonalized. The surprising result is the presence of an emergent exponential degeneracy: All states satisfying the condition:

$$W_{j,1} = W_{j,2} \ , \tag{4.11}$$

have the same energy. Therefore, for a given energy, there is a 2^{N_c}-dimensional Hilbert space, where N is the number of spins and $N_c = N/4$ is the number of unit cells. This is a sign of a phase instability in the tetrahedral chain: Any operator coupling locally to a chirality in a unit cell would lift this degeneracy. We will address this problem in the next section.

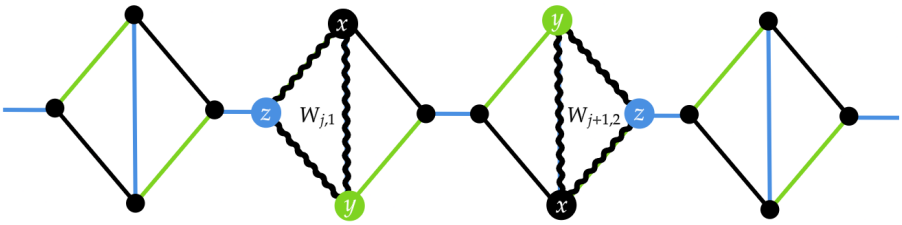

Figure 4.3: Definition of flux operators on the tetrahedral chain: They are defined on each of the two triangular plaquettes on every unit cell.

4.3 1d Chiral Spin State

Let us go back to the tetrahedral chain. We want to identify the exponentially degenerate ground state manifold with a simpler hamiltonian. This can be archieved by dropping the $\sigma^z\sigma^z$ terms connecting different unit cells in Fig. 4.2. Then H_{tet} becomes a sum of unit cell hamiltonians, involving four spins each, of the form:

$$H_{\text{tet}}^{\text{u.c}} = J_x(\sigma^x_{1,A}\sigma^x_{1,B} + \sigma^x_{2,A}\sigma^x_{2,B}) + J_y(\sigma^x_{1,A}\sigma^x_{2,A} + \sigma^x_{1,B}\sigma^x_{2,B}) + J_z\ \sigma^z_{2,A}\sigma^z_{1,B}\ , \tag{4.12}$$

which can be numerically diagonalized. Of course, $W_1 = \sigma^z_{1,A}\sigma^y_{1,B}\sigma^x_{2,A}$ and $W_2 = \sigma^x_{1,B}\sigma^z_{2,B}\sigma^y_{2,A}$ remain good quantum numbers. In general, a twofold degenerate ground state is found, corresponding to the flux eigenstates on the triangular plaquettes $W_1 = W_2 = \pm 1$. We define a basis $\{|u_1\rangle, |u_2\rangle\}$, chosen such that:

$$P^{-1}W_1P = P^{-1}W_2P = \tau^y\ , \tag{4.13}$$

where $P = \sum_{a=1,2} |u_a\rangle\langle u_a|$ is the ground state projector, and τ^y is the y-component of a pseudospin describing the two energy levels on each unit cell. One can then define $|\pm\rangle = (|u_1\rangle \pm i|u_2\rangle)/\sqrt{2}$ as the flux eigenstates. For concreteness, we write the results for the isotropic case where $J_\alpha = J$ as:

$$|u_1\rangle = \frac{1}{\sqrt{6}}\left(|\downarrow\downarrow\uparrow\uparrow\rangle + |\downarrow\uparrow\downarrow\uparrow\rangle - |\downarrow\uparrow\uparrow\downarrow\rangle - |\uparrow\downarrow\downarrow\uparrow\rangle + |\uparrow\downarrow\uparrow\downarrow\rangle + |\uparrow\uparrow\downarrow\downarrow\rangle\right)\ , \tag{4.14}$$

$$|u_2\rangle = \frac{1}{\sqrt{6}}\left(|\downarrow\downarrow\downarrow\downarrow\rangle + |\downarrow\downarrow\uparrow\uparrow\rangle - |\downarrow\uparrow\downarrow\uparrow\rangle - |\uparrow\downarrow\uparrow\downarrow\rangle + |\uparrow\uparrow\downarrow\downarrow\rangle + |\uparrow\uparrow\uparrow\uparrow\rangle\right)\ . \tag{4.15}$$

Therefore, by considering this particular limit, we already have the $2^{N/4}$ degeneracy. The previous construction in two dimensions suggests then a perturbation to $H_{\rm tet}$ to stabilize a chiral phase of the form:

$$-Q\sum_{I,J} W_I W_J \ , \tag{4.16}$$

coupling flux operators on different unit cells. We choose to couple the flux operators as:

$$H^1_{\rm CSS} = H_{\rm tet} - Q_1 \sum_j W_{j,1} W_{j+1,2} \ , \tag{4.17}$$

For $Q_1 > 0$, the ground state is a one-dimensional chiral spin state, with the same properties as the two-dimensional case described in the last section: time reversal is spontaneously broken, and flux operators are ordered in a twofold degenerate ground state. In terms of the Majoranas, $Q_1 \neq 0$ induces a uniform background flux into the gauge fields u^α_{ij}. By diagonalizing eq. (4.7), one obtains the dispersion of the a_i fermions in such a background. Any choice of $\{u^\alpha_{ij}\}$ will do, provided that it generates one of the two ground states $\{W_{j,1} = W_{j,2} = 1\}_j$, $\{W_{j,1} = W_{j,2} = -1\}_j$. Explicity writing all the terms:

$$\begin{aligned} H_{\rm tet} = i\sum_{j=1}^{N/4}[\ & a_{j,1,A}\,(J_x u_{1,A;1,B}\ a_{j,1,B} + J_y u_{1,A;2,A}\ a_{j,2,A}) + \\ & + a_{j,1,B}\,(J_z u_{1,B;2,A}\ a_{j,2,A} + J_y u_{1,B;2,B}\ a_{j,2,B}) + \\ & + J_x u_{2,A;2,B}\ a_{j,2,A} a_{j,2,B} + J_z u_{2.B;1,A}\ a_{j,2,B} a_{j+1,1,A}]\ , \end{aligned} \tag{4.18}$$

where $u_{M;M'}$ is the gauge field in the link connecting sublattices M and M'. In the above equation, we have already assumed uniformity in the background on the unit cells. For concreteness, consider the following gauge choice:

$$u_{1,A;1,B} = u_{2,B;1,A} = u_{1,B;2,A} = u_{1,B;2,B} = u_{2,A;2,B} = 1 \tag{4.19}$$

$$u_{1,A;2,A} = -1 \ . \tag{4.20}$$

It can be checked that this indeed holds $W_{j,1} = W_{j,2} = 1$. The translation invariance can be exploited to define momentum modes. Let:

$$a_{j,M} = \sqrt{\frac{2}{N/4}} \sum_{k=-\pi}^{\pi} e^{ikj} a_{k,M} \ . \tag{4.21}$$

Note that the momentum modes at k are dependent on the mode defined on $-k$, as briefly commented in the solution of the TFIM: the reality condition $a_i^\dagger = a_i$ implies $a_k^\dagger = a_{-k}$. It can be checked that given $k, q \in [-\pi, \pi)$, $\{a_{k,M}, a_{q,M'}\} = \delta_{k,-q}\delta_{M,M'}$. Therefore, $\{a_{k,M}, a^\dagger_{q,M'}\} = \delta_{k,q}\delta_{M,M'}$, which is the usual fermionic algebra defined on the momentum space. This means that if one works in half of a Brillouin zone (say $k \in [0, \pi)$), where independent Majorana modes are defined, one can treat the quadratic Majorana hamiltonian as an ordinary free fermion hamiltonian, filling up the bands to construct the spectrum.

Given that there are four sublattices, a four-component spinor is defined:

$$A_k = \begin{pmatrix} a_{k,1,A} \\ a_{k,1,B} \\ a_{k,2,A} \\ a_{k,2,B} \end{pmatrix} \ . \tag{4.22}$$

Eq. (4.7) can then be rewritten in a uniform background as:

$$H_{\text{tet}} = \sum_{0<k<\pi} A_k^\dagger \, h_{\text{tet}}(k) \, A_k \equiv \sum_{0<k<\pi} A_k^\dagger \, 2i \begin{pmatrix} 0 & J_x & -J_y & -J_z e^{-ik} \\ -J_x & 0 & J_z & J_y \\ J_y & -J_z & 0 & J_x \\ J_z e^{ik} & -J_y & -J_x & 0 \end{pmatrix} A_k \ , \tag{4.23}$$

where we are counting only the modes on half of the Brillouin zone. We can now treat A_k as a complex fermion spinor and obtain the spectrum by diagonalizing the above matrix. The obtained energy spectrum is given as:

$$\varepsilon(k) = \pm 2 \sqrt{(J_x^2 + J_y^2 + J_z^2) \pm 2|J_z| \sqrt{J_x^2 + J_y^2} \cos\left(\frac{k}{2}\right)} \ . \tag{4.24}$$

The four bands corresponds to choosing the signs inside and outside the square root. The energy gap Δ, defined as the difference between the negative bands and the minimum of the positive energy bands is shown in Fig. 4.4, alongside with the plot of the spectrum in three distinct cases. For $J_x^2 + J_y^2 > J_z^2$ or $J_x^2 + J_y^2 < J_z^2$, there is an energy gap between the filled states with $\varepsilon(k) < 0$ and empty states. This is what we expect for a symmetry-breaking phase. However, for $J_x^2 + J_y^2 = J_z^2$, a gapless point occurs at $k = 0$, indicating a continuous phase transition!

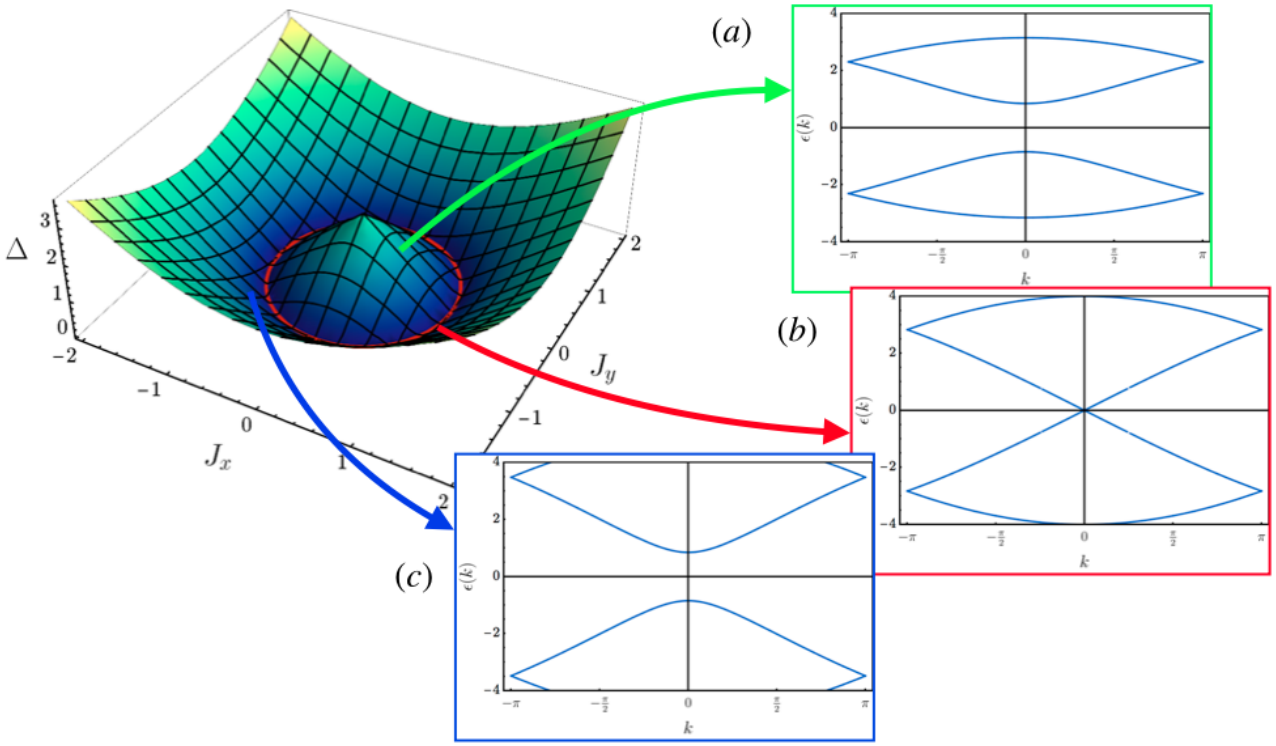

Figure 4.4: Energy gap and spectrum of a fermions. (a) and (c): Gapped spectrum at the topological and trivial phases, respectively; (b): Gapless spectrum at the critical region.

This is a surprise, since one expects a gapped phase by stabilizing the exponential degeneracy. Note the similarity with the TFIM: By writing the spin variables as real (Majorana) fermions (by introducing non-locality in the Jordan-Wigner transformation or redundancy in the parton approach), a gapless spectrum in the fermions indicates a continuous phase transition between two different one-dimensional phases (a ferromagnet-paramagnet transition in the Ising model). Less discussed, however, was the interpretation of each gapped side in terms of the fermions. This is a subtle matter, and is an example of a *topological* phase transition. "Topological" refers here to the absence of a local order parameter. On a side of the transition, both models are an example of a one-dimensional topological superconductor [89], and

the fermions behave as a trivial insulator on the other side. They are distinguished by the Majorana number [90]:

$$\mathcal{M} = \text{sgn}\left(\text{Pf } h_{\text{tet}}(0)\right) \text{sgn}\left(\text{Pf } h_{\text{tet}}(\pi)\right) \ , \tag{4.25}$$

where Pf is called the Pfaffian, a function of skew-symmetric matrices which squares to the determinant and can be numerically evaluated [91]. By numerically evaluating the Pfaffian in the first quantized hamiltonian at $k = 0, \pi$, we find that $\mathcal{M} = -1$ for $J_x^2 + J_y^2 < J_z^2$, which corresponds to the topological superconductor phase, and $\mathcal{M} = 1$ for $J_x^2 + J_y^2 > J_z^2$, characterizing the insulating phase.

There is an interesting interpretation of such a number, supporting the "topological" denomination: If open boundary conditions are considered in the $\mathcal{M} = -1$ phase, it is found that there are two degenerate energy levels sitting at $E = 0$, whose wavefunctions are exponentially localized on the corresponding boundaries of the chain. Those are *Majorana zero modes*, and they cannot exist in isolation, since we have determined that real fermions are half of a complex fermion (on which it is possible to construct a Hilbert space). In the case of the TFIM, this topological phase maps to the usual symmetry breaking phase: A pair of Majoranas at the ends of the chain are paired up to construct a two-dimensional Hilbert space, representing the two degenerate states in the ferromagnetic phase. The insulating state, where the Majorana fermions are all paired up and filling the negative-energy bands, is the trivial paramagnet state.

For the perturbed tetrahedral chain, we already know that it must have a twofold degeneracy from the ordering of the fluxes. Furthermore, the mapping between the Majorana states and spin states is more subtle due to the nature of the parton construction, as explained below. Since our interest lies in the overall properties of the symmetry-breaking state and its transitions, we will focus our efforts on understanding the $J_x^2 + J_y^2 > J_z^2$ region of the phase diagram, which we will continue to refer as the chiral spin state or chiral state. In the rest of this chapter, we work in the isotropic limit $J_x = J_y = J_z = J > 0$, and the physics of both the complementary region $J_x^2 + J_y^2 < J_z^2$ and corresponding transition will be discussed in the fifth chapter.

Let us now turn to excitations, which can be created by the Majorana modes b^α, a. The ground state is spanned by $|U_\pm\rangle \otimes |\Omega\rangle$, where $|U_\pm\rangle$ are the gauge field

configurations giving the uniform flux states, and $|\Omega\rangle$ is the filled Fermi sea of a fermions in the half Brillouin zone. Naively, excited states are constructed by defining $a_k^\dagger|\text{gs}\rangle$, and so forth. However, there is an important subtlety: only gauge invariant sates satisfying $D = 1$ are allowed [92]. If $|\text{gs}\rangle$ is in the ground state, the first non-trivial states which can be constructed are $b_i^\alpha a_i|\text{gs}\rangle$, since $a_i \to \zeta_i a_i$ and $b_i^\alpha \to \zeta_i b_i^\alpha$.

It can be checked that if the site i is a corner of one of the two triangles in the unit cell, $b_i^\alpha a_i|\text{gs}\rangle \propto \sigma_i^\alpha|\text{gs}\rangle$ will carry the opposite flux. We will refer to such states as vortex excitations. In order to construct them explicitly, we must study the spectrum in the presence of flux insertions. First, let us consider again the ground state with $W_{j,1/2} = 1$, and periodic boundary conditions. The first non-trivial excitation one can think of is a *single vortex*, drawn in Fig. 4.5(a): A particular flux on a triangle is flipped, and a vortex is created if the spin operator acts on $1, A$ or $2, B$. A second type of excitation is a *vortex pair*, where the flux of both triangles are flipped, as shown in Fig 4.5(b). It can be created by the action of a single spin operator on $1, B$ and $2, A$, for example.

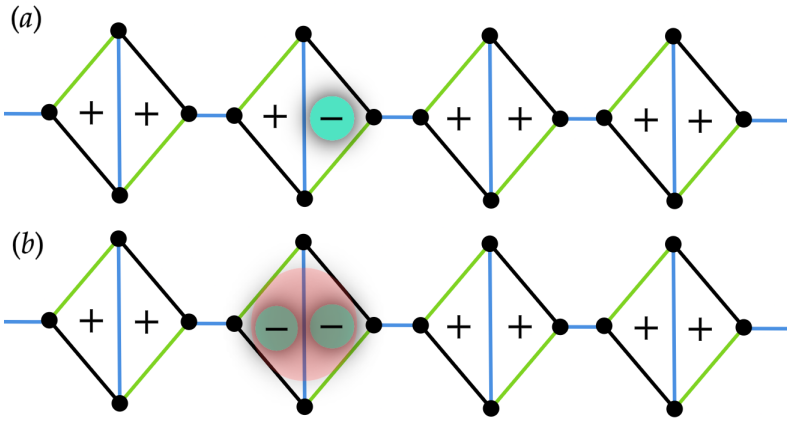

Figure 4.5: A (a) single vortex and (b) vortex pair in the uniform ground state. The ± labelling in the plaquettes corresponds to $W = \pm 1$.

At first, this distinction seems trivial: flux operators provide a $\mathbb{Z}_2$ classification for the excitations: the sign of the fluxes indicate the presence/absence of a vortex, and one can understand a vortex pair as two single vortices bound together, costing twice the energy. This, however, does not happen in general. Remember that H_{tet} had an exponential degeneracy: In fact, the ground state condition corresponds to the proliferation of vortex pairs: $W_{j,1}W_{j,2} = 1$. In contrast, a single vortex has a finite energy gap of $\simeq 0.29J$, computed by numerically diagonalizing eq. (4.10)

flipping a flux operator in a uniform background.

Since our interest lies in the chiral spin state, this picture must be understood for $Q_1 > 0$. Since the coupling of the flux is just like a classical Ising model, the values of the energy costs for each excitation in Fig 4.5 is readily evaluated:

$$\text{Single vortex}: \quad \Delta_v^{(\mathrm{a})} = 0.29J + 2Q_1 \ , \tag{4.26}$$

$$\text{Vortex pair}: \quad \Delta_v^{(\mathrm{b})} = 4Q_1 \ . \tag{4.27}$$

$$\tag{4.28}$$

For $Q_1 \ll J$, vortex pairs remains the low energy excitations, albeit now gapped. In the opposite regime $Q_1 \gg J$, single vortices costs less energy, and take the place as the first excited states. That is, there is an energy level crossing at $Q_1^* \approx 0.15J$.

We will be interested, however, in open boundary conditions. Since we are dealing with a symmetry-broken phase in one spatial dimension, the natural excitations in this case are domain walls, as explained in Sec. 2.1. Indeed, domain walls with a vortex pair interface, as shown in Fig. 4.6, cost energy $\Delta_{\mathrm{dw}} = 2Q_1$, lower than both $\Delta_v^{(\mathrm{a})}, \Delta_v^{(\mathrm{b})}$. We then conclude that, in this limit, gapped domain walls dominate the bottom part of the spectrum.

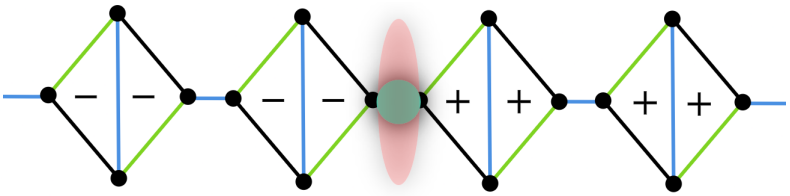

Figure 4.6: A domain wall between the two degenerate ground states of the chiral spin state.

4.4 Zigzag chain

In order to estabilish the chiral spin state as a stable phase, it is necessary to study perturbations. We choose to preserve the quoted symmetries of the tetrahedral chain, by studying a particular perturbation:

$$\delta H = J'_x \sum_j \sum_{l=1,2} \sigma^x_{j,l,B} \sigma^x_{j+1,l,A} \ , \tag{4.29}$$

transforming the tetrahedral chain into a "zigzag chain", with the full hamiltonian

$$H_1 = H_{\rm tet} - Q_1 \sum_j W_{j,1} W_{j,2} + J'_x \sum_j \sum_{l=1,2} \sigma^x_{j,l,B} \sigma^x_{j+1,l,A} \ , \tag{4.30}$$

see Fig. 4.7(a). This choice is motivated by the Kitaev model on the triangular lattice, where the hamiltonian is of the form of eq. (4.4), where the Ising bonds are distributed equally between the six nearest-neighbors of the lattice. One can see then this zigzag chain as a strip of the full lattice, see Fig. 4.7(b). There is an ongoing debate on the nature of its ground state: Early numerical studies pointed to a nematic phase [93, 94], but recent work showed convincing numerical evidence that there is an antiferromanetic stripe-ordered phase [95]. Therefore, our model is of interest even for $Q_1 = 0$, since it can shine light on ground state properties in one higher dimension in a simpler environment.

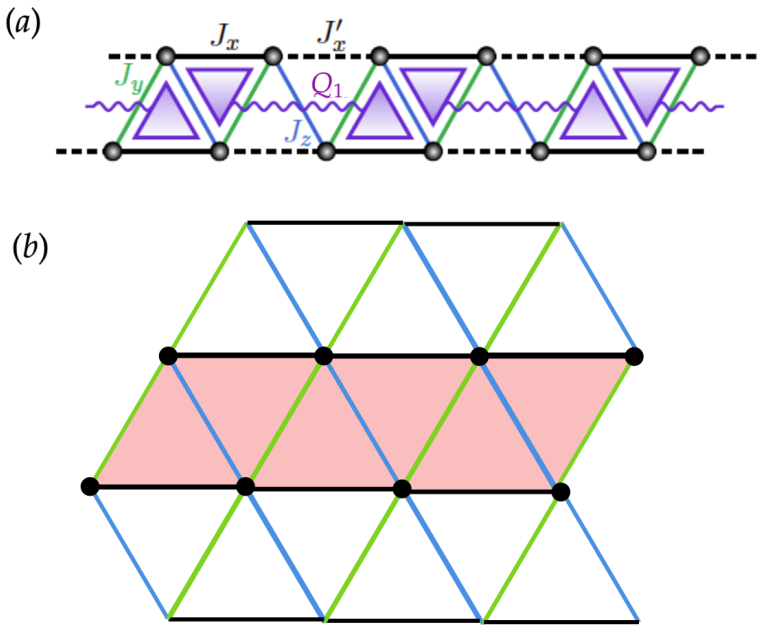

Figure 4.7: (a) Zigzag chain highlighting all terms in the hamiltonian, (b) The zigzag chain as a strip of a triangular lattice, highlighted in red.

In this section, we will study the perturbative limit where $J'_x, Q_1 \ll J$. To

deal with the exponential degeneracy of the ground states for $Q_1 = J'_x = 0$, we will use degenerate perturbation theory, following in similar steps as [27]. Consider $H = H_0 + V$, where H_0 is an unperturbed hamiltonian and V is a perturbation. We seek H_{eff}, called the effective hamiltonian, which describes the physics of H_0 eigenstates due to the perturbation V. It can be shown that the effective hamiltonian can be obtained from the expansion:

$$H_{\text{eff}} = E_0 + P^{-1}\left(V + VG'_0V + VG'_0VG'_0V + \cdots\right)P \,, \tag{4.31}$$

where E_0 is the ground state energy, and $G'_0 = (E_0 - H_0)^{-1}$ is the Green's function, where the $'$ indicates that $G'_0 = 0$ if acted on the ground state, and is non-trivial otherwise. Take H_0 to be the sum of decoupled unit cells, each described by eq. (4.12), with each site having a local Hilbert space spanned by $\{|u_1\rangle, |u_2\rangle\}$. However, to do perturbation theory, the full spectrum must be numerically computed. The idea is that, in the expansion above, the perturbation V generates excitations in the ground state, whose energy cost is measured by each factor of $G'_0 \sim -(\Delta E)^{-1}$. By creating and removing such excitations, we are left with an operator acting on the ground state manifold.

The perturbation V accommodates all the perturbations left out of H_0:

$$V = J\sum_j \sigma^z_{j,2,B}\sigma^z_{j+1,1,A} + J'_x\sum_j\sum_{l=1,2}\sigma^x_{j,l,B}\sigma^x_{j+1,l,A} - Q_1\sum_j W_{j,2}W_{j+1,1} \,. \tag{4.32}$$

The first term might be worrying, since is controlled by a "large energy scale". However, as argued in the exact solution, the exponential degeneracy still remains if this term is present. In fact, we will compute H_{eff} up to second order, and this term only leads to a correction to the ground state energy, which will be ignored.

The first order term acts as a pseudospin Ising term:

$$H^{(1)}_{\text{eff}} = P^{-1}VP = -Q_1\sum_j \tau^y_j\tau^y_{j+1} \,, \tag{4.33}$$

as derived from eq. (4.13). Ordering τ^y corresponds to the chiral spin state, and the corresponding excitations are vortex pairs. Note that single vortices are not

captured by degenerate perturbation theory, since we are probing energetics with the constraint $W_{j,1} = W_{j,2}$. No further non-trivial first order terms are generated. The second order terms are computed by evaluating the matrix elements:

$$\langle a|H_{\text{eff}}^{(2)}|b\rangle = \langle a|VG_0'V|b\rangle = \sum_{n\notin \text{G.S}} \langle a|V|n\rangle \frac{1}{E_0 - E_n}\langle n|V|b\rangle \ , \tag{4.34}$$

where $|n\rangle$ are the excited eigenstates of H_0, and $|a\rangle, |b\rangle$ are two elements of the ground state basis. There is no need to compute a $2^{N/4}$-dimensional matrix: Note that every perturbation is a sum over terms of the form:

$$V^{\text{pair}} = \lambda\, O_1 \otimes O_2 \ , \tag{4.35}$$

where O_1, O_2 acts on neighboring unit cells, and λ is an energy scale. For example, for the flux coupling, $O_1 = W_{j,2}$, and $O_2 = W_{j+1,1}$. Since all perturbations only couple neighboring unit cells, the sum over excited states and $|a\rangle, |b\rangle$ can be decomposed into a product of two excited states of individual unit cells, and $|u_1\rangle, |u_2\rangle$, respectively. At second order, one can then just compute the matrix elements:

$$\begin{aligned}\langle u_a, u_b|H_{\text{eff}}^{\text{pair}}|u_c, u_d\rangle = \lambda\lambda' \sum_{n_1,n_2\notin \text{G.S}} &\langle u_a|O_1|n_1\rangle\langle u_b|O_2|n_2\rangle\times \\ &\times \frac{1}{E_0 - E_{n_1} - E_{n_2}}\langle n_1|O_1'|u_c\rangle\langle n_2|O_2'|u_d\rangle \ ,\end{aligned} \tag{4.36}$$

where $a, b, c, d = 1, 2$, and the double sum is over excited states of a single unit cell. The primed index distinguishes between two different terms generating the perturbation. By computing the above matrix elements, one can write this $2^2 = 4$-dimensional matrix in the pseudospin basis of the corresponding unit cells:

$$H_{\text{eff}}^{\text{pair}} = \lambda\lambda' \sum_{\alpha,\beta} c_{\alpha,\beta}\tau_1^\alpha\tau_2^\beta \ , \tag{4.37}$$

the dimensionless coefficients $c_{\alpha\beta}$ are given by $c_{\alpha,\beta} = \text{Tr}(\tau_1^\alpha\tau_2^\beta H_{\text{eff}}^{\text{pair}})/(4\lambda\lambda')$. By evaluating those matrix elements, it turns out that the only non-trivial contribution comes from the J_x' term:

$$H_{\text{eff}}^{(2)} = \frac{(J'_x)^2}{J} \sum_j \left[c_{x,x} \tau_j^x \tau_{j+1}^x + c_{z,z} \tau_j^z \tau_{j+1}^z + c_{x,z} \left(\tau_j^x \tau_{j+1}^z + \tau_j^z \tau_{j+1}^x \right) \right] , \tag{4.38}$$

which can be rewritten as:

$$H_{\text{tet}} = \frac{(J'_x)^2}{J} \sum_j \boldsymbol{\tau}_j^T \begin{pmatrix} c_{x,x} & 0 & c_{x,z} \\ 0 & 0 & 0 \\ c_{x,z} & 0 & c_{z,z} \end{pmatrix} \boldsymbol{\tau}_{j+1} . \tag{4.39}$$

One can diagonalize this quadratic form by rotating the pseudospin in the y direction, and we get:

$$H_{\text{eff}}^{(2)} = -\frac{(J'_x)^2}{J} \sum_j \left[\alpha \ \tau_j^x \tau_{j+1}^x + \beta \ \tau_j^z \tau_{j+1}^z \right] , \tag{4.40}$$

where $\alpha \simeq 0.90589$ and $\beta \simeq 1.51424 \times 10^{-3}$. Since $\beta/\alpha \sim 10^{-3}$, the second term can be safely discarded. Therefore, the effective hamiltonian up to second order is:

$$H_{\text{eff}} = -\sum_j \left[Q_1 \ \tau_j^y \tau_{j+1}^y + \alpha \frac{(J'_x)^2}{J} \ \tau_j^x \tau_{j+1}^x \right] + \cdots . \tag{4.41}$$

This is nothing more than the XY chain! A new phase transition at $Q_1 \simeq \alpha (J'_x)^2/J$ is predicted from the chiral spin state to a $\langle \tau_j^x \rangle \neq 0$ phase, in the $c = 1$ universality class. However, the pseudospin is a low energy operator, which can be described by multiple "high-energy" operators defined on the lattice scale. If O is an operator defined on the lattice, computing the projected part $P^{-1}OP$ corresponds to constructing all low-energy operators to which it reduces to. Therefore, we can identify the nature of the phase by studying the symmetries of lattice operators which project into τ^x. The most general operator we can construct in a unit cell is $O = \sigma_{j,M_1}^{\alpha} \sigma_{j,M_2}^{\beta} \sigma_{j,M_3}^{\gamma} \sigma_{j,M_4}^{\delta}$, where $M_{1,2,3,4}$ are one of the four sublattices in the unit cell. We list some of the operators which contains τ^x upon projection:

$$P^{-1}\sigma^x_{j,1,A}\sigma^x_{j,2,A}P = P^{-1}\sigma^x_{j,1,B}\sigma^x_{j,2,B}P \sim A_1\tau^x_j + \cdots \tag{4.42}$$
$$P^{-1}\sigma^y_{j,1,A}\sigma^y_{j,1,B}P = P^{-1}\sigma^y_{j,2,A}\sigma^y_{j,2,B}P \sim A_2\tau^x_j + \cdots \tag{4.43}$$
$$\cdots \tag{4.44}$$

$A_{1,2}$ are numerical coefficients. We checked that all of such operators are odd only to $\mathcal{K}_1$ or $\mathcal{K}_2$. In the examples above, both operators are clearly even under time reversal and transform into each other under rotations. Therefore, the symmetry-breaking phase in question has a breaking pattern $\mathcal{K} \simeq \mathbb{Z}_2 \times \mathbb{Z}_2 \to \mathbb{Z}_2$. We will refer to this phase as a *Klein paramagnet* (KPM), since it only breaks the Klein symmetry. This is, indeed, the conjectured phase of [88], and, to our knowledge, it was not found previously in any of the two-dimensional or one-dimensional variants of Kitaev-like models. For concreteness, we will define a corresponding order parameter as:

$$K_{j,N} = \sigma^x_{j,1,N}\sigma^x_{j,2,N} \quad ; \quad N = A, B \ , \tag{4.45}$$

but any of the operators which projects to τ^x is viable.

We can indeed conclude that the chiral spin state is stable, and is not destroyed immediately if a $\mathcal{T}-$preserving perturbation is added. Independently, if one considers the pure zigzag chain for $Q_1 = 0$, the system orders to a time-reversal invariant phase for $J'_x \ll J$. Since it is described by the XY chain, the transition is indeed beyond the LGW paradigm. It is also worth noting the stark difference of the KPM to the stripe ordered phase, obtained in the triangular lattice Kitaev model. However, the comparison to the triangular lattice model is premature, since we are far away from homogeneity $J'_x \simeq J$.

It is interesting to note that the domain walls remain as robust low energy excitations in the presence of small J'_x, now corresponding to an Ising domain wall in the τ^y variable. Similarly, this analysis predicts domain walls in the KPM phase, in the τ^x direction. A continuous transition is then the point where both excitations become gapless. We will later see that the domain wall physics also plays an important role in other transitions.

However, we are interested in the full zigzag chain in eq. (4.30), and numerical confirmation is needed for this transition. Conveniently, the model is one-dimensional, where the method of density matrix renormalization group (DMRG)

[96–98] is effective. The main idea is to construct an ansatz for the ground state by truncating the Hilbert space by ignoring small eigenvalues of the reduced density matrix. The property that allows DMRG to work well in one dimension is twofold: (1) The cost scales polynomially with the number of lattice sites; (2) Gapped, one-dimensional systems have a constant bipartite *entanglement entropy* [47]. This means that a constant number of parameters can be fixed while the system size is increased, since the eigenvalues are directly related to the entanglement entropy.

Entanglement-based probes can also be used to detect quantum phase transitions. In general, one may compute the order parameters of the corresponding phases and study the analytic behaviour at the transition in the scaling limit (taking $N \to \infty$ by studying larger and larger systems sizes) Following earlier work [99], one can point to a phase transition if the largest eigenvalue of the reduced density matrix hits a minimum. For small J'_x and Q_1, this was plotted in Fig. 4.8 along with the transition line computed from perturbation theory. It has very good agreement for small enough values of the parameters, indicating, in fact, a Gaussian second order phase transition.

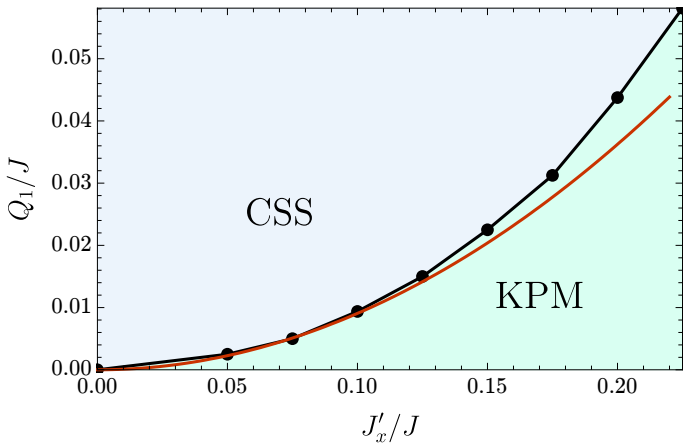

Figure 4.8: Phase diagram for $Q, J'_x \ll J = 1$. DMRG estimates (black dots) are compared to the perturbation theory calculation $Q_1 = \alpha(J'_x)^2/J$ (red line).

DMRG is not constrained to any energy scale. The ground state phase diagram can then be computed for any value of Q, J'_x, shown in Fig. 4.9. Remarkably, a fourfold degenerate stripe-ordered phase emerges for strong enough J'_x, ordering $\langle \sigma^x \rangle \neq 0$. It breaks all symmetries, and is of antiferromagnetic nature, see Fig. 4.10.

It is then confirmed that at the limit $J'_x \simeq J$, the zigzag chain reproduces the results found two-dimensional triangular lattice with an antiferromagnetic stripe phase. Furthermore, at the intersections of the CSS-Stripe, CSS-KPM and KPM-

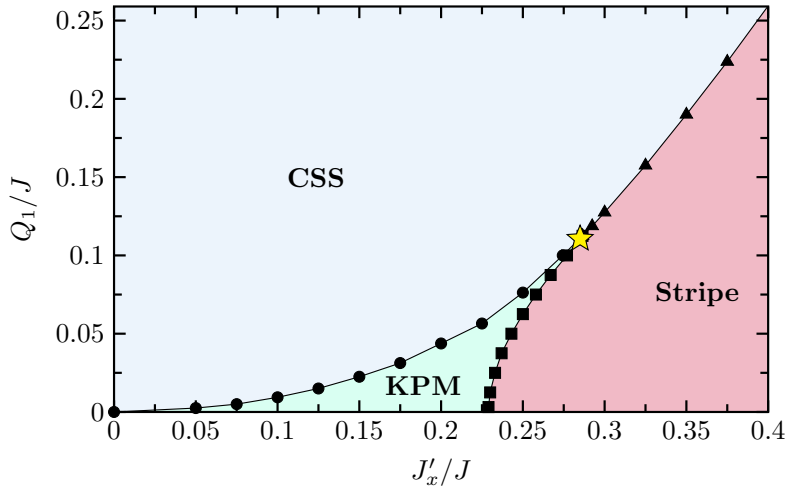

Figure 4.9: Phase diagram of the zigzag chain in the isotropic regime. For small enough J'_x, only the CSS and KPM phases can be seen with the transition between them. For strong enough J'_x, a stripe ordered phase appear. The yellow star pinpoints the tricritical point.

Stripe transitions, a tricritical point is found.

In the big picture of the LGW paradigm, the CSS-Klein transition would be first order or fine-tuned, say, due to $J_x = J_y = J_z = J$, since they live between ordered phases. However, we already see this is not the case: If we take $J_{x,y,z}$ different from each other (keeping $J_x^2 + J_y^2 > J_z^2$), the ground state manifold on which eq. (4.31) is defined remains the same. In the next chapter, we will take a different limit and show that all three transitions can become continuous, and discuss possible exotic transitions.

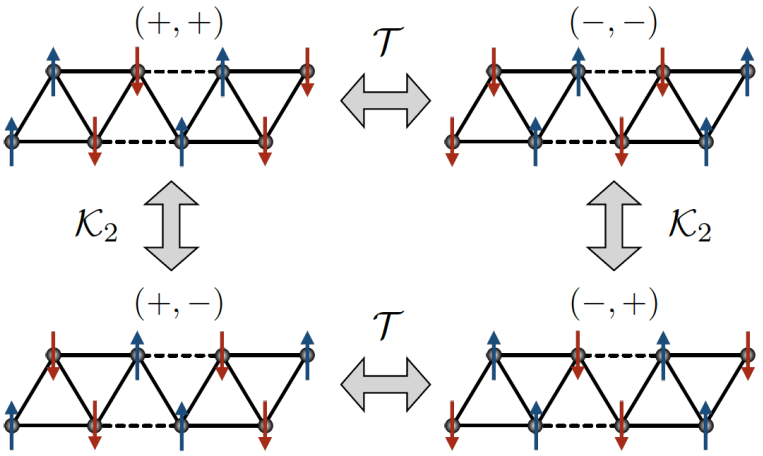

Figure 4.10: The four degenerate ground states of the stripe phase, where the spins are pointing in the σ^x direction. They can be labelled by $(\mathrm{sgn}\langle\sigma^x_{j,1,A}\rangle, \mathrm{sgn}\langle\sigma^x_{j,2,A}\rangle)$, and related by the action of $\mathcal{T}, \mathcal{K}_{n=1,2}$. The states $(+,+)$ and $(-,-)$ explicitly breaks $\mathcal{R}$, meanwhile $(+,-)$ and $(-,+)$ preserves it.

Chapter 5

Phase transitions of the zigzag chain

We will now turn our attention to a different limit of the zigzag chain. In doing so, both the nature of the phase transitions involving the stripe phase and the connection to DQC will become clear. In the first section, we introduce a new set of pseudospins suitable in the anisotropic limit that we are interested in. Following this construction, an effective spin ladder model is obtained, followed by a phase diagram analysis in the second section. We show that all three transitions found in the last chapter are present in the effective model, and the central charge of the KPM-Stripe transition can be obtained. In the third section, the zigzag chain is modified slightly without changing the symmetries. The modification allows a field theory analysis of the CSS-Stripe transition.

All this chapter is composed with original work.

5.1 Pseudospin representation

To further understand the phase transitions, we will study different limits, by relaxing the isotropic condition on the tetrahedral chain. Note a particular aspect of the tetrahedral chain (which is true in general for compass models): If only one of the spin directions is retained, the hamiltonian becomes a classical Ising model on dangling bonds:

$$H_{\text{tet}} \to J_\alpha \sum_{\langle i,j\rangle_\alpha} \sigma_i^\alpha \sigma_j^\alpha \ . \tag{5.1}$$

The ground state is exponentially degenerate where each separate bond is in an antiferromagnetic state between the two spins. It can also be understood as a local conservation law: For every $\langle i,j\rangle_\alpha$ bond, the operator $\sigma_i^\alpha\sigma_j^\alpha$ commutes with the hamiltonian. If other Ising-like interactions are reinstated, fluctuations spoil this conservation law, however weakly if $J_{\beta\neq\alpha} \ll J_\alpha$. We will develop a procedure to construct an effective hamiltonian in this limit. The order parameters for the three symmetry-breaking phases are:

$$\text{Chiral Spin State} \quad W_{j,1} = \sigma^z_{j,1,A}\sigma^y_{j,1,B}\sigma^x_{j,2,A} \quad ; \quad W_{j,2} = \sigma^x_{j,1,B}\sigma^z_{j,2,B}\sigma^y_{j,2,A} \tag{5.2}$$

$$\text{Klein paramagnet} \quad K_{j,N} = \sigma^x_{j,1,N}\sigma^x_{j,2,N} \quad ; \quad N = A,B \tag{5.3}$$

$$\text{AFM Stripe} \quad S_{j,M} = \sigma^x_{j,M} \quad ; \quad M = (1,A),(2,A),(1,B),(2,B)\ . \tag{5.4}$$

In practice, the Klein order parameter can be fully constructed from the stripe order parameter. Furthermore, we note the algebraic relations:

$$\{W_{j,1}, S_{j,1,A}\} = \{W_{j,1}, S_{j,1,B}\} = \{W_{j,2}, S_{j,2,A}\} = \{W_{j,2}, S_{j,2,B}\} = 0\ . \tag{5.5}$$

It can be verified that all other combinations of W and S commute. The full zigzag chain model already has a natural anisotropy: For $J_x, J_x' \neq 0$, ordering in the x-directions is preferred. Therefore, one can then study the limit in which J_x is much larger than all other energy scales. Of course, there is no guarantee that the same phase diagram structure emerges a priori. Keeping this possibility in mind, define:

$$\rho^x_{j,l} \equiv \sigma^x_{j,l,A}\sigma^x_{j,l,B} \quad ; \quad l = 1,2\ . \tag{5.6}$$

In the limit where $J_y, J_z \to 0$, $[\rho^x_{j,1/2}, H_1] = 0$, generating the extensive degeneracy. The interesting aspect of this limit is that ρ^x also commutes with the order parameters. Therefore, as suggested by the algebra between the stripe and chiral order parameters, one can then define pseudospin variables as:

$$X_{j,1} = W_{j,1} = \sigma^y_{j,1,B}\sigma^x_{j,2,A}\sigma^z_{j,1,A} \ , \tag{5.7}$$
$$Z_{j,1} = S_{j,1,B} = \sigma^x_{j,1,B} \ , \tag{5.8}$$
$$Y_{j,1} = iZ_{j,1}X_{j,1} = \sigma^z_{j,1,B}\sigma^x_{j,2,A}\sigma^z_{j,1,A} \ , \tag{5.9}$$
$$X_{j,2} = W_{j,2} = \sigma^x_{j,1,B}\sigma^z_{j,2,B}\sigma^y_{j,2,A} \ , \tag{5.10}$$
$$Z_{j,2} = S_{j,2,A} = \sigma^x_{j,2,A} \ , \tag{5.11}$$
$$Y_{j,2} = iZ_{j,2}X_{j,2} = \sigma^z_{j,2,A}\sigma^x_{j,1,B}\sigma^z_{j,2,B} \ , \tag{5.12}$$
$$\rho^x_{j,1} = S_{j,1,A}S_{j,1,B} = S_{j,1,A}Z_{j,1} = \sigma^x_{j,1,A}\sigma^x_{j,1,B} \ , \tag{5.13}$$
$$\rho^z_{j,1} = \sigma^z_{j,1,A} \ , \tag{5.14}$$
$$\rho^y_{j,1} = i\rho^x_{j,1}\rho^z_{j,1} = \sigma^y_{j,1,A}\ \sigma^x_{j,1,B} \ , \tag{5.15}$$
$$\rho^x_{j,2} = S_{j,2,A}S_{j,2,B} = S_{j,2,B}Z_{j,2} = \sigma^x_{j,2,A}\sigma^x_{j,2,B} \ , \tag{5.16}$$
$$\rho^z_{j,2} = \sigma^z_{j,2,B} \ , \tag{5.17}$$
$$\rho^y_{j,2} = i\rho^x_{j,2}\rho^z_{j,2} = \sigma^x_{j,2,A}\ \sigma^y_{j,2,B} \ . \tag{5.18}$$

One can check that no degrees of freedom are added or removed, since there are four copies of the $\mathfrak{su}(2)$ algebra per unit cell. The full hamiltonian is then rewritten, for both couplings of flux operators:

$$\begin{aligned} H_1 = {} & J_x \sum_j \sum_{l=1,2} \rho^x_{j,l} + J'_x \sum_j \left(Z_{j,1}\rho^x_{j+1,1}Z_{j+1,1} + Z_{j,2}\rho^x_{j,2}Z_{j+1,2} \right) + \\ & + J_y \sum_j \left(\rho^y_{j,1}\rho^z_{j,2}X_{j,2} + \rho^y_{j,2}\rho^z_{j,1}X_{j,1} \right) + J_z \sum_j \left(\rho^z_{j,2}\rho^z_{j+1,1} + \rho^z_{j,1}\rho^z_{j,2}X_{j,1}X_{j,2} \right) \\ & - Q_1 \sum_j X_{j,1}X_{j+1,2} \ , \end{aligned} \tag{5.19}$$

We now proceed to do degenerate perturbation theory. The degenerate subspace is now unique, defined by the projector:

$$P = |\{\rho^x_{j,l} = -1\}_{j,l}\rangle\langle\{\rho^x_{j,l} = -1\}_{l,j}| \otimes \mathbb{I}_{X,Y,Z} \ , \tag{5.20}$$

where $\mathbb{I}_{X,Y,Z}$ is the identity on the Hilbert space constructed from the second set of pseudospins. This means that, in this limit, the low energy physics is completely dictated from a pair of pseudospins per unit cell. By computing the terms in eq.

(4.31), the first order terms are $-J'_x \sum_{j,l} Z_{j,l}Z_{j+1,l}$ and $-Q_1 \sum_j X_{j,1}X_{j+1,2}$. It can be checked that at second order, the only term which contributes is:

$$J_y^2 \sum_{j,j'} P^{-1} \left[\left(\rho^y_{j,1}\rho^z_{j,2} X_{j,2} + \rho^z_{j,1}\rho^y_{j,2} X_{j,1} \right) G'_0 \left(\rho^y_{j',1}\rho^z_{j',2} X_{j',2} + \rho^z_{j',1}\rho^y_{j',2} X_{j',1} \right) \right] P \quad (5.21)$$

$$= -\frac{J_y^2}{2J_x} \sum_j X_{j,1}X_{j,2} \, . \quad (5.22)$$

Again, we are ignoring constant terms. Up to second order, then:

$$H^1_{\text{eff}} = -J'_x \sum_j \sum_{l=1,2} Z_{j,l}Z_{j+1,l} - Q_1 \sum_j X_{j,1}X_{j+1,2} - \frac{J_y^2}{2J_x} \sum_j X_{j,1}X_{j,2} + \cdots \, , \quad (5.23)$$

which is a spin ladder model, see Fig. 5.1. This chapter will be dedicated to understanding the phase structure of this hamiltonian, connecting to the earlier phase diagram found in the isotropic case.

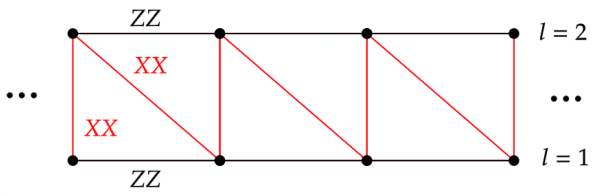

Figure 5.1: Effective spin ladder model obtained in the anisotropic limit of the zigzag chain: Two ising chains, labelled by l, are coupled by Ising interactions in the transverse direction.

Before tackling this task, it is useful to consider symmetries. From the pseudospin mapping, the previously discussed symmetries act as (explicitly adding translations):

$$\mathcal{T} : \{ i \to -i, \; X_{j,l} \to -X_{j,l}, \; Z_{j,l} \to -Z_{j,l}, \; Y_{j,l} \to -Y_{j,l}, \} \, , \quad (5.24)$$

$$\mathcal{R} : \{ j \to -j, \; X_{j,2} \leftrightarrow X_{j,1}, \; Z_{j,2} \leftrightarrow Z_{j,1} \; Y_{j,2} \leftrightarrow Y_{j,1}, \} \, , \quad (5.25)$$

$$\mathcal{K}_{n=1,2} : \{ Z_{j,n} \to -Z_{j,n}, \; Y_{j,n} \to -Y_{j,n} \} \, , \quad (5.26)$$

$$T_x : \{ j \to j+1 \} \quad (5.27)$$

The action of the symmetries on the ρ^α pseudospins are omitted since they are gapped out at low energies. Note that the Klein subgroup is generated by an Ising parity $\prod_j X_{j,n}$ on each chain, the lattice rotation symmetry exchanges the two chains, and time reversal has the expected action. At this order in perturbation theory, there are also "fragile symmetries", which are not guaranteed to survive at higher orders in perturbation theory. For eq. (5.23):

$$\bar{\mathcal{K}}_{n=1,2} : \{X_{j,n} \to -X_{j,n},\ Y_{j,n} \to -Y_{j,n}\} \ . \tag{5.28}$$

For eq. (5.47):

$$\bar{\mathcal{K}} : \{X_{j,l} \to -X_{j,l},\ Y_{j,l} \to -Y_{j,l}\} \ . \tag{5.29}$$

Those symmetries are fragile since they are not satisfied non-pertubatively, and thus expected to be broken at higher order contributions. Therefore, they will be ignored. Let us explore limits of the above models and show that the three gapped phases are found.

5.2 Triangulating the phase diagram

Define $J_\perp = J_y^2/(2J_x)$, the term being responsible for the coupling between the two chains. Consider another set of pseudospins:

$$q_j^z = Z_{j,1}Z_{j,2} \ , \tag{5.30}$$
$$q_j^x = X_{j,2} \ , \tag{5.31}$$
$$\eta_j^z = Z_{j,1} \ , \tag{5.32}$$
$$\eta_j^x = X_{j,1}X_{j,2} \ . \tag{5.33}$$

We then have:

$$H^1_{\text{eff}} = -J'_x \sum_j (1 + q_j^z q_{j+1}^z)\eta_j^z\eta_{j+1}^z - J_\perp \sum_j \eta_j^x - Q_1 \sum_j q_j^x \eta_{j+1}^x q_{j+1}^x \ . \tag{5.34}$$

It turns out, for $Q_1 = 0$, eq. (5.23) is a model known as the quantum compass ladder, discussed by Brzezicki and Olés [100]. Only the z component of q^α appears in the hamiltonian. In the original paper, it was argued that the ground state must order in the q^z variables, essentially reproducing the ground state of a classical Ising chain. By imposing ferromagnetic order in $\langle q^z \rangle = \langle Z_{j,1} Z_{j,2} \rangle \neq 0$, the Klein symmetry is immediately broken down to $\mathbb{Z}_2$. Then, in this limit, we basically have a TFIM at low energies:

$$H^1_{\text{eff}}(Q_1 \to 0) = -2J'_x \sum_j \eta^z_j \eta^z_{j+1} - J_\perp \sum_j \eta^x_j \ . \tag{5.35}$$

For $|J'_x| \gg |J_\perp|$, we have ferromagnetic order in $\langle q^z \rangle = \langle Z_{j,1} Z_{j,2} \rangle \neq 0$ and $\langle \eta^z \rangle = \langle Z_{j,1} \rangle \neq 0$, which corresponds to a fourfold stripe ordered phase (two degenerate states in q^z order and another two in η^z) in the original spin variables, since $\rho^x = -1$. Otherwise, for $|J'_x| \ll |J_\perp|$, $\langle q^z \rangle = \langle Z_{j,1} Z_{j,2} \rangle \neq 0$ and $\langle \eta^x \rangle = \langle X_{j,1} X_{j,2} \rangle \neq 0$ corresponds then to the Klein paramagnet state. This leads to a prediction that the KPM-Stripe transition is an Ising transition with $c = 1/2$.

Consider again another limit, where $J_\perp \gg J'_x, Q_1$. We again apply perturbation theory in the ground state, now defined as $|\{\eta^x_j = 1\}\rangle$. The first order term is $-Q_1 \sum_j q^x_j q^x_{j+1}$. There is a $\sim (J'_x)^2$ second order term, which generates a $q^z q^z$ interaction. The effective hamiltonian is of the form:

$$H^1_{\text{eff}}(J_\perp \gg J'_x, Q_1) \simeq -\frac{(J'_x)^2}{\Delta} \sum_j q^z_j q^z_{j+1} - Q_1 \sum_j q^x_j q^x_{j+1} \ , \tag{5.36}$$

where $\Delta \propto J_\perp$. This is the XY chain, and indeed does correspond to the CSS-Klein transition: ordering q^z and η^x leads to the Klein phase, whereas ordering $\eta^x_j = X_{j,1} X_{j,2}$ and $q^x_j = X_{j,2}$ leads to the twofold degenerate chiral spin state. This agrees with the previous calculation. A third limit of interest is where $Q_1 = J_\perp$:

$$H^1_{\text{eff}}(J_\perp = Q_1) = -J'_x \sum_j (1 + q^z_j q^z_{j+1}) \eta^z_j \eta^z_{j+1} - J_\perp \sum_j (1 + q^x_j q^x_{j+1}) \eta^x_{j+1} \ . \tag{5.37}$$

Taking $J'_x \gg J_\perp$, q^z, η^z are ordered, corresponding to the stripe phase. On the other hand, in $J'_x \ll J_\perp$, q^x, η^x are ordered into the chiral spin state. This is the

CSS-Stripe transition, however, its nature is not clear from the above model, and will be dealt in the next section.

There is a hidden duality in this spin ladder model. Let us redefine (5.30-5.33) as:

$$\tilde{q}_j^z = Z_{j+1,1}Z_{j,2} \ , \tag{5.38}$$
$$\tilde{q}_j^x = X_{j,2} \ , \tag{5.39}$$
$$\tilde{\eta}_j^z = Z_{j+1,1} \ , \tag{5.40}$$
$$\tilde{\eta}_j^x = X_{j+1,1}X_{j,2} \ , \tag{5.41}$$

where the hamiltonian is rewritten as:

$$H^1_{\text{eff}} = -J'_x \sum_j (1 + \tilde{q}_j^z \tilde{q}_{j+1}^z)\tilde{\eta}_j^z \tilde{\eta}_{j+1}^z - Q_1 \sum_j \tilde{\eta}_j^x - J_\perp \sum_j \tilde{q}_j^x \tilde{\eta}_j^x \tilde{q}_{j+1}^x \ , \tag{5.42}$$

which, in the thermodynamic limit, is the same as eq. (5.34) with exchanged couplings $J_\perp \leftrightarrow Q_1$: This means that the full phase diagram must be symmetric under $J_\perp$ and Q_1 [1]. For $J_\perp \neq Q_1$, we found the CSS-Klein and Klein-Stripe transitions, which, under this duality, must also occur for $Q_1 \gg J'_x, J_\perp$ and $J_\perp = 0$, respectively. This places constraints on the phase diagram. We conjecture the form shown in Fig. 5.2: Ising transitions occur at $J_\perp = 0$ and $Q_1 = 0$ planes and generically at the Klein-Stripe transition. The Gaussian transitions occur between the CSS and Klein phases also generically.

Two objections may be raised at this point: (1) Why is there no intermediate gapped phase between the three already discussed? (2) How do these results connect to the phase diagram shown in Fig. 4.9, since they are at completely different limits? The partial answer comes from trying to extract a phase diagram for $J_\perp = \text{const.}$ from the conjectured 3d phase diagram, as illustrated in Fig. 5.3. It predicts a tricritical point between the three phases, which corresponds to the CSS-Stripe transition in the self-dual line $J_\perp = Q_1$. In the DMRG results previously described, the KPM phase only emerges for $Q_1 \ll J, J'_x$. However, in the light of those results,

[1] It can be checked by studying the same limits and list all possible orderings of $\tilde{\boldsymbol{\eta}}$ and $\tilde{\mathbf{q}}$, that all three phases remains.

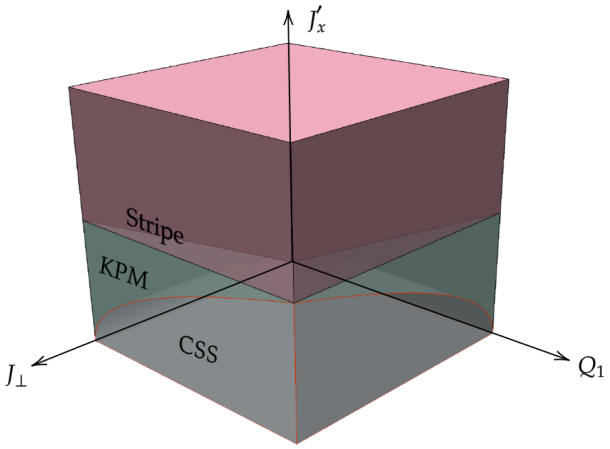

Figure 5.2: Conjectured phase diagram of eq. (5.23). The red lines indicate a $c = 1$ transition, while $c = 1/2$ transitions are in black. The CSS-Stripe transition at $Q_1 = J_\perp$ occurs for $J_\perp = Q_1$.

it may be that there is a Klein phase "hiding" at $Q_1 \gg J'_x, J$. Indeed, a DMRG sweep at Q_1 large of eq.(4.30) finds a Klein paramagnet between the CSS and stripe phases.

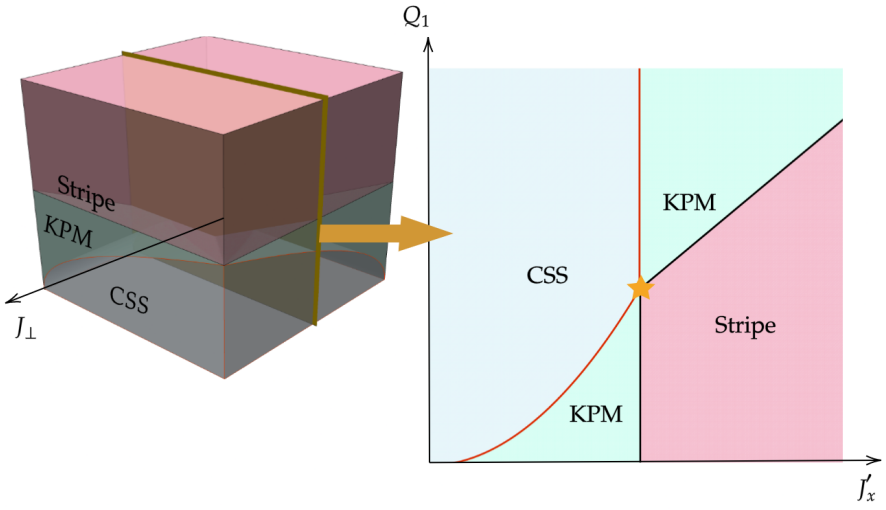

Figure 5.3: Two dimensional slice of fig 5.2 at $J_\perp = \text{const}$ shows a two-dimensional phase diagram with a Klein paramagnet phase emerging for large enough Q_1. Compare to Fig 4.9.

There is also an important property of conformal field theories which can be exploited to find out about universality classes numerically. The entanglement entropy of a one dimensional cut of length ℓ in a conformal field theory on a torus of radius $L/2\pi$ is given as [101]:

$$S(\ell) = \text{const.} + \frac{c}{6} \ln \left[\frac{L}{\pi} \sin \left(\frac{\pi}{L} \ell \right) \right] , \tag{5.43}$$

where the first term is a non-universal constant, and c is the central charge. The entanglement entropy can be computed in a straightforward manner from a MPS state. Two points at the phase transition between the CSS and Klein phase are chosen from Fig. 4.9 , and the corresponding entanglement entropy is computed in Fig. 5.4, fitting with the expression derived from the CFT. Both fits agree with good precision with an Ising CFT with $c = 1/2$, derived in the anisotropic limit.

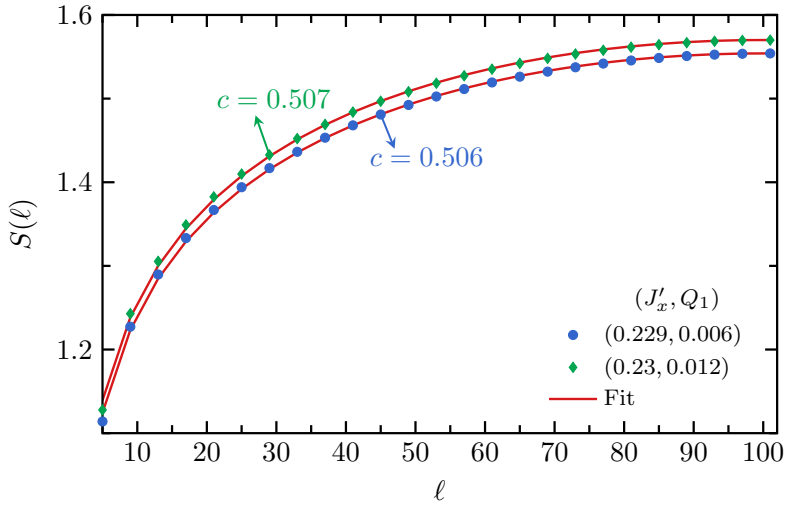

Figure 5.4: Entanglement entropy as a function of ℓ, the partition length, of two points in the phase diagram sitting on the KPM-Stripe transition in the zigzag chain.

Since both the Klein paramagnet and the stripe order are ordered phases separated by a continuous transition, one may label this transition as beyond the LGW paradigm. Note, however, that $\langle \sigma_i^x \sigma_j^x \rangle \simeq \langle \sigma_i^x \rangle \langle \sigma_j^x \rangle$ in the stripe phase, which means that the Klein order parameter is non-zero. This is due to an important subtlety: The group of preserved symmetries of the KPM phase is generated by $\{\mathcal{T}, \mathcal{R}, \mathcal{K}_1 \cdot \mathcal{K}_2\} \in G_{p=\text{KPM}}$, then one can verify that $G_{p=\text{stripe}} \lhd G_{p=\text{KPM}}$. Therefore, this transition is LGW-allowed, as discussed in Sec. 2.1. From the transitions found in Figs. 4.9, 5.2, this is the only one where this subgroup structure is found.

In our model, it turns out another ordered-ordered transition is also an exception: the transition found using the Majorana construction in the tetrahedral chain on Sec. 4.3. We will revisit it in the light of the pseudospin representation. In eq. (5.19), by taking $Q_1 > 0$ and $J'_x = 0$, one can see that $X_{j,l}$ orders in one of the two

degenerate chiral spin states. This is equivalent to applying the pseudospin mapping on eq. (4.17). For $X_{j,1} = X_{j,2} = +1$:

$$H^1_{\text{CSS}} = J_x \sum_j \sum_{l=1,2} \rho^x_{j,l} + J_y \sum_j \left(\rho^y_{j,1}\rho^z_{j,2} + \rho^y_{j,2}\rho^z_{j,1}\right) + J_z \sum_j \left(\rho^z_{j,2}\rho^z_{j+1,1} + \rho^z_{j,1}\rho^z_{j,2}\right) - Q_1 \ . \tag{5.44}$$

For $J_y = 0$, this reduces to the TFIM. For $J_x > J_z$, the $\boldsymbol{\rho}$ pseudospin is in a trivial paramagnet phase, which corresponds to the previously found CSS phase. On the other hand, for $J_z > 0$, $\langle \rho^z_{j,1} \rangle = \langle \sigma^z_{j,1,A} \rangle \neq 0$ and $\langle \rho^z_{j,2} \rangle = \langle \sigma^z_{j,2,B} \rangle \neq 0$ orders, breaking both lattice rotation and Klein symmetries. This is a chiral magnetic phase, which we will denote as CSS_m. Indeed $G_{p=\text{CSS}_\text{m}} \lhd G_{p=\text{CSS}}$, and thus the Ising $\text{CSS}_\text{m} - \text{CSS}$ transition is LGW allowed. This transition is realized in the Majorana representation for $J_z^2 = J_x^2 + J_y^2$ exactly, matching eq. (3.56), describing a gapless Majorana cone in the Ising transition. The robustness of this transition was further verified numerically for $J_y \neq 0$, exactly diagonalizing eq. (5.44) for small chains.

In the CSS-Klein and CSS-Stripe transitions, however, one must consider two independent order parameters and from the overall discussion in Sec. 2.1, it follows that they must be of first order or second order if fine-tuned.

5.3 CSS-Stripe transition and deconfined quantum criticality

The last hanging fruit is the transition between the chiral spin state and the stripe ordered phase. To do so, we will introduce a similar model respecting all symmetries, where the chiralities are coupled in a slightly different manner:

$$H_2 = H_{\text{tet}} + J'_x \sum_j \sum_{l=1,2} \sigma^x_{j,l,B}\sigma^x_{j+1,l,A} - Q_2 \sum_j \sum_{l=1,2} W_{j,l}W_{j+1,l} \ , \tag{5.45}$$

see Fig. 5.5(a). The main properties of the model we have been studying so far are also satisfied:

- At $J'_x = 0$, a chiral spin state is obtained exactly for any $Q_2 > 0$. The argument

is exactly the same, the previously degenerate manifold is frozen out in the ordered states and the low-energy spectrum is constructed from domain walls;

- The results derived in Sec. 4.4 also follow. Since $W_{j,1} = W_{j,2}$, in the ground state, it can be shown that the flux coupling renormalizes to $-2Q_2 \sum_j \tau^y_j \tau^y_{j+1}$ at first order, and the exact same transition still occurs.

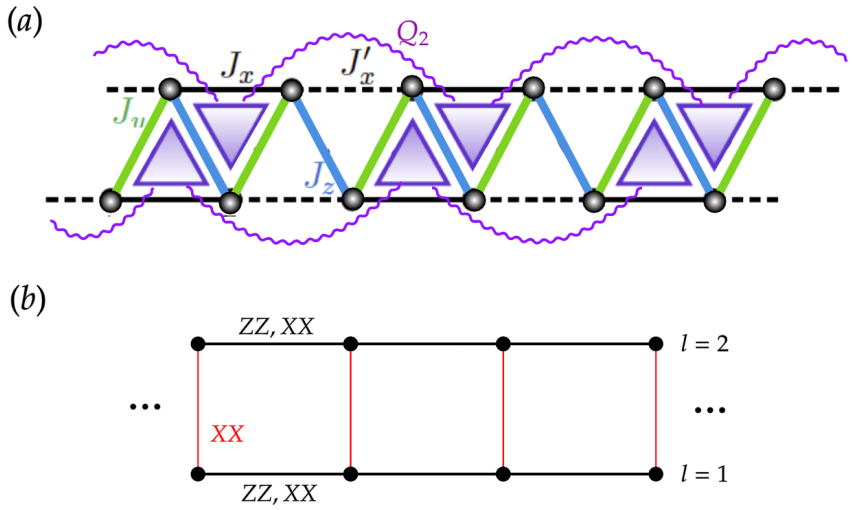

Figure 5.5: (a) Zigzag chain, where the triangular flux operators are now coupled preserving the "triangle direction", (b) Effective spin ladder model obtained in the anisotropic limit of eq. (5.45).

There is also a simple description in the anisotropic limit where J_x is taken to be much larger than all other energy scales. By using the mapping in eqs. (5.7-5.18),

$$\begin{aligned} H_2 = {} & J_x \sum_j \sum_{l=1,2} \rho^x_{j,l} + J'_x \sum_j \left(Z_{j,1} \rho^x_{j+1,1} Z_{j+1,1} + Z_{j,2} \rho^x_{j,2} Z_{j+1,2} \right) + \\ & + J_y \sum_j \left(\rho^y_{j,1} \rho^z_{j,2} X_{j,2} + \rho^y_{j,2} \rho^z_{j,1} X_{j,1} \right) + J_z \sum_j \left(\rho^z_{j,2} \rho^z_{j+1,1} + \rho^z_{j,1} \rho^z_{j,2} X_{j,1} X_{j,2} \right) \\ & - Q_2 \sum_j \sum_{l=1,2} X_{j,l} X_{j+1,l} \ . \end{aligned} \tag{5.46}$$

The same $J_y, J_z \to 0$ limit can be taken and perturbed. The effective hamiltonian up to second order is written:

$$H^2_{\text{eff}} = - \sum_j \sum_{l=1,2} \left(J'_x \ Z_{j,l} Z_{j+1,l} + Q_1 \ X_{j,l} X_{j+1,l} \right) - J_\perp \sum_j X_{j,1} X_{j,2} \ , \tag{5.47}$$

which is a distinct spin ladder from H^1_{eff}, see Fig. 5.5(b). One can try to further introduce the $\boldsymbol{\eta}, \mathbf{q}$ pseudospins in eqs.(5.30-5.33):

$$H^2_{\text{eff}} = -J'_x \sum_j (1 + q^z_j q^z_{j+1}) \eta^z_j \eta^z_{j+1} - J_\perp \sum_j \eta^x_j - Q_2 \sum_j (1 + \eta^x_j \eta^x_{j+1}) q^x_j q^x_{j+1} \ , \quad (5.48)$$

Some of the transitions which were previously discussed also follow: For $Q_2 = 0$, there is an Ising transition, corresponding to KPM-Stripe, and an effective XY chain is found in the limit $J_\perp \gg Q_1, J'_x$, describing the CSS-KPM transition. However, now the phase diagram is "assymetrical": For $J_\perp = 0$, it can be checked by analyzing the limits that a CSS-Stripe transition occurs. We will be focused on the nature of this transition.

In fact, note that for $J_\perp = 0$, eq. (5.47) describes two decoupled XY chains, suggesting a $c = 2$ transition between fourfold degenerate phases. For $J_\perp > 0$, note that the degeneracy of the chiral spin state is lifted to two, justifying the use of this alternative model to study both phases. We will argue that for $J_\perp > 0$, a $c = 1$ transition occurs. The insights from deconfined quantum criticality are manifested in the low energy physics, and the role of emergent symmetries at the transition are discussed.

We will weakly couple the XY chains, working at the limit $Q_1 \simeq J'_x \gg J_\perp$. The Jordan-Wigner transformation in eqs. (3.41-3.43) are now redefined to be quantized in the Y direction:

$$X_{j,l} = B_{j,l}(f^\dagger_{j,l} + f_{j,l}) \ , \quad (5.49)$$

$$Z_{j,l} = iB_{j,l}(f^\dagger_{j,l} - f_{j,l}) \quad ; \quad B_{j,l} = \prod_{j'<j} (1 - 2f^\dagger_{j',l} f_{j',l}) \ , \quad (5.50)$$

$$Y_{j,l} = 2f^\dagger_{j,l} f_{j,l} - 1 \ . \quad (5.51)$$

There are then two pairs of compact bosons from which we write the spin operators, see App. A, as:

$$X_{j,l} \sim \sqrt{\frac{2}{\pi}} \cos \sqrt{\pi}\theta_l \ , \tag{5.52}$$

$$Z_{j,l} \sim -\sqrt{\frac{2}{\pi}} \sin \sqrt{\pi}\theta_l \ , \tag{5.53}$$

$$Y_{j,l} \sim \frac{2}{\sqrt{\pi}} \partial_x \varphi_l - (-1)^x \frac{2}{\pi} \sin \sqrt{4\pi}\varphi_l \ . \tag{5.54}$$

where we have shifted $(\varphi_l \to \varphi_l + \sqrt{\pi}/4, \theta_l + \sqrt{\pi}/4)$ compared to the expressions derived in the Appendix. From eqs. (5.24-5.27), one can derive the action of the bosonic fields under the symmetries:

$$\mathcal{T} : \{i \to -i, \ \theta_l \to \theta_l + \sqrt{\pi}, \ \varphi_l \to -\varphi_l\} \ , \tag{5.55}$$

$$\mathcal{R} : \{x \to -x, \ \theta_2 \leftrightarrow \theta_1, \ \varphi_2 \leftrightarrow \varphi_1\} \ , \tag{5.56}$$

$$\mathcal{K}_{n=1,2} : \{\theta_n \to -\theta_n, \varphi_n \to -\varphi_n\} \ . \tag{5.57}$$

$$T_x : \{x \to x + 1, \ \theta_l \to \theta_l, \ \varphi_l \to \varphi_l + \sqrt{\pi}/2\} \ . \tag{5.58}$$

Therefore, in the continuum, the hamiltonian density of the decoupled chains must be similar to eq. (3.64):

$$\mathcal{H}_{\text{eff}} = \sum_{l=1,2} \left\{ \frac{v_F}{2} [(\partial_x \varphi_l)^2 + (\partial_x \theta_l)^2] + g_l \ \cos\left(\sqrt{4\pi}\theta_\ell\right) \right\} + \cdots \ ., \tag{5.59}$$

where $v_F \propto (J'_x + Q_1)$. The bare value of the coupling in the cosine term is $g_{l=1,2} \propto (J'_x - Q_1)/v_F$. In the field theory, coupling the two chains can be obtained by adding the term, using eq.(5.52):

$$-J_\perp \ X_{j,1} X_{j,2} \sim g_{12} \ \cos \sqrt{\pi}\theta_1 \cos \sqrt{\pi}\theta_2 \ . \tag{5.60}$$

where $g_{12} \propto -J_\perp/v_F$. As explained in Chapter 2, to compute the relevant low energy states of a field theory, all symmetry-allowed terms must be included taken into account in the renormalization group flow. The free (unperturbed) action is given by:

$$\mathcal{S}^0_{\text{eff}} = \sum_{l=1,2} \int \mathrm{dxd}\tau \, \left\{ \frac{v_F}{2} \left[(\partial_x \theta_l)^2 + (\partial_x \varphi_l)^2 \right] - i \partial_x \theta_l \partial_\tau \varphi_l \right\} . \tag{5.61}$$

Some of the terms allowed by symmetry are:

$$\begin{aligned} \mathcal{S}_{\text{eff}} = \mathcal{S}^0_{\text{eff}} + \int \mathrm{d}^2\mathbf{x} \, \{ \sum_{l=1,2} [& g_l \, \cos \sqrt{4\pi} \theta_l + \lambda_l \, \cos \sqrt{16\pi} \varphi_l + \frac{\delta K_l}{2} (\nabla \theta_l)^2 + \\ & + \frac{\delta K_l^{-1}}{2} (\nabla \varphi_l)^2] + \lambda_{12} \, \cos \sqrt{4\pi} \varphi_1 \cos \sqrt{4\pi} \varphi_2 + \\ & + g_{12} \, \cos \sqrt{\pi} \theta_1 \cos \sqrt{\pi} \theta_2 + \cdots \} , \end{aligned} \tag{5.62}$$

where we have ignored terms with higher scaling dimensions and, since they are not generated on the lattice, all the couplings $\lambda_{12}, \lambda_l, \delta K_l$ are initially zero at high energies ($\ell = 0$). Putting off the analysis of vertex operators and the calculation of the renormalization group flow in App. B, the results are as follows:

$$\frac{dg_{12}}{d\ell} = \left(2 - \frac{1}{4K_1} - \frac{1}{4K_2} \right) g_{12} - \pi (g_1 + g_2) g_{12} , \tag{5.63}$$

$$\frac{dg_l}{d\ell} = \left(2 - \frac{1}{K_\ell} \right) g_l - \frac{\pi}{4} g_{12}^2 \quad ; \quad l = 1, 2 , \tag{5.64}$$

$$\frac{dK_l}{d\ell} = \frac{\pi^2}{4} g_{12}^2 + 2\pi^2 (g_1^2 + g_2^2) - \pi^2 \lambda_{12}^2 K_l^2 - 8\pi^2 (\lambda_1^2 + \lambda_2^2) K_l^2 , \tag{5.65}$$

$$\frac{d\lambda_{12}}{d\ell} = (2 - K_1 - K_2) \lambda_{12} - \pi (\lambda_1 + \lambda_2) g_{12} , \tag{5.66}$$

$$\frac{d\lambda_l}{d\ell} = (2 - 4K_l) \lambda_l - \frac{\pi}{4} \lambda_{12}^2 \quad ; \quad l = 1, 2 , \tag{5.67}$$

forming eight coupled differential equations, which can be cut down to five if one consider the flow of $\lambda_+ = \lambda_1 + \lambda_2$, $K_+ = K_1 + K_2$ and $g_+ = g_1 + g_2$, since the corresponding antisymmetric combination does not flow due to $\mathcal{R}$ symmetry. The equations are solved numerically. Remarkably, at low energies, by taking $\ell \to \infty$, all vertex perturbations involving φ are irrelevant, that is, $\lambda_1(\ell \to \infty) = \lambda_2(\ell \to \infty) = \lambda_{12}(\ell \to \infty) = 0$, and thus can be ignored. The intuition from the spin model follows in the gapped regimes, by taking any $J_\perp \neq 0$: For J_x' sufficient larger than Q_1, $g_{l=1,2} \sim \mathcal{O}(1)$, while $g_{12} \to 0^-$, representing the fourfold stripe phase with the vacua:

$$\left(\theta_1 = \frac{\sqrt{\pi}}{2},\ \theta_2 = \frac{\sqrt{\pi}}{2}\right) \quad ; \quad \left(\theta_1 = \frac{3\sqrt{\pi}}{2},\ \theta_2 = \frac{3\sqrt{\pi}}{2}\right) , \tag{5.68}$$

$$\left(\theta_1 = \frac{3\sqrt{\pi}}{2},\ \theta_2 = \frac{\sqrt{\pi}}{2}\right) \quad ; \quad \left(\theta_1 = \frac{\sqrt{\pi}}{2},\ \theta_2 = \frac{3\sqrt{\pi}}{2}\right) . \tag{5.69}$$

On the other hand, for Q_1 sufficiently larger than J'_x, we have both $\lambda_{l=1,2}$ and λ_{12} as large and negative. By minimizing the cosine perturbations, we have a twofold chiral spin state:

$$(\theta_1 = 0,\ \theta_2 = 0) \quad ; \quad (\theta_1 = \sqrt{\pi},\ \theta_2 = \sqrt{\pi}) . \tag{5.70}$$

Both phases can be checked by evaluating X_l and Z_l. One may then expect a fixed point in the renormalization group equations, corresponding to a phase transition. Since both Luttinger parameters grow with the length scale, and we have $K(\ell \to \infty) \to \infty$ a fixed point is found from the zeros of the beta function. Indeed, there is a non-trivial zero, which depends on the specific value of the Luttinger parameter. For $K_{l=1,2} \to \infty$, and denoting $g_1^* = g_2^* = g^*$ at the fixed point:

$$g^* = \frac{3}{2\pi} \simeq 0.4775 \quad ; \quad g_{12}^* = -\sqrt{\frac{2g^*}{\pi}} \simeq -0.5513 . \tag{5.71}$$

It can be verified that the beta function vanishes in this limit. This corresponds to a strongly interacting theory, whose properties are not clear from the perturbation theory around the $c = 2$ fixed point. We will need another approach to understand what happens at the phase transition.

First, note the absence of $\varphi_{l=1,2}$ fields at low energies, since all deformations related to it vanish. One can use $T-$duality to write the effective theory with only the θ boson. At criticality:

$$\mathcal{L}_{\text{eff}} \sim \sum_{l=1,2} \left[\frac{v_\infty}{2}(\nabla\theta_l)^2 + g^* \cos\left(\sqrt{4\pi}\theta_l\right)\right] + g_{12}^* \cos\left(\sqrt{\pi}\theta_1\right)\cos\left(\sqrt{\pi}\theta_2\right) , \tag{5.72}$$

where v_∞ denotes the renormalized boson velocity at criticality. Define two $O(2)$ vectors:

$$\mathbf{n}_l = (X_l, Z_l) \sim (\cos\left(\sqrt{\pi}\theta_l\right), \sin\left(\sqrt{\pi}\theta_l\right)) \,, \tag{5.73}$$

which may be reminiscent of the Néel order parameter. In fact, we will draw some similarities to the Néel-VBS transition. Locally, a rotation of the order parameter, deep in a ordered phase, from a state to another corresponds to a domain wall. More specifically, one can take the vacua of any of the phases in eqs. (5.68, 5.70), and shift by $\sqrt{\pi}$: It generally will remain in the same phase, however, in a different state. As was the case for the one dimensional Néel-VBS transition in Fig. 3.3, the order parameter of the "dual phase" is generated in between, exemplified in Fig. 5.6.

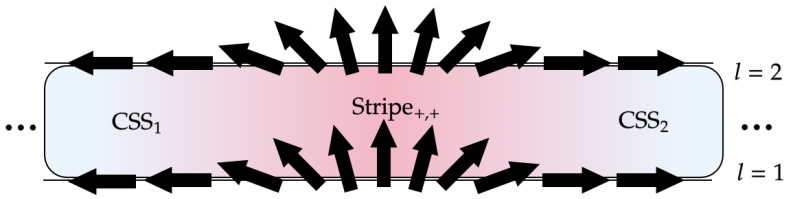

Figure 5.6: An example of a domain wall in the CSS phase. The bold vectors denote the direction of $\mathbf{n}_l$, $\text{CSS}_{1,2}$ denotes the states with positive and negative chirality respectively, and $\text{Stripe}_{(}+,+)$ denotes the $(+,+)$ state depicted in Fig 4.10.

Let us make this statement concrete. From the algebra of dual bosons in eq. (3.30), one can show that:

$$V^\dagger_{\sqrt{\pi},l}(y)\theta_l(x)V_{\sqrt{\pi},l}(y) = \theta_l - \sqrt{\pi}H(x-y) \quad ; \quad V_{\sqrt{\pi},l}(y) = \exp\left[i\sqrt{\pi}\varphi_l(y)\right] \,. \tag{5.74}$$

That is, vertex operators of the dual boson correspond to the topological defects of both phases, domain walls. This is equivalent to the monopole operator $\mathcal{M}$, whose profileration generates the VBS phase. However, in the CSS-Stripe transition, such operators are irrelevant on both sides of the transition. As one would expect, there is a charge associated to such domain walls, generated from the winding of the θ bosons:

$$\mathbf{j}_l = \frac{1}{2\sqrt{\pi}}\hat{z} \times \nabla\theta_l \quad \rightarrow \quad Q_l = \frac{1}{\sqrt{\pi}}\int \mathrm{dx}\, \partial_x\tilde{\theta}_l \,, \tag{5.75}$$

where we have defined $\tilde{\theta}_l = \theta_l/2$ and $\tilde{\varphi}_l = 2\varphi_l$. As defined, $V_{\sqrt{\pi},l}|Q_l\rangle = |Q_l - 1\rangle$. Invoking bosonization, one can introduce chiral fermions $\tilde{\Psi}_l = (\tilde{\psi}_{L,l}, \tilde{\psi}_{R,l})^T$ related to this domain wall as:

$$\tilde{\psi}_{R/L,l} \sim \frac{1}{\sqrt{2\pi}} \exp[-i\sqrt{\pi}\left(\tilde{\varphi}_l \mp \tilde{\theta}_l\right)] \,, \tag{5.76}$$

where the winding charges now corresponds to the fermionic charges, if properly normalized in units of e_1, e_2:

$$Q_l = e_l \int \mathrm{d}x \; \tilde{\Psi}_l^\dagger \tilde{\Psi}_l \,. \tag{5.77}$$

The reasoning behind defining two charge units will be become clear later. In terms of the $\tilde{\theta}$ boson:

$$\mathcal{L}_{\text{eff}} \sim \sum_{l=1,2} \left[\frac{\tilde{v}_\infty}{2}(\nabla\tilde{\theta}_l)^2 + g^* \cos\left(\sqrt{16\pi}\tilde{\theta}_l\right)\right] + g_{12}^* \cos\left(\sqrt{4\pi}\tilde{\theta}_1\right)\cos\left(\sqrt{4\pi}\tilde{\theta}_2\right) \,. \tag{5.78}$$

We want a dual description of this transition in terms of the "domain wall" fermions $\tilde{\Psi}$. By using the bosonization dictionary in eqs. (3.36-3.39) for $\psi_{L/R} \to \tilde{\psi}_{L/R}$, $\varphi \to \tilde{\theta}$, $\theta \to \tilde{\varphi}$,

$$X_{j,l} \sim \cos 2\sqrt{\pi}\tilde{\theta}_l \sim \tilde{\Psi}_l^\dagger \; \sigma^x \; \tilde{\Psi}_l \,, \tag{5.79}$$

$$Z_{j,l} \sim \sin 2\sqrt{\pi}\tilde{\theta}_l \sim \tilde{\Psi}_l^\dagger \; \sigma^y \; \tilde{\Psi}_l \,, \tag{5.80}$$

$$Y_{j,l} \sim \partial_x\tilde{\varphi}_l \sim -\tilde{\Psi}_l^\dagger \; \sigma^z \; \tilde{\Psi}_l \,. \tag{5.81}$$

there are "low energy constraints" on this fermion: first, physical states at low energies must satisfy $\langle Y_{j,l}\rangle = 0$, from which we add a delta functional in the partition function of the form $\prod_{l=1,2}\delta\left(\tilde{\Psi}_l^\dagger \; \sigma^z \; \tilde{\Psi}_l\right)$. A second constraint comes from the fact that domain wall operators are irrelevant: One can fix a charge sector $\prod_{l=1,2}\delta\left(\tilde{\Psi}_l^\dagger\tilde{\Psi}_l - Q_l/L\right)$, where L spatial length. As done in Sec. 2.3 for the $\mathbb{CP}^1$ model, the constraints can be applied by introducing a gauge field $\mathbf{a}$:

$$\delta\mathcal{L} = \sum_{l=1,2} \left[a_2^l e_l \bar{\tilde{\Psi}} \gamma_2 \tilde{\Psi} + a_1^l e_l \bar{\tilde{\Psi}} \gamma_1 \tilde{\Psi} \right] , \tag{5.82}$$

where the γ are the same as defined in Chapter 3, satisfying the euclidean Clifford algebra in eq. (3.12). The presence of the gauge fields can also be understood as a consequence of a "parton construction": the physical operators, described by eqs. (5.79-5.81) has a gauge redundancy $\tilde{\Psi}_l \to e^{ie_l\alpha_l(\mathbf{x})}\tilde{\Psi}_l$, whose $U(1)$ gauge field needs to be introduced transforming as $\mathbf{a}^l \to \mathbf{a}^l + \nabla\alpha_l$, In order to have gauge invariant dynamics, both terms above needs to be introduced [102–104].

Then by the bosonization dictionary, at the transition:

$$\begin{aligned}
\mathcal{L}_{\text{eff}} &\sim \sum_{l=1,2} \left[\frac{\tilde{v}_\infty}{2} (\nabla\tilde{\theta}_l)^2 + g^* \cos\left(\sqrt{16\pi}\tilde{\theta}_l\right) \right] + g_{12}^* \cos\left(\sqrt{4\pi}\tilde{\theta}_1\right) \cos\left(\sqrt{4\pi}\tilde{\theta}_2\right) \\
&\sim \sum_{l=1,2} \left\{ i\tilde{v}_\infty \bar{\tilde{\Psi}}_l \gamma \cdot (\nabla - ie_l\mathbf{a}^l)\tilde{\Psi}_l + g^* \left[\left(\tilde{\psi}_{R,l}^\dagger \tilde{\psi}_{L,l} \right)^2 + \text{h.c.} \right] \right\} + \\
&+ g_{12}^* \left(\bar{\tilde{\Psi}}_1 \gamma_1 \tilde{\Psi}_1 \right) \left(\bar{\tilde{\Psi}}_2 \gamma_1 \tilde{\Psi}_2 \right) ,
\end{aligned} \tag{5.83}$$

which is still a strongly coupled theory: the order $\mathcal{O}(g^*, g_{12}^*)$ terms describes four-fermion scattering tuned to a non-trivial critical point. First, consider a mean-field approach, in the gapped phases. The hamiltonian density is written as:

$$\begin{aligned}
\mathcal{H}_{\text{eff}} \sim \sum_{l=1,2} \Big[& i\tilde{v}_\infty \tilde{\Psi}_l^\dagger \sigma^z \partial_x \tilde{\Psi}_l + + g(: \tilde{\psi}_{R,l}^\dagger \tilde{\psi}_{L,l} :: \tilde{\psi}_{R,l}^\dagger \tilde{\psi}_{L,l} : + \text{h.c}) \Big] \\
& + g_{12} : (\tilde{\Psi}_1^\dagger \sigma^x \tilde{\Psi}_1) :: (\tilde{\Psi}_2^\dagger \sigma^x \tilde{\Psi}_2) : ,
\end{aligned} \tag{5.84}$$

where we have properly normal-ordered $: O := O - \langle O \rangle$ the quadratic terms. A mean-field description is found by ignoring quartic terms and defining $M_l^x = \langle \tilde{\Psi}_l^\dagger \sigma^x \Psi_l \rangle$ and $M_l^z = \langle \tilde{\Psi}_l^\dagger \sigma^y \Psi_l \rangle$, we have:

$$\mathcal{H}^{\text{MF}}_{\text{CSL}-\text{Stripe}} = \sum_{l=1,2} \tilde{\Psi}_l^\dagger \left[i\sigma^z \partial_x - (gM_l^x + g_{12}M_{-l}^x)\sigma^x + gM_l^z \sigma^y \right] \tilde{\Psi}_l + \varepsilon^{(0)} , \tag{5.85}$$

$$\varepsilon^{(0)} = \frac{g}{2} \sum_\ell \left[(M_l^x)^2 - (M_l^z)^2 \right] + g_{12} M_1^x M_2^x , \tag{5.86}$$

where $M^x_{-1} = M_2$, $M^x_{-2} = x_1$. By minimizing the ground state energy to find $(M^x_1, M^x_2, M^z_1, M^z_2)$, the mean-field spectrum indeed describes both phases correctly, including degeneracies. This is analogous to the mean-field result discussed at the Néel-VBS transition in one dimension in section 3.2. Corresponding domain walls trap the fermions in zero modes, which are the elementary excitations. At the transition however, taking $M^x_l, M^z_l \to 0$ results in two chiral fermions, with central charge $c = 2$: This is not surprising, since it comes from a mean-field result. However, as discussed, the fermions are charged under a gauge field. This discussion resembles the easy-plane Néel-VBS transition in two dimensions, where the fermionic degrees of freedom play the role of $\psi_{1/2}$, responsible for creating topological excitations in the Néel phase. Moreover, the continous criticality in DQC is reliant on the gauge field dynamics: Inspired by this case, one then adds dynamics to the gauge field:

$$\mathcal{L}_{\text{eff}} \sim \sum_{l=1,2} i\tilde{v}_\infty \bar{\tilde{\Psi}}_l \gamma \cdot (\nabla - ie_l \mathbf{a}^l)\tilde{\Psi}_l + \mathcal{L}_4 - \frac{1}{G^2}\sum_{\square} \mathcal{W}_\square \ , \tag{5.87}$$

where $\mathcal{L}_4$ contains all four-fermion terms and $\mathcal{W}_\square$ are the Wilson lines on the elementary plaquettes. There are four terms which contribute to this sum:

$$\sum_{\square} \mathcal{W}_\square = \sum_l \cos(\partial_2 a^l_1 - \partial_1 a^l_2) + \cos(a^1_2 - a^2_2 - \partial_2 a_y) + \cos(a^1_1 - a^2_1 - \partial_1 a_y) \ , \tag{5.88}$$

where a_y is the gauge field component in the links between the chains; in our case, $a_y = 0$. Then, defining $\mathbf{a} = \mathbf{a}^1 + \mathbf{a}^2$ and $\mathbf{a}^- = \mathbf{a}^1 - \mathbf{a}^2$, the antisymmetric combination is gapped out by the last two cosine terms. The first terms can be safely expanded out, due to the absence of monopoles. One has then:

$$\mathcal{L}_{\text{eff}} \sim \sum_{l=1,2} i\tilde{v}_\infty \bar{\tilde{\Psi}}_l \gamma \cdot (\nabla - ie_l \mathbf{a})\tilde{\Psi}_l + \mathcal{L}_4 + \frac{1}{2G^2}(\nabla \times \mathbf{a}) \ , \tag{5.89}$$

which, for $\mathcal{L}_4 = 0$, corresponds to two fermionic flavors of $1+1$ quantum electrodynamics, denoted by $N_f = 2$ QED_2. This theory can be exactly solved, and we are interested in the infrared dynamics where $G^2 \to \infty$. [103, 104]. Gauge fix $a_2 = 0$ and integrate out a_1, using techniques from Gaussian integration:

$$\int \mathcal{D}a_1 \exp\left\{-\int \mathrm{x}^2\mathbf{x}\left[\sum_l\left(\bar{\tilde{\Psi}}_l i\boldsymbol{\gamma}\cdot\nabla\tilde{\Psi}_l - a_1 e_l \bar{\tilde{\Psi}}_l\gamma^1\tilde{\Psi}_l\right)+\frac{1}{2G^2}(\partial_2 a_1)^2\right]\right\}$$
$$\sim \exp\{-\int \mathrm{d}^2\mathbf{x}\left[\frac{1}{2}\sum_\ell(\partial_\mu\tilde{\theta}_\ell)^2\right]+ \tag{5.90}$$
$$-G^2\int \mathrm{dx}_1\mathrm{dx}_2'\mathrm{dx}_2|x_2-x_2'|\left[\sum_l e_l(\partial_2\tilde{\theta}_l)\right]\left[\sum_{l'} e_{l'}(\partial_{2'}\tilde{\theta}_{l'})\right]\}\ ,$$

where we have bosonized again in the second line. Redefine the bosonic modes in a $O(2)$ rotation:

$$\tilde{\theta}_s = \frac{e_1\tilde{\theta}_1+e_2\tilde{\theta}_2}{\sqrt{e_1^2+e_2^2}} \quad ; \quad \tilde{\theta}_a = \frac{e_1\tilde{\theta}_1-e_2\tilde{\theta}_2}{\sqrt{e_1^2+e_2^2}}\ , \tag{5.91}$$

Let $e=|e_l|$. We have two choices, $e_1=\pm e_2=e$. The lagrangian is then written, including the terms from $\mathcal{L}_4$:

$$\mathcal{L}_{\text{eff}} \sim \sum_{\sigma=a,s}\left[\frac{\tilde{v}_\infty}{2}(\nabla\tilde{\theta}_\sigma)^2+\frac{g_{12}}{2}\cos\left(\sqrt{8\pi}\tilde{\theta}_\sigma\right)\right]+2G^2e^2(\tilde{\theta}_s)^2+2g\cos\left(\sqrt{8\pi}\tilde{\theta}_a\right)\cos\left(\sqrt{8\pi}\tilde{\theta}_s\right)\ , \tag{5.92}$$

In the strong coupling limit, $G^2\to\infty$, the symmetric mode is gapped. Therefore, at first order, one can pin down $\tilde{\theta}_s$ in the action and obtain an effective sine-Gordon theory:

$$\mathcal{L}_{\text{eff}} \sim \frac{\tilde{v}_\infty}{2}(\partial_\mu\tilde{\theta}_a)^2 + M(g,g_{12})\cos 2\sqrt{2\pi}\tilde{\theta}_a\ , \tag{5.93}$$

where $M=g_{12}/2+2gC$, and $C\sim\mathcal{O}(1)$ is a non-universal constant. This indeed describes both phases:

- $e_1=-e_2$: This corresponds to states where $\tilde{\theta}_1=\tilde{\theta}_2$. For $M\gg 0$, (large and positive) there are two degenerate states corresponding to $Z_1=Z_2=1$ and $Z_1=Z_2=1$, and for $M\ll 0$ (big and negative), we have the CSS ground states $X_1=X_2=\pm 1$;

- $e_1 = e_2$: This corresponds to $\tilde{\theta}_1 = -\tilde{\theta}_2$. For $M \gg 0$, there are two states $Z_1 = -Z_2 = 1$, and $Z_1 = -Z_2 = -1$. For $M \ll 0$, there are the usual CSS ground states.

For $M(g^*, g_{12}^*) = 0$, we have a free compact boson at the transition. We claim that this is the critical point found in eq. (5.71). Both couplings g^*, g_{12}^* are $\mathcal{O}(1)$ and oppositely signed, and the corresponding perturbations lead to the correct phases in the infrared. Therefore, we conclude that the CSS-Stripe transition is a $c = 1$ transition. By computing the entanglement entropy in DMRG, for the spin ladder model, this result was found for any $J_\perp > 0$. In the original zigzag chain model, the large correlation length at the transition prevented a good numerical estimate of the central charge.

Physically, this means that the "dual theory" of domain walls is as good as original variables, and is a good description at the transition. This point is in complete agreement with the DQC phenomenology. Note also that the critical region also has an emergent $U(1) \times U(1)$ symmetry structure, as the one-dimensional Néel-VBS transition or FM-VBS transitions. In all those cases, the topological excitations play an important role and generically become massless at the transition. Alas, one may distance themselves to naming the CSS-Stripe transition as "deconfined", due to the confining nature of gauge fields in one dimension: In our example, our critical boson at the CSS-Stripe transition would not exist if one coupled only one fermionic flavor to the $U(1)$ gauge field, and the theory is completely gapped. One can for example, compute the photon propagator and verify the shift of the massless pole to a massive pole [104]

However, those examples still remain as the best analogies to deconfined criticality in one dimension, due to the existence of this "charged domain wall" description. This was explored in [32], where the wide range of tools in one dimension was used to show that a $c = 1$ FM-ordered transition can be cast as a gauge theory with bosonic or fermionic matter. All descriptions depend on the symmetry properties of domain walls and how they must be charged. In our model, the continuum limit suggested the symmetry properties of the domain wall, and the transformation properties of other lattice symmetries were not as important.

Chapter 6

Conclusion

In this thesis, we presented a one-dimensional chiral spin state and discussed its perturbations. We found a family of continuous phase transitions, and the corresponding universality classes were computed. We discussed how the properties of domain walls can generate DQC-like behaviour in one dimension, supporting previous arguments in the literature [5, 32]. Other symmetry-breaking phases which were found are also of interest: The stripe phase supports the numerical results on an analogue model in two dimensions [95] and the presence of a Klein paramagnet was shown confirming previous conjectures [88]. Furthermore, evidence for the robustness of such continuous transitions was shown, by working at different energy scales.

There are two lines of further research questions related to different aspects of our work. From the perspective of model building:

- It is interesting to ask about models with $SU(2)$ spin symmetry. There is evidence of chiral spin states in one dimension when four-spin interactions are introduced [37, 38], but further theoretical understanding of the nature of the transitions is still lacking. Spin symmetry allows us to construct lattice dualities between the chiralities and spin operators, which may aid this endeavor [105]. It is an open question if chiral phases can exist if only two spin interactions are constructed;
- There is an exactly solvable two-dimensional model exhibiting similar phenomenology to the tetrahedral chain, known as the Yao-Kivelson model [106], where two chiral spin liquid phases, a topological and a trivial one, are separated by a continuous phase transition. It remains to see if similar methods,

such as the pseudspin approach, can be applied in the two-dimensional setting to study possible perturbations and unconventional phase transitions.

There are also questions relating to the bigger picture of the classification of quantum phases and transitions in one dimension:

- In one dimension there are Lieb-Schultz-Mattis (LSM) theorems and its generalizations [107–110], which state that a translationally-invariant spin chain with a given symmetry group G (with a projective action on the half-spin degrees of freedom), the ground state must be either gapless or in a symmetry-breaking state, and no unique disordered ground state can exist. First proposed by LSM for $G = U(1)$, it was shown that it is also valid for $G = \mathcal{T}$ or $G = \mathbb{Z}_2 \times \mathbb{Z}_2$. This is satisfied by the model on eq.(3.66), and explains why the phase diagram was composed only by symmetry-breaking phases. However, both the zigzag chain models in eqs.(4.30,5.45) and the simpler anisotropic counterparts in eqs.(5.23, 5.47) does not satisfy such criteria, since it contains a larger unit cell. In both numerical and analytical analysis, no disordered state was found. It suggests a LSM-type constraint for spin ladders;

- Our model adds to the list of examples of deconfined transitions due to domain walls. As highlighted in [32], ordered-ordered transitions in one dimension seems to have generally this structure. On a bigger goal, one may then ask if there is a combination of methods in order to "bootstrap" [111] one-dimensional deconfined quantum criticality in a model-independent way, since: (1) The topological nature of domain walls could not become simpler, since there is only one non-trivial homotopic classification $\pi_1(S^1) = \mathbb{Z}$ [55], (2) imposing conformal invariance in the transition may be used to classify the deformations, (3) topological effects, such as instantons and what are known as Wess-Zumino-Witten (WZW) for continuous groups are well classified in one dimension [17], (4) If a LSM constraint is present, recent works have showed that this implies that the low-energy field theory must carry a t'Hooft anomaly [112–114], further constraining what field theories are physical. This approach was used to understand possible transitions without explicit models in two-dimensional quantum systems [115]. A combination of some (or all) of this techniques may shed light on what ordered-ordered transitions are possible in spin chains and ladders.

Appendix A

Bosonization of spin operators

In this appendix, we will combine the Jordan-Wigner transformation with the bosonization of chiral fermions, obtaining an explicit formula of lattice spin operators in terms of the dual bosons. Assume the quantization axis in the x axis as eqs.(3.41-3.43) assuming that the fermions can be expanded in chiral modes as eq.(3.59).

At the continuum, operators are defined as excitations of some ground state, or vacuum. For the Jordan-Wigner fermions, this corresponds to half-filling, where $\langle c_i^\dagger c_i \rangle = 1/2$. To prevent single-point singularities, one must take the continuum limit of normal ordered operators, defined as $:O := O - \langle O \rangle$. Then, eq.(3.41) is rewritten as:

$$\begin{aligned} \sigma_j^x &\simeq 2 : c_j^\dagger c_j : \\ &\sim : \rho_R : + : \rho_L : + \left(e^{-i2k_F x} : \psi_R^\dagger \psi_L : + \text{h.c} \right) \sim 2 \left[\frac{1}{\sqrt{\pi}} \partial_x \varphi + \frac{1}{\pi} \cos(\sqrt{4\pi}\varphi + 2k_F x) \right] \\ &\sim 2 \left[\frac{1}{\sqrt{\pi}} \partial_x \varphi + \frac{(-1)^x}{\pi} \cos \sqrt{4\pi}\varphi \right] , \end{aligned} \tag{A.1}$$

where we have used the bosonization dictionary in eqs.(3.36, 3.37, 3.38), and $k_F = \pi/2$. To obtain the continuum expression for other components requires a subtle analysis of fusing single-point operators. For example, we will need the following identity:

$$e^A e^B = e^{\frac{1}{2}[A,B]} e^{A+B} , \tag{A.2}$$

which is true for $[A, B] \in \mathbb{C}$. The continuum of the string operator can be written as:

$$\begin{aligned} B_j &= \exp\left(i\pi \sum_{j'<j} n_{j'}\right) \\ &\sim \exp\left(i\pi \int_{-\infty}^{x} \mathrm{d}x' \, [: \rho_R(x') : + : \rho_L(x') : +1/2]\right) \sim e^{ik_F x} e^{i\sqrt{\pi}\varphi(x)} \, . \end{aligned} \tag{A.3}$$

We now need to specify a point-splitting operation. That is, let us define:

$$\lim_{x\to y} O(x)O(y) :=: O(x)O(x-\epsilon) : \, , \tag{A.4}$$

and $A^{\pm}(x) = c^{\dagger}(x) \pm c(x)$. By eqs.(3.41,3.42):

$$\begin{aligned} \sigma_j^z &\sim : B(x)A^{+}(x-\epsilon) : \\ &\sim \frac{1}{\sqrt{2\pi}} : e^{ik_F(x-\epsilon)} e^{i\sqrt{\pi}\varphi(x-\epsilon)} \{ e^{-ik_F x} e^{i\sqrt{\pi}[\theta(x)-\varphi(x)]} + e^{ik_F x} e^{i\sqrt{\pi}[\theta(x)+\varphi(x)]} \\ &+ e^{ik_F x} e^{-i\sqrt{\pi}[\theta(x)-\varphi(x)]} + e^{-ik_F x} e^{-i\sqrt{\pi}[\theta(x)+\varphi(x)]} \} : \, , \end{aligned} \tag{A.5}$$

using eq.(A.2,3.30) with $H(x \to 0) = 1/2$, the fusion rule is derived:

$$: e^{i\sqrt{\pi}\varphi(x-\epsilon)} e^{i\sqrt{\pi}\lambda_1[\theta(x)+\lambda_2\varphi(x)]} := e^{-i\pi\lambda_1/4} \exp\left\{ i\sqrt{\pi}\left[\lambda_1\theta(x) + (\lambda_1\lambda_2 - 1)\varphi(x)\right] \right\} \, , \tag{A.6}$$

then, taking $\epsilon \to 0$ in the full expression, we arrive at:

$$\sigma_j^z \sim \sqrt{\frac{2}{\pi}} \cos\left[\sqrt{\pi}\left(\theta - \frac{\sqrt{\pi}}{4}\right)\right] + \sqrt{\frac{2}{\pi}}(-1)^x \cos\left[\sqrt{\pi}\left(\theta - 2\varphi_\ell - \frac{\sqrt{\pi}}{4}\right)\right] \, . \tag{A.7}$$

By using the same identities, the product $\lim_{x\to y} B(x)A^{-}(y)$ can be worked out and one derives:

$$\sigma_j^y \sim -\sqrt{\frac{2}{\pi}} \sin\left[\sqrt{\pi}\left(\theta - \frac{\sqrt{\pi}}{4}\right)\right] - \sqrt{\frac{2}{\pi}}(-1)^x \sin\left[\sqrt{\pi}\left(\theta - 2\varphi_\ell - \frac{\sqrt{\pi}}{4}\right)\right] \ . \quad \text{(A.8)}$$

Appendix B

Vertex operators and RG flow

In this appendix, we will compute OPEs of vertex operators and the corresponding scale dimensions. The results are then used to compute the one-loop RG flow equations from the action in eq. (5.62).

B.1 Operator product expansion of vertex operators

Consider the free action in eq.(3.27), where the velocity is made explicit and defined in euclidean time:

$$\mathcal{S}_{\mathrm{LL}} \to \int \mathrm{d}\tau \mathrm{dx} \left\{ \frac{v}{2} \left[\frac{1}{2K} (\partial_x \theta)^2 + \frac{K}{2} (\partial_x \varphi)^2 \right] - i \partial_x \theta \partial_\tau \varphi \right\} . \tag{B.1}$$

We want to study the OPEs of the charged vertex operators $V_\alpha, \tilde{V}_\beta$ in eqs.(3.31, 3.32). We also use the expressions of the shift currents $\mathbf{j}_s^\theta = \nabla\theta$, $\mathbf{j}_s^\varphi = \nabla\varphi$. First, we must compute the logarithmically divergent correlations of the free bosons in $1+1$ dimensions. Let $\mathbf{x} = (\tau, x)$ denote as a spacetime point. Consider the *regulated* correlation functions:

$$G_\varphi(\mathbf{x}) = \langle \varphi(\mathbf{x}) \varphi(0) \rangle - \langle \varphi(0)^2 \rangle , \tag{B.2}$$

$$G_\theta(\mathbf{x}) = \langle \theta(\mathbf{x}) \theta(0) \rangle - \langle \theta(0)^2 \rangle , \tag{B.3}$$

introduce momentum modes:

$$\varphi(\mathbf{x}) = \int \frac{\mathrm{dkd}\omega}{(2\pi)^2} e^{-i(kx+\omega\tau)} \varphi(\mathbf{k}) \ . \tag{B.4}$$

The action can be written as a quadratic form:

$$\mathcal{S}_{\mathrm{LL}} = \frac{1}{2} \int \frac{\mathrm{dkd}\omega}{(2\pi)^2} \begin{pmatrix} \theta(-\mathbf{k}) & \varphi(-\mathbf{k}) \end{pmatrix} A(\mathbf{k}) \begin{pmatrix} \theta(\mathbf{k}) \\ \varphi(\mathbf{k}) \end{pmatrix} \ , \tag{B.5}$$

from which the momentum-space propagator is derived:

$$A^{-1}(\mathbf{k}) = \begin{pmatrix} \langle\theta(-\mathbf{k})\theta(\mathbf{k})\rangle & \langle\theta(-\mathbf{k})\varphi(\mathbf{k})\rangle \\ \langle\varphi(-\mathbf{k})\theta(\mathbf{k})\rangle & \langle\varphi(-\mathbf{k})\varphi(\mathbf{k})\rangle \end{pmatrix} = \begin{pmatrix} \frac{K^{-1}}{vk^2+v^{-1}\omega^2} & \frac{-i\omega}{kv(vk^2+v^{-1}\omega^2)} \\ \frac{-i\omega}{kv(vk^2+v^{-1}\omega^2)} & \frac{K}{vk^2+v^{-1}\omega^2} \end{pmatrix} \ . \tag{B.6}$$

Let us compute then eq.(B.2), imposing a cutoff in $\mathbf{k} = (k, v^{-1}\omega)$:

$$\begin{aligned} G_\varphi(\mathbf{x}) &= K \int \frac{\mathrm{d}\omega\mathrm{dk}}{(2\pi)^2} \frac{e^{-i(kx+\omega\tau)} - 1}{vk^2 + v^{-1}\omega^2} = K \int_{|\mathbf{k}|<1/a} \frac{\mathrm{d}^2\mathbf{k}}{(2\pi)^2} \frac{e^{-i\mathbf{k}\cdot\mathbf{x}} - 1}{|\mathbf{k}|^2} \\ &\simeq -\frac{K}{2\pi} \ln\left(\frac{|\mathbf{x}|}{2a}\right) = -\frac{K}{2\pi} \ln|\mathbf{x}| \ . \end{aligned} \tag{B.7}$$

where we choose to measure lengths in units of $2a$. Therefore:

$$G_\varphi(\mathbf{x}) = -\frac{K}{2\pi} \ln|\mathbf{x}| \ , \tag{B.8}$$

$$G_\theta(\mathbf{x}) = -\frac{1}{2\pi K} \ln|\mathbf{x}| \ , \tag{B.9}$$

where a similar computation gives the second correlation. OPEs must satisfy the selection rules of the symmetries of the CFT. In our case, it is manifested as a $U(1)_\varphi \times U(1)_\theta$ symmetry, organized into a $\mathbb{Z} \times \mathbb{Z}$ structure labelling the irreducible representations in terms of the charges (Q_φ, Q_θ). As mentioned, V_α is charged in the $(\alpha, 0)$ representation and $\tilde{V}_\beta$ in the $(0, \beta)$ rep. Schematically, this already constraint

the OPEs. Let $\Delta_\alpha, \tilde{\Delta}_\beta$ be the scaling dimensions of V_α and $\tilde{V}_\beta$, respectively. From the expression of the correlations, one can take derivatives to show that the scaling dimension of the currents are 1. Then, one must have:

$$V_\alpha(\mathbf{x}) \cdot V_{\alpha'}(\mathbf{y}) \sim \frac{1}{|\mathbf{x}-\mathbf{y}|^{\Delta_\alpha+\Delta_{\alpha'}-\Delta_{\alpha+\alpha'}}} V_{\alpha+\alpha'} + \delta_{\alpha+\alpha',0} \frac{\#}{|\mathbf{x}-\mathbf{y}|^{\Delta_\alpha+\Delta_{\alpha'}-2}} (\nabla\varphi)^2 + \cdots , \tag{B.10}$$

$$\tilde{V}_\beta(\mathbf{x}) \cdot \tilde{V}_{\beta'}(\mathbf{y}) \sim \frac{1}{|\mathbf{x}-\mathbf{y}|^{\tilde{\Delta}_\beta+\tilde{\Delta}_{\beta'}-\tilde{\Delta}_{\beta+\beta'}}} \tilde{V}_{\beta+\beta'} + \delta_{\beta+\beta',0} \frac{\#}{|\mathbf{x}-\mathbf{y}|^{\tilde{\Delta}_\beta+\tilde{\Delta}_{\beta'}-2}} (\nabla\theta)^2 + \cdots , \tag{B.11}$$

where # denotes numerical prefactors, corresponding to the structure constants, which will be computed [1]. Since we have this Hilbert space structure where vertex operators are defined, one may use canonical quantization (correlations of vertex operators can also be computed using the path integral formalism). To have well-behaved vertex operators, consider the normal-ordered product, which can be safely expanded:

$$: V_\alpha(\mathbf{x}) :: V_{\alpha'}(\mathbf{y}) := \sum_{n,m=0}^{\infty} \frac{(i\alpha)^n}{n!} \frac{(i\alpha')^m}{m!} : \varphi^n(\mathbf{x}) :: \varphi^m(\mathbf{y}) : , \tag{B.12}$$

we will only need to evaluate this expression for $\alpha = -\beta$. Furthermore, we will also only need the terms:

$$\begin{aligned} : V_\alpha(\mathbf{x}) :: V_{-\alpha}(\mathbf{y}) : &= \sum_{n,m=0}^{\infty} \frac{(\alpha^2)^n}{n!} \langle\varphi(\mathbf{x})\varphi(\mathbf{y})\rangle^n \left[1 + \alpha^2 : \varphi(\mathbf{x})\varphi(\mathbf{y}) : - \frac{\alpha^2}{2} \left(: \varphi^2(\mathbf{x}) : + : \varphi^2(\mathbf{y}) :\right) + \cdots \right. \\ &= \exp\left(\alpha^2 \langle\varphi(\mathbf{x})\varphi(\mathbf{y})\rangle\right) \left[1 - \frac{\alpha^2}{2} : (\varphi(\mathbf{x}) - \varphi(\mathbf{y}))^2 : + \cdots\right] , \end{aligned} \tag{B.13}$$

where we have used Wick's theorem to simplify the terms. The relation between vertex operators and its normal ordered counterpart, as can also be shown by expanding the exponential is a "screening factor":

[1] the absence of a prefactor in the "fusion term" comes from imposing that correlation function of scaling operators follow eq. (2.32)

$$V_\alpha(\mathbf{x}) = e^{-\alpha^2/2\langle\varphi^2(\mathbf{0})\rangle} : V_\alpha(\mathbf{x}) : , \tag{B.14}$$

therefore:

$$\begin{aligned} V_\alpha(\mathbf{x})V_{-\alpha}(\mathbf{y}) &= \exp\left(\alpha^2 G_\varphi(\mathbf{x})\right)\left[1 - \frac{\alpha^2}{2} : (\varphi(\mathbf{x}) - \varphi(\mathbf{y}))^2 : + \cdots\right] , \\ &= \frac{1}{|\mathbf{x}-\mathbf{y}|^{\alpha^2 K/2\pi}}\left[1 - \frac{\alpha^2}{2} : (\varphi(\mathbf{x}) - \varphi(\mathbf{y}))^2 : + \cdots\right] , \end{aligned} \tag{B.15}$$

to obtain the OPE, one must take $\mathbf{x} = \mathbf{y} \to \mathbf{R} = (\mathbf{x}+\mathbf{y})/2$. Then, for example, $\varphi(\mathbf{x}) \sim \varphi(\mathbf{R}) + \frac{1}{2}(\mathbf{x}-\mathbf{y})\cdot\nabla\varphi$. Then we have:

$$V_\alpha(\mathbf{x}) \cdot V_{-\alpha}(\mathbf{y}) \sim \frac{1}{|\mathbf{x}-\mathbf{y}|^{\alpha^2 K/2\pi}} + \frac{\alpha^2/2}{|\mathbf{x}-\mathbf{y}|^{\alpha^2 K/2\pi - 2}}(\nabla\varphi)^2 + \cdots , \tag{B.16}$$

$$\tilde{V}_\beta(\mathbf{x}) \cdot \tilde{V}_{\beta'}(\mathbf{y}) \sim \frac{1}{|\mathbf{x}-\mathbf{y}|^{\beta^2/2\pi K}} + \frac{\beta^2/2}{|\mathbf{x}-\mathbf{y}|^{\beta^2/2\pi K - 2}}(\nabla\theta)^2 + \cdots , \tag{B.17}$$

where we read the scaling dimensions:

$$\Delta_\alpha = \frac{\alpha^2 K}{4\pi} \quad ; \quad \tilde{\Delta}_\beta = \frac{\beta^2}{4\pi K} , \tag{B.18}$$

and also the missing constants in eqs. (B.10,B.11):

$$V_\alpha(\mathbf{x}) \cdot V_{\alpha'}(\mathbf{y}) \sim \frac{1}{|\mathbf{x}-\mathbf{y}|^{-\alpha\alpha' K/2\pi}} V_{\alpha+\alpha'} + \frac{\alpha^2/2}{|\mathbf{x}-\mathbf{y}|^{\alpha^2 K/2\pi - 2}}(\nabla\varphi)^2 + \cdots , \tag{B.19}$$

$$\tilde{V}_\beta(\mathbf{x}) \cdot \tilde{V}_{\beta'}(\mathbf{y}) \sim \frac{1}{|\mathbf{x}-\mathbf{y}|^{-\beta\beta'/2\pi K}} \tilde{V}_{\beta+\beta'} + \frac{\beta^2/2}{|\mathbf{x}-\mathbf{y}|^{\beta^2/2\pi K - 2}}(\nabla\theta)^2 + \cdots , \tag{B.20}$$

in the above identities, operators of higher scaling dimensions are ignored, since they are generally irrelevant.

B.2 Renormalization group equations

In eq. (5.62), all deformations to the fixed point can be written as vertex operators:

$$O_{\theta_l} \equiv \cos\sqrt{4\pi}\theta_l = \frac{1}{2}(\tilde{V}_{\sqrt{4\pi},l} + \tilde{V}_{-\sqrt{4\pi}}) \ , \tag{B.21}$$

$$O_{\varphi_l} \equiv \cos\sqrt{16\pi}\varphi_l = \frac{1}{2}(V_{\sqrt{16\pi},l} + V_{-\sqrt{16\pi},l}) \ , \tag{B.22}$$

$$\begin{aligned} O_{\theta_{12}} &\equiv \cos\sqrt{\pi}\theta_1 \cos\sqrt{\pi}\theta_2 \\ &= \frac{1}{4}\left(\tilde{V}_{\sqrt{\pi},1}\tilde{V}_{\sqrt{\pi},2} + \tilde{V}_{-\sqrt{\pi},1}\tilde{V}_{-\sqrt{\pi},2} + \tilde{V}_{-\sqrt{\pi},1}\tilde{V}_{\sqrt{\pi},2} + \tilde{V}_{\sqrt{\pi},1}\tilde{V}_{-\sqrt{\pi},2}\right) \ , \end{aligned} \tag{B.23}$$

$$\begin{aligned} O_{\varphi_{12}} &\equiv \cos\sqrt{4\pi}\varphi_1 \cos\sqrt{4\pi}\varphi_2 \\ &= \frac{1}{4}\left(V_{\sqrt{4\pi},1}V_{\sqrt{4\pi},2} + V_{-\sqrt{4\pi},1}V_{-\sqrt{4\pi},2} + V_{-\sqrt{4\pi},1}V_{\sqrt{4\pi},2} + V_{\sqrt{4\pi},1}V_{-\sqrt{4\pi},2}\right) \ . \end{aligned} \tag{B.24}$$

with coupling constants $g_l, \lambda_l, g_{12}, \lambda_{12}$, respectively, and $V_{\alpha,l} = \exp[i\alpha\varphi_l]$, $\tilde{V}_{\beta,l} = \exp[i\beta\theta_l]$. The corresponding scaling dimensions are:

$$\Delta_{\theta_l} = \frac{1}{K_l} \ , \tag{B.25}$$

$$\Delta_{\varphi_l} = 4K_l \ , \tag{B.26}$$

$$\Delta_{\theta_{12}} = \frac{1}{4K_1} + \frac{1}{4K_2} \ , \tag{B.27}$$

$$\Delta_{\varphi_{12}} = K_1 + K_2 \ . \tag{B.28}$$

$$\tag{B.29}$$

The one-loop contribution to the beta function, described in eq.(2.36), is computed by evaluating the operator product expansion of the above operators. Equipped with the results of the last section, one can compute each $\mathcal{O}_i$ *cdot*$\mathcal{O}_j$, aided by the following identity: If V_1, V_2, V_3, V_4 are vertex operators, the OPE decomposes as

$$[V_1(\mathbf{x})V_2(\mathbf{x})]\cdot[V_3(\mathbf{y})V_4(\mathbf{y})] \sim [V_1(\mathbf{x})V_3(\mathbf{y})]\cdot[V_2(\mathbf{x})V_4(\mathbf{y})] + [V_2(\mathbf{x})V_3(\mathbf{y})]\cdot[V_1(\mathbf{x})V_4(\mathbf{y})] \tag{B.30}$$

which is a consequence of Wick's theorem. We will state the results:

$$O_{\theta_1}(\mathbf{x})O_{\theta_{12}}(\mathbf{y}) = O_{\theta_2}(\mathbf{x})O_{\theta_{12}}(\mathbf{y}) \sim \frac{1}{2}\frac{1}{|\mathbf{x}-\mathbf{y}|} : \cos\sqrt{\pi}\theta_1 \cos\sqrt{\pi}\theta_2 : , \tag{B.31}$$

$$O_{\theta_{12}}(\mathbf{x})O_{\theta_{12}}(\mathbf{y}) \sim \sum_{l=1,2}\left[\frac{1}{4} : \cos\sqrt{4\pi}\theta_l : -\frac{1}{2}\left(\frac{\pi}{4}\right)|\mathbf{x}-\mathbf{y}| : (\nabla\theta_l)^2 :\right] , \tag{B.32}$$

$$O_{\theta_1}(\mathbf{x})O_{\theta_1}(\mathbf{y}) \sim -\frac{1}{2}(2\pi)(\nabla\theta_1)^2 , \tag{B.33}$$

$$O_{\theta_2}(\mathbf{x})O_{\theta_2}(\mathbf{y}) \sim -\frac{1}{2}(2\pi)(\nabla\theta_2)^2 , \tag{B.34}$$

$$O_{\varphi_1}(\mathbf{x})O_{\varphi_{12}}(\mathbf{y}) = O_{\varphi_2}(\mathbf{x})O_{\varphi_{12}}(\mathbf{y}) \sim \frac{1}{2}\frac{1}{|\mathbf{x}-\mathbf{y}|^4} : \cos\sqrt{4\pi}\varphi_1 \cos\sqrt{4\pi}\varphi_2 : , \tag{B.35}$$

$$O_{\varphi_{12}}(\mathbf{x})O_{\varphi_{12}}(\mathbf{y}) \sim \sum_{l=1,2}\left[\frac{1}{4} : \cos\sqrt{16\pi}\varphi_l : -\frac{1}{2}(\pi)|\mathbf{x}-\mathbf{y}|^2 : (\nabla\varphi_l)^2 :\right] , \tag{B.36}$$

$$O_{\varphi_1}(\mathbf{x})O_{\varphi_1}(\mathbf{y}) \sim -\frac{1}{2}(8\pi)\frac{:(\nabla\varphi_1)^2:}{|\mathbf{x}-\mathbf{y}|^6} , \tag{B.37}$$

$$O_{\varphi_2}(\mathbf{x})O_{\varphi_2}(\mathbf{y}) \sim -\frac{1}{2}(8\pi)\frac{:(\nabla\varphi_2)^2:}{|\mathbf{x}-\mathbf{y}|^6} . \tag{B.38}$$

From the above expression, the coefficients are extracted:

$$c(\lambda_1,\lambda_{12};\lambda_{12}) = c(\lambda_{12},\lambda_1;\lambda_{12}) = c(\lambda_2,\lambda_{12};\lambda_{12}) = c(\lambda_{12},\lambda_2;\lambda_{12}) = \frac{1}{2} , \tag{B.39}$$

$$c(\lambda_{12},\lambda_{12};\lambda_1) = c(\lambda_{12},\lambda_{12};\lambda_2) = \frac{1}{4} , \tag{B.40}$$

$$c(\lambda_{12},\lambda_{12};K_1) = c(\lambda_{12},\lambda_{12};K_2) = -\pi , \tag{B.41}$$

$$c(\lambda_1,\lambda_1;K_1) = c(\lambda_2,\lambda_2;K_2) = -8\pi , \tag{B.42}$$

$$c(g_1,g_{12};g_{12}) = c(g_{12},g_1;g_{12}) = c(g_2,g_{12};g_{12}) = c(g_{12},g_2;g_{12}) = \frac{1}{2} , \tag{B.43}$$

$$c(g_{12},g_{12};g_1) = c(g_{12},g_{12};g_2) = \frac{1}{4} , \tag{B.44}$$

$$c(g_{12},g_{12};K_1^{-1}) = c(g_{12},g_{12};K_2^{-1}) = -\frac{\pi}{4} , \tag{B.45}$$

$$c(g_1,g_1;K_1^{-1}) = c(g_2,g_2;K_2^{-1}) = -2\pi , \tag{B.46}$$

appearing as c_{ijk} in eq.(2.36). Noting that:

$$\frac{dK_l^{-1}}{d\ell} = -\frac{1}{K_l^2}\frac{dK_l}{d\ell} \quad \rightarrow \quad c(\cdots,\cdots,K_l^{-1}) = -K_l^2 c(\cdots,\cdots,K_l) , \tag{B.47}$$

one can substitute $S_{d=2} = 2\pi$, the scaling dimensions in eqs.(B.25-B.28) and the OPE coefficients in eqs.(B.39-B.46) in eq.(2.36) and eqs.(5.63-5.67) are derived, as promised.

Bibliography

[1] Piers Coleman. *Introduction to many-body physics*. Cambridge University Press, 2015.

[2] John Cardy. *Scaling and renormalization in statistical physics*, volume 5. Cambridge university press, 1996.

[3] Alexander Altland and Ben D Simons. *Condensed matter field theory*. Cambridge university press, 2010.

[4] T. Senthil, Ashvin Vishwanath, Leon Balents, Subir Sachdev, and Matthew P. A. Fisher. Deconfined quantum critical points. *Science*, 303(5663):1490–1494, 2004.

[5] Christopher Mudry, Akira Furusaki, Takahiro Morimoto, and Toshiya Hikihara. Quantum phase transitions beyond landau-ginzburg theory in one-dimensional space revisited. *Phys. Rev. B*, 99:205153, May 2019.

[6] X. G. Wen, Frank Wilczek, and A. Zee. Chiral spin states and superconductivity. *Phys. Rev. B*, 39:11413–11423, Jun 1989.

[7] Lev Davidovich Landau. On the theory of phase transitions. i. *Zh. Eksp. Teor. Fiz.*, 11:19, 1937.

[8] Lev Davidovich Landau. On the theory of phase transitions. ii. *Zh. Eksp. Teor. Fiz.*, 11:627, 1937.

[9] Mehran Kardar. *Statistical physics of fields*. Cambridge University Press, 2007.

[10] Jean Zinn-Justin. *Quantum field theory and critical phenomena*. Oxford University Press, 2021.

[11] Kenneth G. Wilson and Michael E. Fisher. Critical exponents in 3.99 dimensions. *Phys. Rev. Lett.*, 28:240–243, Jan 1972.

[12] Kenneth G Wilson and John Kogut. The renormalization group and the ϵ expansion. *Physics reports*, 12(2):75–199, 1974.

[13] Kenneth G. Wilson. The renormalization group: Critical phenomena and the kondo problem. *Rev. Mod. Phys.*, 47:773–840, Oct 1975.

[14] Kenneth G. Wilson. The renormalization group and critical phenomena. *Rev. Mod. Phys.*, 55:583–600, Jul 1983.

[15] T. Senthil, Leon Balents, Subir Sachdev, Ashvin Vishwanath, and Matthew P. A. Fisher. Quantum criticality beyond the landau-ginzburg-wilson paradigm. *Phys. Rev. B*, 70:144407, Oct 2004.

[16] Cenke Xu. Unconventional quantum critical points. *International Journal of Modern Physics B*, 26(18):1230007, 2012.

[17] Philippe Francesco, Pierre Mathieu, and David Sénéchal. *Conformal field theory*. Springer Science & Business Media, 2012.

[18] Subir Sachdev. *Quantum phase transitions*. Cambridge university press, 2011.

[19] Lars Onsager. Crystal statistics. i. a two-dimensional model with an order-disorder transition. *Phys. Rev.*, 65:117–149, Feb 1944.

[20] Xiao-Gang Wen. Colloquium: Zoo of quantum-topological phases of matter. *Rev. Mod. Phys.*, 89:041004, Dec 2017.

[21] Michael Pretko, Xie Chen, and Yizhi You. Fracton phases of matter. *International Journal of Modern Physics A*, 35(06):2030003, 2020.

[22] Rahul M. Nandkishore and Michael Hermele. Fractons. *Annual Review of Condensed Matter Physics*, 10(1):295–313, 2019.

[23] V. Kalmeyer and R. B. Laughlin. Equivalence of the resonating-valence-bond and fractional quantum hall states. *Phys. Rev. Lett.*, 59:2095–2098, Nov 1987.

[24] Lucile Savary and Leon Balents. Quantum spin liquids: a review. *Reports on Progress in Physics*, 80(1):016502, nov 2016.

[25] J. Knolle and R. Moessner. A field guide to spin liquids. *Annual Review of Condensed Matter Physics*, 10(1):451–472, 2019.

[26] C. Broholm, R. J. Cava, S. A. Kivelson, D. G. Nocera, M. R. Norman, and T. Senthil. Quantum spin liquids. *Science*, 367(6475):eaay0668, 2020.

[27] Alexei Kitaev. Anyons in an exactly solved model and beyond. *Annals of Physics*, 321(1):2–111, 2006.

[28] Stephen M Winter, Alexander A Tsirlin, Maria Daghofer, Jeroen van den Brink, Yogesh Singh, Philipp Gegenwart, and Roser Valentí. Models and materials for generalized kitaev magnetism. *Journal of Physics: Condensed Matter*, 29(49):493002, 2017.

[29] Maria Hermanns, Itamar Kimchi, and Johannes Knolle. Physics of the kitaev model: Fractionalization, dynamic correlations, and material connections. *Annual Review of Condensed Matter Physics*, 9:17–33, 2018.

[30] Hans Bethe. Zur theorie der metalle. *Zeitschrift für Physik*, 71(3):205–226, 1931.

[31] Steven R. White and Ian Affleck. Dimerization and incommensurate spiral spin correlations in the zigzag spin chain: Analogies to the kondo lattice. *Phys. Rev. B*, 54:9862–9869, Oct 1996.

[32] Shenghan Jiang and Olexei Motrunich. Ising ferromagnet to valence bond solid transition in a one-dimensional spin chain: Analogies to deconfined quantum critical points. *Phys. Rev. B*, 99:075103, Feb 2019.

[33] Brenden Roberts, Shenghan Jiang, and Olexei I. Motrunich. Deconfined quantum critical point in one dimension. *Phys. Rev. B*, 99:165143, Apr 2019.

[34] Rui-Zhen Huang, Da-Chuan Lu, Yi-Zhuang You, Zi Yang Meng, and Tao Xiang. Emergent symmetry and conserved current at a one-dimensional incarnation of deconfined quantum critical point. *Phys. Rev. B*, 100:125137, Sep 2019.

[35] Alexander A. Nersesyan, Alexander O. Gogolin, and Fabian H. L. Eßler. Incommensurate spin correlations in spin- 1/2 frustrated two-leg heisenberg ladders. *Phys. Rev. Lett.*, 81:910–913, Jul 1998.

[36] Toshiya Hikihara, Lars Kecke, Tsutomu Momoi, and Akira Furusaki. Vector chiral and multipolar orders in the spin-$\frac{1}{2}$ frustrated ferromagnetic chain in magnetic field. *Phys. Rev. B*, 78:144404, Oct 2008.

[37] A. Läuchli, G. Schmid, and M. Troyer. Phase diagram of a spin ladder with cyclic four-spin exchange. *Phys. Rev. B*, 67:100409, Mar 2003.

[38] Tessa Cookmeyer, Johannes Motruk, and Joel E. Moore. Four-spin terms and the origin of the chiral spin liquid in mott insulators on the triangular lattice. *Phys. Rev. Lett.*, 127:087201, Aug 2021.

[39] Abhinav Saket, S. R. Hassan, and R. Shankar. Manipulating unpaired majorana fermions in a quantum spin chain. *Phys. Rev. B*, 82:174409, Nov 2010.

[40] Sachio Watanabe and Tunemaru Usui. Phase Transition in Coupled Order Parameter System. *Progress of Theoretical Physics*, 73(6):1305–1319, 06 1985.

[41] Eduardo Fradkin. *Quantum field theory: an integrated approach*. Princeton University Press, 2021.

[42] Vitaly L Ginzburg and Lev D Landau. On the theory of superconductivity. In *On Superconductivity and Superfluidity*, pages 113–137. Springer, 2009.

[43] Nivaldo A Lemos. *Mecânica analítica*. Editora Livraria da Física, 2007.

[44] Anthony Zee. *Group theory in a nutshell for physicists*, volume 17. Princeton University Press, 2016.

[45] Matthew B Hastings and Tohru Koma. Spectral gap and exponential decay of correlations. *Communications in mathematical physics*, 265(3):781–804, 2006.

[46] M. B. Hastings. Lieb-schultz-mattis in higher dimensions. *Phys. Rev. B*, 69:104431, Mar 2004.

[47] Bei Zeng, Xie Chen, Duan-Lu Zhou, and Xiao-Gang Wen. *Quantum information meets quantum matter: From quantum entanglement to topological phases of many-body systems*. Springer, 2019.

[48] Richard P Feynman, Albert R Hibbs, and Daniel F Styer. *Quantum mechanics and path integrals*. Courier Corporation, 2010.

[49] Michael E Peskin. *An introduction to quantum field theory*. CRC press, 2018.

[50] Horatiu Nastase. *Introduction to Quantum Field Theory*. Cambridge University Press, 2019.

[51] John Cardy. Conformal field theory and statistical mechanics. *Exact Methods in Lowdimensional Statistical Physics and Quantum Computing (Oxford University Press, Oxford, 2010)*, pages 65–98, 2010.

[52] Assa Auerbach. *Interacting electrons and quantum magnetism*. Springer Science & Business Media, 2012.

[53] F. D. M. Haldane. $O(3)$ nonlinear σ model and the topological distinction between integer- and half-integer-spin antiferromagnets in two dimensions. *Phys. Rev. Lett.*, 61:1029–1032, Aug 1988.

[54] N. Read and Subir Sachdev. Valence-bond and spin-peierls ground states of low-dimensional quantum antiferromagnets. *Phys. Rev. Lett.*, 62:1694–1697, Apr 1989.

[55] Charles Nash and Siddhartha Sen. *Topology and geometry for physicists*. Elsevier, 1988.

[56] J M Kosterlitz and D J Thouless. Ordering, metastability and phase transitions in two-dimensional systems. *Journal of Physics C: Solid State Physics*, 6(7):1181–1203, apr 1973.

[57] A. D'Adda, M. Lüscher, and P. Di Vecchia. A 1/n expandable series of nonlinear σ models with instantons. *Nuclear Physics B*, 146(1):63–76, 1978.

[58] Edward Witten. Instatons, the quark model, and the 1/n expansion. *Nuclear Physics B*, 149(2):285–320, 1979.

[59] Aleksandr Michajlovič Polyakov. *Gauge fields and strings*. Taylor & Francis, 1987.

[60] Heinz J Rothe. *Lattice gauge theories: an introduction*. World Scientific Publishing Company, 2012.

[61] Nathan Seiberg, T. Senthil, Chong Wang, and Edward Witten. A duality web in 2+1 dimensions and condensed matter physics. *Annals of Physics*, 374:395–433, 2016.

[62] Carl Turner. Lectures on dualities in 2+ 1 dimensions. *arXiv preprint arXiv:1905.12656*, 2019.

[63] Nicholas R. Poniatowski. Superconductivity, broken gauge symmetry, and the higgs mechanism. *American Journal of Physics*, 87(6):436–443, 2019.

[64] Subir Sachdev and R Jalabert. Effective lattice models for two-dimensional quantum antiferromagnets. *Modern Physics Letters B*, 4(16):1043–1052, 1990.

[65] C. Lannert, Matthew P. A. Fisher, and T. Senthil. Quantum confinement transition in a d-wave superconductor. *Phys. Rev. B*, 63:134510, Mar 2001.

[66] C. Dasgupta and B. I. Halperin. Phase transition in a lattice model of superconductivity. *Phys. Rev. Lett.*, 47:1556–1560, Nov 1981.

[67] Michael E Peskin. Mandelstam-'t hooft duality in abelian lattice models. *Annals of Physics*, 113(1):122–152, 1978.

[68] Andreas Karch and David Tong. Particle-vortex duality from 3d bosonization. *Phys. Rev. X*, 6:031043, Sep 2016.

[69] Michael Kamal and Ganpathy Murthy. New o(3) transition in three dimensions. *Phys. Rev. Lett.*, 71:1911–1914, Sep 1993.

[70] Olexei I. Motrunich and Ashvin Vishwanath. Emergent photons and transitions in the O(3) sigma model with hedgehog suppression. *Phys. Rev. B*, 70:075104, Aug 2004.

[71] Hui Shao, Wenan Guo, and Anders W. Sandvik. Quantum criticality with two length scales. *Science*, 352(6282):213–216, 2016.

[72] Adam Nahum, J. T. Chalker, P. Serna, M. Ortuño, and A. M. Somoza. Deconfined quantum criticality, scaling violations, and classical loop models. *Phys. Rev. X*, 5:041048, Dec 2015.

[73] Chong Wang, Adam Nahum, Max A. Metlitski, Cenke Xu, and T. Senthil. Deconfined quantum critical points: Symmetries and dualities. *Phys. Rev. X*, 7:031051, Sep 2017.

[74] Kenji Harada, Takafumi Suzuki, Tsuyoshi Okubo, Haruhiko Matsuo, Jie Lou, Hiroshi Watanabe, Synge Todo, and Naoki Kawashima. Possibility of deconfined criticality in su(n) heisenberg models at small n. *Phys. Rev. B*, 88:220408, Dec 2013.

[75] D. Charrier, F. Alet, and P. Pujol. Gauge theory picture of an ordering transition in a dimer model. *Phys. Rev. Lett.*, 101:167205, Oct 2008.

[76] Zhen Bi and T. Senthil. Adventure in topological phase transitions in $3 + 1$-d: Non-abelian deconfined quantum criticalities and a possible duality. *Phys. Rev. X*, 9:021034, May 2019.

[77] E Miranda. Introduction to bosonization. *Brazilian Journal of Physics*, 33:3–35, 2003.

[78] David Tong. Gauge theory, 2018.

[79] Thierry Giamarchi. *Quantum physics in one dimension*, volume 121. Clarendon press, 2003.

[80] Jan Von Delft and Herbert Schoeller. Bosonization for beginners—refermionization for experts. *Annalen der Physik*, 7(4):225–305, 1998.

[81] L A Takhtadzhan and Lyudvig D Faddeev. THE QUANTUM METHOD OF THE INVERSE PROBLEM AND THE HEISENBERG XYZ MODEL. *Russian Mathematical Surveys*, 34(5):11–68, oct 1979.

[82] Ian Affleck and F. D. M. Haldane. Critical theory of quantum spin chains. *Phys. Rev. B*, 36:5291–5300, Oct 1987.

[83] R. Jackiw and C. Rebbi. Solitons with fermion number 1/2. *Phys. Rev. D*, 13:3398–3409, Jun 1976.

[84] Michael Levin and T. Senthil. Deconfined quantum criticality and néel order via dimer disorder. *Phys. Rev. B*, 70:220403, Dec 2004.

[85] Hendrik Antoon Kramers. Théorie générale de la rotation paramagnétique dans les cristaux. *Proc. Acad. Amst*, 33(6), 1930.

[86] Hal Tasaki. *Physics and mathematics of quantum many-body systems*. Springer Nature, 2020.

[87] Zohar Nussinov and Jeroen Van Den Brink. Compass models: Theory and physical motivations. *Reviews of Modern Physics*, 87(1):1, 2015.

[88] Itamar Kimchi and Ashvin Vishwanath. Kitaev-heisenberg models for iridates on the triangular, hyperkagome, kagome, fcc, and pyrochlore lattices. *Phys. Rev. B*, 89:014414, Jan 2014.

[89] A Yu Kitaev. Unpaired majorana fermions in quantum wires. *Physics-uspekhi*, 44(10S):131, 2001.

[90] Ching-Kai Chiu, Jeffrey C. Y. Teo, Andreas P. Schnyder, and Shinsei Ryu. Classification of topological quantum matter with symmetries. *Rev. Mod. Phys.*, 88:035005, Aug 2016.

[91] Michael Wimmer. Algorithm 923: Efficient numerical computation of the pfaffian for dense and banded skew-symmetric matrices. *ACM Transactions on Mathematical Software (TOMS)*, 38(4):1–17, 2012.

[92] Fabio L. Pedrocchi, Stefano Chesi, and Daniel Loss. Physical solutions of the kitaev honeycomb model. *Phys. Rev. B*, 84:165414, Oct 2011.

[93] Kazuya Shinjo, Shigetoshi Sota, Seiji Yunoki, Keisuke Totsuka, and Takami Tohyama. Density-matrix renormalization group study of kitaev–heisenberg model on a triangular lattice. *Journal of the Physical Society of Japan*, 85(11):114710, 2016.

[94] Michael Becker, Maria Hermanns, Bela Bauer, Markus Garst, and Simon Trebst. Spin-orbit physics of $j = \frac{1}{2}$ mott insulators on the triangular lattice. *Phys. Rev. B*, 91:155135, Apr 2015.

[95] P. A. Maksimov, Zhenyue Zhu, Steven R. White, and A. L. Chernyshev. Anisotropic-exchange magnets on a triangular lattice: Spin waves, accidental degeneracies, and dual spin liquids. *Phys. Rev. X*, 9:021017, Apr 2019.

[96] Steven R White. Density matrix formulation for quantum renormalization groups. *Physical review letters*, 69(19):2863, 1992.

[97] Steven R White. Density-matrix algorithms for quantum renormalization groups. *Physical review b*, 48(14):10345, 1993.

[98] Ulrich Schollwöck. The density-matrix renormalization group. *Reviews of modern physics*, 77(1):259, 2005.

[99] Erik S Sørensen, Andrei Catuneanu, Jacob S Gordon, and Hae-Young Kee. Heart of entanglement: Chiral, nematic, and incommensurate phases in the kitaev-gamma ladder in a field. *Physical Review X*, 11(1):011013, 2021.

[100] Wojciech Brzezicki and Andrzej M. Oleś. Exact solution for a quantum compass ladder. *Phys. Rev. B*, 80:014405, Jul 2009.

[101] Pasquale Calabrese and John Cardy. Entanglement entropy and quantum field theory. *Journal of Statistical Mechanics: Theory and Experiment*, 2004(06):P06002, jun 2004.

[102] D. N. Sheng, Olexei I. Motrunich, Simon Trebst, Emanuel Gull, and Matthew P. A. Fisher. Strong-coupling phases of frustrated bosons on a two-leg ladder with ring exchange. *Phys. Rev. B*, 78:054520, Aug 2008.

[103] Yutaka Hosotani. Gauge theory description of spin chains and ladders. In *Solitons*, pages 69–73. Springer, 2000.

[104] Don H Kim and Patrick A Lee. Theory of spin excitations in undoped and underdoped cuprates. *Annals of Physics*, 272(1):130–164, 1999.

[105] Toshiya Hikihara, Tsutomu Momoi, and Xiao Hu. Spin-chirality duality in a spin ladder with four-spin cyclic exchange. *Phys. Rev. Lett.*, 90:087204, Feb 2003.

[106] Hong Yao and Steven A. Kivelson. Exact chiral spin liquid with non-abelian anyons. *Phys. Rev. Lett.*, 99:247203, Dec 2007.

[107] Elliott Lieb, Theodore Schultz, and Daniel Mattis. Two soluble models of an antiferromagnetic chain. *Annals of Physics*, 16(3):407–466, 1961.

[108] Xie Chen, Zheng-Cheng Gu, and Xiao-Gang Wen. Classification of gapped symmetric phases in one-dimensional spin systems. *Physical review bB*, 83(3):035107, 2011.

[109] Haruki Watanabe, Hoi Chun Po, Ashvin Vishwanath, and Michael Zaletel. Filling constraints for spin-orbit coupled insulators in symmorphic and nonsymmorphic crystals. *Proceedings of the National Academy of Sciences*, 112(47):14551–14556, 2015.

[110] Yoshiko Ogata and Hal Tasaki. Lieb–schultz–mattis type theorems for quantum spin chains without continuous symmetry. *Communications in Mathematical Physics*, 372(3):951–962, 2019.

[111] David Poland, Slava Rychkov, and Alessandro Vichi. The conformal bootstrap: Theory, numerical techniques, and applications. *Reviews of Modern Physics*, 91(1):015002, 2019.

[112] Gil Young Cho, Chang-Tse Hsieh, and Shinsei Ryu. Anomaly manifestation of lieb-schultz-mattis theorem and topological phases. *Physical Review B*, 96(19):195105, 2017.

[113] Chao-Ming Jian, Zhen Bi, and Cenke Xu. Lieb-schultz-mattis theorem and its generalizations from the perspective of the symmetry-protected topological phase. *Physical Review B*, 97(5):054412, 2018.

[114] Max A Metlitski and Ryan Thorngren. Intrinsic and emergent anomalies at deconfined critical points. *Physical Review B*, 98(8):085140, 2018.

[115] Weicheng Ye, Meng Guo, Yin-Chen He, Chong Wang, and Liujun Zou. Topological characterization of lieb-schultz-mattis constraints and applications to symmetry-enriched quantum criticality. *arXiv preprint arXiv:2111.12097*, 2021.